

Application of Non-local Quantum Hydrodynamics to the Description of the Charge Density Waves in the Graphene Crystal Lattice.

Boris V. Alexeev^{*}, Irina V. Ovchinnikova

Moscow Lomonosov University of Fine Chemical Technologies (MITHT)
Prospekt Vernadskogo, 86, Moscow 119570, Russia

e-mail: boris.vlad.alexeev@gmail.com

ABSTRACT

The motion of the charged particles in graphene in the frame of the quantum non-local hydrodynamic description is considered. It is shown as results of the mathematical modeling that the mentioned motion is realizing in the soliton forms. The dependence of the size and structure of solitons on the different physical parameters is investigated.

Keywords: The theory of solitons; Generalized hydrodynamic equations; Quantum non-local hydrodynamics; Theory of transport processes in graphene.

1. INTRODUCTION

We deliver here some main ideas and deductions of the generalized Boltzmann physical kinetics and non-local physics developed by B. Alexeev (see for example [1 – 10]). For simplicity, the fundamental methodic aspects are considered from the qualitative standpoint of view avoiding excessively cumbersome formulas. A rigorous description can be found, for example, in the monograph [6].

In 1872 L Boltzmann [11, 12] published his kinetic equation for the one-particle distribution function (DF) $f(\mathbf{r}, \mathbf{v}, t)$. He expressed the equation in the form

$$Df/Dt = J^B(f), \quad (1.1)$$

where J^B is the local collision integral, and $\frac{D}{Dt} = \frac{\partial}{\partial t} + \mathbf{v} \cdot \frac{\partial}{\partial \mathbf{r}} + \mathbf{F} \cdot \frac{\partial}{\partial \mathbf{v}}$ is the substantial (particle) derivative, \mathbf{v} and \mathbf{r} being the velocity and radius vector of the particle, respectively. Boltzmann equation (1.1) governs the transport processes in a one-component gas, which is sufficiently rarefied that only binary collisions between particles are of importance and valid only for two character scales, connected with the hydrodynamic time-

^{*} Tel.: +xx xx 265xxxxx; fax: +xx aa 462xxxxx.
E-mail address: xyz@abc.com.

scale and the time-scale between particle collisions. While we are not concerned here with the explicit form of the collision integral, note that it should satisfy conservation laws of point-like particles in binary collisions. Integrals of the distribution function (i.e. its moments) determine the macroscopic hydrodynamic characteristics of the system, in particular the number density of particles n and the temperature T . The Boltzmann equation (BE) is not of course as simple as its symbolic form above might suggest, and it is in only a few special cases that it is amenable to a solution. One example is that of a maxwellian distribution in a locally, thermodynamically equilibrium gas in the event when no external forces are present.

In this case the equality $J^B = 0$ and $f = f_0$ is met, giving the maxwellian distribution function f_0 . A weak point of the classical Boltzmann kinetic theory is the way it treats the dynamic properties of interacting particles. On the one hand, as the so-called “physical” derivation of the BE suggests, Boltzmann particles are treated as material points; on the other hand, the collision integral in the BE brings into existence the cross sections for collisions between particles. A rigorous approach to the derivation of the kinetic equation for f (noted in following as KE_f) is based on the hierarchy of the Bogolyubov-Born-Green-Kirkwood-Yvon (BBGKY) [1, 6, 13, 14] equations.

A KE_f obtained by the multi-scale method turns into the BE if one ignores the change of the distribution function (DF) over a time of the order of the collision time (or, equivalently, over a length of the order of the particle interaction radius). It is important to note [1 - 6] that accounting for the third of the scales mentioned above leads (*prior* to introducing any approximation destined to break the Bogolyubov chain) to additional terms, generally of the same order of magnitude, appear in the BE. If the correlation functions is used to derive KE_f from the BBGKY equations, then the passage to the BE means the neglect of non-local effects.

Given the above difficulties of the Boltzmann kinetic theory, the following clearly inter related questions arise. First, what is a physically infinitesimal volume and how does its introduction (and, as the consequence, the unavoidable smoothing out of the DF) affect the kinetic equation? This question can be formulated in (from the first glance) the paradox form – what is the size of the point in the physical system? Second, how does a systematic account for the proper diameter of the particle in the derivation of the KE_f affect the Boltzmann equation? In the theory developed by B. Alexeev, we refer to the corresponding KE_f as Generalized Boltzmann Equation (GBE). The derivation of the GBE and the applications of GBE are presented, in particular, in monograph [6]. Accordingly, our purpose is first to explain the essence of the physical generalization of the BE.

Let a particle of finite radius be characterized, as before, by the position vector \mathbf{r} and velocity \mathbf{v} of its center of mass at some instant of time t . Let us introduce physically small volume (**PhSV**) as element of measurement of macroscopic characteristics of physical system for a point containing in this **PhSV**. We should hope that **PhSV** contains sufficient particles N_{ph} for statistical description of the system. In other words, a net of physically small volumes covers the whole investigated physical system.

Every **PhSV** contains entire quantity of point-like Boltzmann particles, and *the same DF f is prescribed for whole **PhSV** in Boltzmann physical kinetics*. Therefore, Boltzmann particles are fully “packed” in the reference volume. Let us consider two adjoining physically small volumes **PhSV₁** and **PhSV₂**. We have in principle another situation for the particles of finite size moving in physical small volumes, which are *open* thermodynamic systems.

Then, the situation is possible where, at some instant of time t , the particle is located on the interface between two volumes. In so doing, the lead effect is possible (say, for

PhSV₂), when the center of mass of particle moving to the neighboring volume **PhSV₂** is still in **PhSV₁**. However, the delay effect takes place as well, when the center of mass of particle moving to the neighboring volume (say, **PhSV₂**) is already located in **PhSV₂** but a part of the particle still belongs to **PhSV₁**.

Moreover, even the point-like particles (starting after the last collision near the boundary between two mentioned volumes) can change the distribution functions in the neighboring volume. The adjusting of the particles dynamic characteristics for translational degrees of freedom takes several collisions. As result, we have in the definite sense "the Knudsen layer" between these volumes. This fact unavoidably leads to fluctuations in mass and hence in other hydrodynamic quantities. Existence of such "Knudsen layers" is not connected with the choice of space nets and fully defined by the reduced description for ensemble of particles of finite diameters in the conceptual frame of open physically small volumes, therefore – with the chosen method of measurement.

This entire complex of effects defines non-local effects in space and time. The corresponding situation is typical for the theoretical physics – we could remind about the role of probe charge in electrostatics or probe circuit in the physics of magnetic effects.

Suppose that DF f corresponds to **PhSV₁** and DF $f - \Delta f$ is connected with **PhSV₂** for Boltzmann particles. In the boundary area in the first approximation, fluctuations will be proportional to the mean free path (or, equivalently, to the mean time between the collisions). Then for **PhSV** the correction for DF should be introduced as

$$f^a = f - \tau Df / Dt \quad (1.2)$$

in the left hand side of classical BE describing the translation of DF in phase space. As the result

$$Df^a / Dt = J^B, \quad (1.3)$$

where J^B is the Boltzmann local collision integral.

Important to notice that it is only qualitative explanation of GBE derivation obtained earlier (see for example [6]) by different strict methods from the BBGKY – chain of kinetic equations. The structure of the KE_f is generally as follows

$$\frac{Df}{Dt} = J^B + J^{nonlocal}, \quad (1.4)$$

where $J^{nonlocal}$ is the non-local integral term incorporating the non-local time and space effects. The generalized Boltzmann physical kinetics, in essence, involves a local approximation

$$J^{nonlocal} = \frac{D}{Dt} \left(\tau \frac{Df}{Dt} \right) \quad (1.5)$$

for the second collision integral, here τ being the mean time *between* the particle collisions. We can draw here an analogy with the Bhatnagar - Gross - Krook (BGK) approximation for J^B ,

$$J^B = \frac{f_0 - f}{\tau}, \quad (1.6)$$

which popularity as a means to represent the Boltzmann collision integral is due to the huge simplifications it offers. In other words – the local Boltzmann collision integral admits approximation via the BGK algebraic expression, but more complicated non-local integral can be expressed as differential form (1.5). The ratio of the second to the first term on the

130 right-hand side of Eq. (1.4) is given to an order of magnitude as $J^{nonlocal}/J^B \approx O(Kn^2)$
 131 and at large Knudsen numbers (Kn defining as ratio of mean free path of particles to the
 132 character hydrodynamic length) these terms become of the same order of magnitude. It
 133 would seem that at small Knudsen numbers answering to hydrodynamic description the
 134 contribution from the second term on the right-hand side of Eq. (1.4) is negligible.
 135 *This is not the case, however.* When one goes over to the hydrodynamic
 136 approximation (by multiplying the kinetic equation by collision invariants and then integrating
 137 over velocities), the Boltzmann integral part vanishes, and the second term on the right-hand
 138 side of Eq. (1.4) gives a single-order contribution in the generalized Navier - Stokes
 139 description. Mathematically, we cannot neglect a term with a small parameter in front of the
 140 higher derivative. Physically, the appearing additional terms are due to viscosity and they
 141 correspond to the small-scale Kolmogorov turbulence [6]. The integral term $J^{nonlocal}$ turns
 142 out to be important both at small and large Knudsen numbers in the theory of transport
 143 processes. Thus, $\tau Df/Dt$ is the distribution function fluctuation, and writing Eq. (1.3)
 144 without taking into account Eq. (1.2) makes the BE non-closed. From viewpoint of the
 145 fluctuation theory, Boltzmann employed the simplest possible closure procedure $f^a = f$.
 146 Then, the additional GBE terms (as compared to the BE) are significant for any Kn,
 147 and the order of magnitude of the difference between the BE and GBE solutions is
 148 impossible to tell beforehand. For GBE the generalized H-theorem is proven [3, 6].
 149 It means that the local Boltzmann equation does not belong even to the class of
 150 minimal physical models and corresponds so to speak to "the likelihood models". This
 151 remark refers also to all consequences of the Boltzmann kinetic theory including "classical"
 152 hydrodynamics.
 153 Obviously the generalized hydrodynamic equations (GHE) will explicitly involve
 154 fluctuations proportional to τ . In the hydrodynamic approximation, the mean time τ
 155 between the collisions is related to the dynamic viscosity μ by
 156
$$\tau p = \Pi \mu, \quad (1.7)$$

 157 [13, 14]. For example, the continuity equation changes its form and will contain terms
 158 proportional to viscosity. On the other hand, if the reference volume extends over the whole
 159 cavity with the hard walls, then the classical conservation laws should be obeyed, and this is
 160 exactly what the monograph [6] proves. Now several remarks of principal significance:
 161 1. All fluctuations are found from the strict kinetic considerations and tabulated [6].
 162 The appearing additional terms in GHE are due to viscosity and they correspond to the
 163 small-scale Kolmogorov turbulence. The neglect of formally small terms is equivalent, in
 164 particular, to dropping the (small-scale) Kolmogorov turbulence from consideration and is the
 165 origin of all principal difficulties in usual turbulent theory. Fluctuations on the wall are equal to
 166 zero, from the physical point of view this fact corresponds to the laminar sub-layer.
 167 Mathematically it leads to additional boundary conditions for GHE. Major difficulties arose
 168 when the question of existence and uniqueness of solutions of the Navier - Stokes equations
 169 was addressed.
 170 O. A. Ladyzhenskaya has shown for three-dimensional flows that under smooth
 171 initial conditions a unique solution is only possible over a finite time interval. Ladyzhenskaya
 172 even introduced a "correction" into the Navier - Stokes equations in order that its unique
 173 solvability could be proved; GHE do not lead to these difficulties.
 174 2. It would appear that in continuum mechanics the idea of discreteness can be
 175 abandoned altogether and the medium under study be considered as a continuum in the
 176 literal sense of the word. Such an approach is of course possible and indeed leads to the
 177 Euler equations in hydrodynamics. However, when the viscosity and thermal conductivity
 178 effects are to be included, a totally different situation arises. As is well known, the dynamical
 179 viscosity is proportional to the mean time τ between the particle collisions, and a continuum

180 medium in the Euler model with $\tau = 0$ implies that neither viscosity nor thermal conductivity
181 is possible.

182 3. The non-local kinetic effects listed above will always be relevant to a kinetic theory
183 using one particle description – including, in particular, applications to liquids or plasmas,
184 where self-consistent forces with appropriately cut-off radius of their action are introduced to
185 expand the capability of GBE [5, 6]. Fluctuation effects occur in any open thermodynamic
186 system bounded by a control surface transparent to particles. GBE (1.3) leads to generalized
187 hydrodynamic equations [6] as the local approximation of non local effects, for example, to
188 the continuity equation

$$189 \quad \frac{\partial \rho^a}{\partial t} + \frac{\partial}{\partial \mathbf{r}} \cdot (\rho \mathbf{v}_0)^a = 0, \quad (1.8)$$

190 where ρ^a , \mathbf{v}_0^a , $(\rho \mathbf{v}_0)^a$ are calculated in view of non-locality effect in terms of gas density
191 ρ , hydrodynamic velocity of flow \mathbf{v}_0 , and density of momentum flux $\rho \mathbf{v}_0$; for locally

192 Maxwellian distribution, ρ^a , $(\rho \mathbf{v}_0)^a$ are defined by the relations

$$193 \quad (\rho - \rho^a)/\tau = \frac{\partial \rho}{\partial t} + \frac{\partial}{\partial \mathbf{r}} \cdot (\rho \mathbf{v}_0), \quad (\rho \mathbf{v}_0 - (\rho \mathbf{v}_0)^a)/\tau = \frac{\partial}{\partial t} (\rho \mathbf{v}_0) + \frac{\partial}{\partial \mathbf{r}} \cdot \rho \mathbf{v}_0 \mathbf{v}_0 + \tilde{\mathbf{I}} \cdot \frac{\partial p}{\partial \mathbf{r}} - \rho \mathbf{a},$$

194 (1.9)

195 where $\tilde{\mathbf{I}}$ is a unit tensor, and \mathbf{a} is the acceleration due to the effect of mass forces.

196 In the general case, the parameter τ is the non-locality parameter; in quantum
197 hydrodynamics, the “time-energy” uncertainty relation defines its magnitude. Obviously the
198 mentioned non-local effects can be discussed from viewpoint of breaking of the Bell’s
199 inequalities [15] because in the non-local theory the measurement (realized in \mathbf{PhSV}_1) has
200 influence on the measurement realized in the adjoining space-time point in \mathbf{PhSV}_2 and
201 verse versa.

202 The violation of Bell’s inequalities [15] is found for local statistical theories, and the
203 transition to non-local description is inevitable.

204 Notice that the application of the above principles also leads to the modification of
205 the system of Maxwell equations. While the traditional formulation of this system does not
206 involve the continuity equation, its derivation explicitly employs the equation

$$207 \quad \frac{\partial \rho^a}{\partial t} + \frac{\partial}{\partial \mathbf{r}} \cdot \mathbf{j}^a = 0, \quad (1.10)$$

208 where ρ^a is the charge per unit volume, and \mathbf{j}^a is the current density, both calculated
209 without accounting for the fluctuations. As a result, the system of Maxwell equations written
210 in the standard notation, namely

$$211 \quad \frac{\partial}{\partial \mathbf{r}} \cdot \mathbf{B} = 0, \quad \frac{\partial}{\partial \mathbf{r}} \cdot \mathbf{D} = \rho^a, \quad \frac{\partial}{\partial \mathbf{r}} \times \mathbf{E} = -\frac{\partial \mathbf{B}}{\partial t}, \quad \frac{\partial}{\partial \mathbf{r}} \times \mathbf{H} = \mathbf{j}^a + \frac{\partial \mathbf{D}}{\partial t} \quad (1.11)$$

212 contains

$$213 \quad \rho^a = \rho - \rho^{fl}, \quad \mathbf{j}^a = \mathbf{j} - \mathbf{j}^{fl}. \quad (1.12)$$

214 The ρ^{fl} , \mathbf{j}^{fl} fluctuations calculated using the generalized Boltzmann equation are given, for
215 example, in Ref. [2, 4, 6].

216 Now we can turn our attention to the quantum hydrodynamic description of individual
217 particles. The abstract of the classical Madelung’s paper [16] contains only one phrase: “It is
218 shown that the Schrödinger equation for one-electron problems can be transformed into the
219 form of hydrodynamic equations”.

220 The following conclusion of principal significance can be done from the generalized
221 quantum consideration [7, 8]:

- 222 1. Madelung's quantum hydrodynamics is equivalent to the Schrödinger equation (SE)
223 and leads to description of the quantum particle evolution in the form of Euler
224 equation and continuity equation.
- 225 2. SE is consequence of the Liouville equation as result of the local approximation of
226 non-local equations.
- 227 3. Generalized Boltzmann physical kinetics defines the strict approximation of non-
228 local effects in space and time and after transmission to the local approximation
229 leads to parameter τ , which on the quantum level corresponds to the uncertainty
230 principle "time-energy".
- 231 4. GHE lead to SE as a deep particular case of the generalized Boltzmann physical
232 kinetics and therefore of non-local hydrodynamics.

233 In principal GHE needn't in using of the "time-energy" uncertainty relation for estimation of
234 the value of the non-locality parameter τ . Moreover, the "time-energy" uncertainty relation
235 does not lead to the exact relations and from position of non-local physics is only the
236 simplest estimation of the non-local effects.

237 Really, let us consider two neighboring physically infinitely small volumes **PhSV₁**
238 and **PhSV₂** in a non-equilibrium system. Obviously the time τ should tend to diminish with
239 increasing of the velocities u of particles invading in the nearest neighboring physically
240 infinitely small volume (**PhSV₁** or **PhSV₂**):

$$241 \quad \tau = H / u^n. \quad (1.13)$$

242 However, the value τ cannot depend on the velocity direction and naturally to tie τ with the
243 particle kinetic energy, then

$$244 \quad \tau = H / mu^2, \quad (1.14)$$

245 where H is a coefficient of proportionality, which reflects the state of physical system. In the
246 simplest case H is equal to Plank constant \hbar and relation (1.14) becomes compatible with
247 the Heisenberg relation.

248 It is known that Ehrenfest adiabatic theorem is one of the most important and widely
249 studied theorems in Schrödinger quantum mechanics. It states that if we have a slowly
250 changing Hamiltonian that depends on time, and the system is prepared in one of the
251 instantaneous eigenstates of the Hamiltonian then the state of the system at any time is
252 given by an the instantaneous eigenfunction of the Hamiltonian up to multiplicative phase
253 factors [17 - 21]. Since the establishment of this theorem many fundamental results have
254 been obtained, such as Landau – Zener transition [17, 18], the Gell-Mann-Low theorem [19],
255 Berry phase [20] and holonomy [21].

256 The adiabatic theory can be naturally incorporated in generalized quantum
257 hydrodynamics based on local approximations of non-local terms. In the simplest case if
258 ΔQ is the elementary heat quantity delivered for a system executing the transfer from one
259 state (the corresponding time moment is t_{in}) to the next one (the time moment t_e) then

$$260 \quad \Delta Q = \frac{1}{\tau} 2\delta(\bar{T}\tau), \quad (1.15)$$

261 where $\tau = t_e - t_{in}$ and \bar{T} is the average kinetic energy. For adiabatic case Ehrenfest
262 supposes that

$$263 \quad 2\bar{T}\tau = \Omega_1, \Omega_2, \dots \quad (1.16)$$

264 where $\Omega_1, \Omega_2, \dots$ are adiabatic invariants. Obviously for Plank's oscillator (compare with
265 (1.14))

$$2\overline{T}\tau = nh. \quad (1.17)$$

267 *Conclusion:* adiabatic theorem and consequences of this theory deliver the general
268 quantization conditions for non-local quantum hydrodynamics.

269 Non-local physics demonstrates its high efficiency in many fields – from the atom
270 structure problems to cosmology [9, 10].

271 The possibility of the non local physics application in the theory of superconductivity
272 is investigated in [22 - 24]. It is shown that by the superconducting conditions the relay
273 ("estafette") motion of the soliton' system ("lattice ion – electron") is realizing without creation
274 of the additional chemical bonds. From the position of the quantum hydrodynamics the
275 problem of creation of the high temperature superconductors leads to finding of materials
276 which lattices could realize the soliton' motion without the soliton destruction. These
277 materials should be created using the technology of quantum dots.

278 This paper is directed on investigation of possible applications of the non-local
279 quantum hydrodynamics in the theory of transport processes in graphene including the
280 effects of the charge density waves (CDW). Is known that graphene, a single-atom-thick
281 sheet of graphite, is a new material which combines aspects of semiconductors and metals.
282 For example the mobility, a measure of how well a material conducts electricity, is higher
283 than for other known material at room temperature. In graphene, a resistivity is of about 1.0
284 microOhm-cm (resistivity defined as a specific measure of resistance; the resistance of a
285 piece material is its resistivity times its length and divided by its cross-sectional area). This is
286 about 35 percent less than the resistivity of copper, the lowest resistivity material known at
287 room temperature.

288 Measurements lead to conclusion that the influence of thermal vibrations on the
289 conduction of electrons in graphene is extraordinarily small. From the other side the typical
290 reasoning exists:

291 "In any material, the energy associated with the temperature of the material causes
292 the atoms of the material to vibrate in place. As electrons travel through the material, they
293 can bounce off these vibrating atoms, giving rise to electrical resistance. This electrical
294 resistance is "intrinsic" to the material: it cannot be eliminated unless the material is cooled
295 to absolute zero temperature, and hence sets the upper limit to how well a material can
296 conduct electricity."

297 Obviously this point of view leads to the principal elimination of effects of the high
298 temperature superconductivity. From the mentioned point of view the restrictions in mobilities
299 of known semiconductors can be explained as the influence of the thermal vibration of the
300 atoms. The limit to mobility of electrons in graphene is about $200,000 \text{ cm}^2 / (V \cdot s)$ at room
301 temperature, compared to about $1,400 \text{ cm}^2 / (V \cdot s)$ in silicon, and $77,000 \text{ cm}^2 / (V \cdot s)$ in
302 indium antimonide, the highest mobility conventional semiconductor known. The opinion of a
303 part of investigators can be formulated as follows: "Other extrinsic sources in today's fairly
304 dirty graphene samples add some extra resistivity to graphene," (see for example [25]) "so
305 the overall resistivity isn't quite as low as copper's at room temperature yet. However,
306 graphene has far fewer electrons than copper, so in graphene the electrical current is carried
307 by only a few electrons moving much faster than the electrons in copper." Mobility
308 determines the speed at which an electronic device (for instance, a field-effect transistor,
309 which forms the basis of modern computer chips) can turn on and off. The very high mobility
310 makes graphene promising for applications in which transistors much switch extremely fast,
311 such as in processing extremely high frequency signals. The low resistivity and extremely
312 thin nature of graphene also promises applications in thin, mechanically tough, electrically
313 conducting, transparent films. Such films are sorely needed in a variety of electronics
314 applications from touch screens to photovoltaic cells.

In the last years the direct observation of the atomic structures of superconducting materials (as usual superconducting materials in the cuprate family like $\text{YBa}_2\text{Cu}_3\text{O}_{6.67}$ ($T_c = 67\text{ K}$)) was realized with the scanning tunneling microscope (STM) and other instruments, STMs scan a surface in steps smaller than an atom.

Superconductivity, in which an electric current flows with zero resistance, was first discovered in metals cooled very close to absolute zero. New materials called cuprates - copper oxides "doped" with other atoms -- superconduct as "high" as minus 123 Celsius. Some conclusions from direct observations [26, 27]:

1. Observations of high-temperature superconductors show an "energy gap" where electronic states are missing. Sometimes this energy gap appears but the material still does not superconduct - a so-called "pseudogap" phase. The pseudogap appears at higher temperatures than any superconductivity, offering the promise of someday developing materials that would superconduct at or near room temperature.

2. STM image of a partially doped cuprate superconductor shows regions with an electronic "pseudogap". As doping increases, pseudogap regions spread and connect, making the whole sample a superconductor.

3. High temperature superconductivity in layered cuprates can develop from an electronically ordered state called a charge density wave (CDW). The results of observation can be interpreted as the creation of the "checkerboard pattern" due to the modulation of the atomic positions in the CuO_2 layers of $\text{YBa}_2\text{Cu}_3\text{O}_{6+x}$ caused by the charge density wave.

4. Application of the method of high-energy X-ray diffraction shows that a CDW develops at zero field in the normal state of superconducting $\text{YBa}_2\text{Cu}_3\text{O}_{6.67}$ ($T_c = 67\text{ K}$). Below T_c the application of a magnetic field suppresses superconductivity and enhances the CDW. It means that the high- T_c superconductivity forms from a pre-existing CDW environment.

Important conclusion: high temperature superconductors demonstrate new type of electronic order and modulation of atomic positions. As it was shown in [22, 24] the mentioned above graphene properties can be explained only in the frame of the self-consistent non-local quantum theory (see for example [7, 8]) which leads to appearance of the soliton waves moving in graphene.

2. GENERALIZED QUANTUM HYDRODYNAMIC EQUATIONS

Strict consideration leads to the following system of the generalized quantum hydrodynamic equations (GHE) [6] written in the dimensional generalized Euler form: Continuity equation for species α :

$$\frac{\partial}{\partial t} \left\{ \rho_\alpha - \tau_\alpha \left[\frac{\partial \rho_\alpha}{\partial t} + \frac{\partial}{\partial \mathbf{r}} \cdot (\rho_\alpha \mathbf{v}_0) \right] \right\} + \frac{\partial}{\partial \mathbf{r}} \cdot \left\{ \rho_\alpha \mathbf{v}_0 - \tau_\alpha \left[\frac{\partial}{\partial t} (\rho_\alpha \mathbf{v}_0) + \frac{\partial}{\partial \mathbf{r}} \cdot (\rho_\alpha \mathbf{v}_0 \mathbf{v}_0) + \tilde{\mathbf{I}} \cdot \frac{\partial \rho_\alpha}{\partial \mathbf{r}} - \rho_\alpha \mathbf{F}_\alpha^{(1)} - \frac{q_\alpha}{m_\alpha} \rho_\alpha \mathbf{v}_0 \times \mathbf{B} \right] \right\} = R_\alpha, \quad (2.1)$$

and continuity equation for mixture

$$\frac{\partial}{\partial t} \left\{ \rho - \sum_\alpha \tau_\alpha \left[\frac{\partial \rho_\alpha}{\partial t} + \frac{\partial}{\partial \mathbf{r}} \cdot (\rho_\alpha \mathbf{v}_0) \right] \right\} + \frac{\partial}{\partial \mathbf{r}} \cdot \left\{ \rho \mathbf{v}_0 - \sum_\alpha \tau_\alpha \left[\frac{\partial}{\partial t} (\rho_\alpha \mathbf{v}_0) + \frac{\partial}{\partial \mathbf{r}} \cdot (\rho_\alpha \mathbf{v}_0 \mathbf{v}_0) + \tilde{\mathbf{I}} \cdot \frac{\partial \rho_\alpha}{\partial \mathbf{r}} - \rho_\alpha \mathbf{F}_\alpha^{(1)} - \frac{q_\alpha}{m_\alpha} \rho_\alpha \mathbf{v}_0 \times \mathbf{B} \right] \right\} = 0. \quad (2.2)$$

354
355

Momentum equation for species

356

$$\begin{aligned}
 & \frac{\partial}{\partial t} \left\{ \rho_\alpha \mathbf{v}_0 - \tau_\alpha \left[\frac{\partial}{\partial t} (\rho_\alpha \mathbf{v}_0) + \frac{\partial}{\partial \mathbf{r}} \cdot \rho_\alpha \mathbf{v}_0 \mathbf{v}_0 + \frac{\partial p_\alpha}{\partial \mathbf{r}} - \rho_\alpha \mathbf{F}_\alpha^{(1)} - \right. \right. \\
 & \left. \left. \frac{q_\alpha}{m_\alpha} \rho_\alpha \mathbf{v}_0 \times \mathbf{B} \right] \right\} - \mathbf{F}_\alpha^{(1)} \left[\rho_\alpha - \tau_\alpha \left(\frac{\partial \rho_\alpha}{\partial t} + \frac{\partial}{\partial \mathbf{r}} (\rho_\alpha \mathbf{v}_0) \right) \right] - \\
 & \frac{q_\alpha}{m_\alpha} \left\{ \rho_\alpha \mathbf{v}_0 - \tau_\alpha \left[\frac{\partial}{\partial t} (\rho_\alpha \mathbf{v}_0) + \frac{\partial}{\partial \mathbf{r}} \cdot \rho_\alpha \mathbf{v}_0 \mathbf{v}_0 + \frac{\partial p_\alpha}{\partial \mathbf{r}} - \rho_\alpha \mathbf{F}_\alpha^{(1)} - \right. \right. \\
 & \left. \left. \frac{q_\alpha}{m_\alpha} \rho_\alpha \mathbf{v}_0 \times \mathbf{B} \right] \right\} \times \mathbf{B} + \frac{\partial}{\partial \mathbf{r}} \cdot \left\{ \rho_\alpha \mathbf{v}_0 \mathbf{v}_0 + p_\alpha \tilde{\mathbf{I}} - \tau_\alpha \left[\frac{\partial}{\partial t} (\rho_\alpha \mathbf{v}_0 \mathbf{v}_0 + \right. \right. \\
 & \left. \left. p_\alpha \tilde{\mathbf{I}}) + \frac{\partial}{\partial \mathbf{r}} \cdot \rho_\alpha (\mathbf{v}_0 \mathbf{v}_0) \mathbf{v}_0 + 2 \tilde{\mathbf{I}} \left(\frac{\partial}{\partial \mathbf{r}} \cdot (p_\alpha \mathbf{v}_0) \right) + \frac{\partial}{\partial \mathbf{r}} \cdot (\tilde{\mathbf{I}} p_\alpha \mathbf{v}_0) - \right. \right. \\
 & \left. \left. \mathbf{F}_\alpha^{(1)} \rho_\alpha \mathbf{v}_0 - \rho_\alpha \mathbf{v}_0 \mathbf{F}_\alpha^{(1)} - \frac{q_\alpha}{m_\alpha} \rho_\alpha [\mathbf{v}_0 \times \mathbf{B}] \mathbf{v}_0 - \frac{q_\alpha}{m_\alpha} \rho_\alpha \mathbf{v}_0 [\mathbf{v}_0 \times \mathbf{B}] \right] \right\} = \\
 & \int m_\alpha \mathbf{v}_\alpha J_\alpha^{st,el} d\mathbf{v}_\alpha + \int m_\alpha \mathbf{v}_\alpha J_\alpha^{st,incl} d\mathbf{v}_\alpha.
 \end{aligned} \tag{2.3}$$

357
358
359

Generalized moment equation for mixture

360

$$\begin{aligned}
 & \frac{\partial}{\partial t} \left\{ \rho \mathbf{v}_0 - \sum_\alpha \tau_\alpha \left[\frac{\partial}{\partial t} (\rho_\alpha \mathbf{v}_0) + \frac{\partial}{\partial \mathbf{r}} \cdot \rho_\alpha \mathbf{v}_0 \mathbf{v}_0 + \frac{\partial p_\alpha}{\partial \mathbf{r}} - \rho_\alpha \mathbf{F}_\alpha^{(1)} - \right. \right. \\
 & \left. \left. \frac{q_\alpha}{m_\alpha} \rho_\alpha \mathbf{v}_0 \times \mathbf{B} \right] \right\} - \sum_\alpha \mathbf{F}_\alpha^{(1)} \left[\rho_\alpha - \tau_\alpha \left(\frac{\partial \rho_\alpha}{\partial t} + \frac{\partial}{\partial \mathbf{r}} (\rho_\alpha \mathbf{v}_0) \right) \right] - \\
 & \sum_\alpha \frac{q_\alpha}{m_\alpha} \left\{ \rho_\alpha \mathbf{v}_0 - \tau_\alpha^{(0)} \left[\frac{\partial}{\partial t} (\rho_\alpha \mathbf{v}_0) + \frac{\partial}{\partial \mathbf{r}} \cdot \rho_\alpha \mathbf{v}_0 \mathbf{v}_0 + \frac{\partial p_\alpha}{\partial \mathbf{r}} - \rho_\alpha \mathbf{F}_\alpha^{(1)} - \right. \right. \\
 & \left. \left. \frac{q_\alpha}{m_\alpha} \rho_\alpha \mathbf{v}_0 \times \mathbf{B} \right] \right\} \times \mathbf{B} + \frac{\partial}{\partial \mathbf{r}} \cdot \left\{ \rho \mathbf{v}_0 \mathbf{v}_0 + p \tilde{\mathbf{I}} - \sum_\alpha \tau_\alpha \left[\frac{\partial}{\partial t} (\rho_\alpha \mathbf{v}_0 \mathbf{v}_0 + \right. \right. \\
 & \left. \left. p_\alpha \tilde{\mathbf{I}}) + \frac{\partial}{\partial \mathbf{r}} \cdot \rho_\alpha (\mathbf{v}_0 \mathbf{v}_0) \mathbf{v}_0 + 2 \tilde{\mathbf{I}} \left(\frac{\partial}{\partial \mathbf{r}} \cdot (p_\alpha \mathbf{v}_0) \right) + \frac{\partial}{\partial \mathbf{r}} \cdot (\tilde{\mathbf{I}} p_\alpha \mathbf{v}_0) - \right. \right. \\
 & \left. \left. \mathbf{F}_\alpha^{(1)} \rho_\alpha \mathbf{v}_0 - \rho_\alpha \mathbf{v}_0 \mathbf{F}_\alpha^{(1)} - \frac{q_\alpha}{m_\alpha} \rho_\alpha [\mathbf{v}_0 \times \mathbf{B}] \mathbf{v}_0 - \frac{q_\alpha}{m_\alpha} \rho_\alpha \mathbf{v}_0 [\mathbf{v}_0 \times \mathbf{B}] \right] \right\} = 0
 \end{aligned} \tag{2.4}$$

361
362
363

364 Energy equation for component

365

366

367

368

$$\begin{aligned}
 & \frac{\partial}{\partial t} \left\{ \frac{\rho_\alpha v_0^2}{2} + \frac{3}{2} p_\alpha + \varepsilon_\alpha n_\alpha - \tau_\alpha \left[\frac{\partial}{\partial t} \left(\frac{\rho_\alpha v_0^2}{2} + \frac{3}{2} p_\alpha + \varepsilon_\alpha n_\alpha \right) + \right. \right. \\
 & \left. \left. \frac{\partial}{\partial \mathbf{r}} \cdot \left(\frac{1}{2} \rho_\alpha v_0^2 \mathbf{v}_0 + \frac{5}{2} p_\alpha \mathbf{v}_0 + \varepsilon_\alpha n_\alpha \mathbf{v}_0 \right) - \mathbf{F}_\alpha^{(1)} \cdot \rho_\alpha \mathbf{v}_0 \right] \right\} + \\
 & \frac{\partial}{\partial \mathbf{r}} \cdot \left\{ \frac{1}{2} \rho_\alpha v_0^2 \mathbf{v}_0 + \frac{5}{2} p_\alpha \mathbf{v}_0 + \varepsilon_\alpha n_\alpha \mathbf{v}_0 - \tau_\alpha \left[\frac{\partial}{\partial t} \left(\frac{1}{2} \rho_\alpha v_0^2 \mathbf{v}_0 + \right. \right. \right. \\
 & \left. \left. \frac{5}{2} p_\alpha \mathbf{v}_0 + \varepsilon_\alpha n_\alpha \mathbf{v}_0 \right) + \frac{\partial}{\partial \mathbf{r}} \cdot \left(\frac{1}{2} \rho_\alpha v_0^2 \mathbf{v}_0 \mathbf{v}_0 + \frac{7}{2} p_\alpha \mathbf{v}_0 \mathbf{v}_0 + \frac{1}{2} p_\alpha v_0^2 \tilde{\mathbf{I}} + \right. \right. \\
 & \left. \left. \frac{5}{2} \frac{p_\alpha^2}{\rho_\alpha} \tilde{\mathbf{I}} + \varepsilon_\alpha n_\alpha \mathbf{v}_0 \mathbf{v}_0 + \varepsilon_\alpha \frac{p_\alpha}{m_\alpha} \tilde{\mathbf{I}} \right) - \rho_\alpha \mathbf{F}_\alpha^{(1)} \cdot \mathbf{v}_0 \mathbf{v}_0 - p_\alpha \mathbf{F}_\alpha^{(1)} \cdot \tilde{\mathbf{I}} - \right. \\
 & \left. \frac{1}{2} \rho_\alpha v_0^2 \mathbf{F}_\alpha^{(1)} - \frac{3}{2} \mathbf{F}_\alpha^{(1)} p_\alpha - \frac{\rho_\alpha v_0^2}{2} \frac{q_\alpha}{m_\alpha} [\mathbf{v}_0 \times \mathbf{B}] - \frac{5}{2} p_\alpha \frac{q_\alpha}{m_\alpha} [\mathbf{v}_0 \times \mathbf{B}] - \right. \\
 & \left. \left. \varepsilon_\alpha n_\alpha \frac{q_\alpha}{m_\alpha} [\mathbf{v}_0 \times \mathbf{B}] - \varepsilon_\alpha n_\alpha \mathbf{F}_\alpha^{(1)} \right] \right\} - \left\{ \rho_\alpha \mathbf{F}_\alpha^{(1)} \cdot \mathbf{v}_0 - \tau_\alpha \left[\mathbf{F}_\alpha^{(1)} \cdot \right. \right. \\
 & \left. \left. \left(\frac{\partial}{\partial t} (\rho_\alpha \mathbf{v}_0) + \frac{\partial}{\partial \mathbf{r}} \cdot \rho_\alpha \mathbf{v}_0 \mathbf{v}_0 + \frac{\partial}{\partial \mathbf{r}} \cdot p_\alpha \tilde{\mathbf{I}} - \rho_\alpha \mathbf{F}_\alpha^{(1)} - q_\alpha n_\alpha [\mathbf{v}_0 \times \mathbf{B}] \right) \right] \right\} = \quad (2.5) \\
 & \int \left(\frac{m_\alpha v_\alpha^2}{2} + \varepsilon_\alpha \right) J_\alpha^{st,el} d\mathbf{v}_\alpha + \int \left(\frac{m_\alpha v_\alpha^2}{2} + \varepsilon_\alpha \right) J_\alpha^{st,incl} d\mathbf{v}_\alpha.
 \end{aligned}$$

$$\begin{aligned}
& \frac{\partial}{\partial t} \left\{ \frac{\rho v_0^2}{2} + \frac{3}{2} p + \sum_{\alpha} \varepsilon_{\alpha} n_{\alpha} - \sum_{\alpha} \tau_{\alpha} \left[\frac{\partial}{\partial t} \left(\frac{\rho_{\alpha} v_0^2}{2} + \frac{3}{2} p_{\alpha} + \varepsilon_{\alpha} n_{\alpha} \right) + \right. \right. \\
& \left. \left. \frac{\partial}{\partial \mathbf{r}} \cdot \left(\frac{1}{2} \rho_{\alpha} v_0^2 \mathbf{v}_0 + \frac{5}{2} p_{\alpha} \mathbf{v}_0 + \varepsilon_{\alpha} n_{\alpha} \mathbf{v}_0 \right) - \mathbf{F}_{\alpha}^{(1)} \cdot \rho_{\alpha} \mathbf{v}_0 \right] \right\} + \\
& \frac{\partial}{\partial \mathbf{r}} \cdot \left\{ \frac{1}{2} \rho v_0^2 \mathbf{v}_0 + \frac{5}{2} p \mathbf{v}_0 + \mathbf{v}_0 \sum_{\alpha} \varepsilon_{\alpha} n_{\alpha} - \sum_{\alpha} \tau_{\alpha} \left[\frac{\partial}{\partial t} \left(\frac{1}{2} \rho_{\alpha} v_0^2 \mathbf{v}_0 + \right. \right. \right. \\
& \left. \left. \frac{5}{2} p_{\alpha} \mathbf{v}_0 + \varepsilon_{\alpha} n_{\alpha} \mathbf{v}_0 \right) + \frac{\partial}{\partial \mathbf{r}} \cdot \left(\frac{1}{2} \rho_{\alpha} v_0^2 \mathbf{v}_0 \mathbf{v}_0 + \frac{7}{2} p_{\alpha} \mathbf{v}_0 \mathbf{v}_0 + \frac{1}{2} p_{\alpha} v_0^2 \tilde{\mathbf{I}} + \right. \right. \\
& \left. \left. \frac{5}{2} \frac{p_{\alpha}^2}{\rho_{\alpha}} \tilde{\mathbf{I}} + \varepsilon_{\alpha} n_{\alpha} \mathbf{v}_0 \mathbf{v}_0 + \varepsilon_{\alpha} \frac{p_{\alpha}}{m_{\alpha}} \tilde{\mathbf{I}} \right) - \rho_{\alpha} \mathbf{F}_{\alpha}^{(1)} \cdot \mathbf{v}_0 \mathbf{v}_0 - p_{\alpha} \mathbf{F}_{\alpha}^{(1)} \cdot \tilde{\mathbf{I}} - \right. \\
& \left. \frac{1}{2} \rho_{\alpha} v_0^2 \mathbf{F}_{\alpha}^{(1)} - \frac{3}{2} \mathbf{F}_{\alpha}^{(1)} p_{\alpha} - \frac{\rho_{\alpha} v_0^2}{2} \frac{q_{\alpha}}{m_{\alpha}} [\mathbf{v}_0 \times \mathbf{B}] - \frac{5}{2} p_{\alpha} \frac{q_{\alpha}}{m_{\alpha}} [\mathbf{v}_0 \times \mathbf{B}] - \right. \\
& \left. \varepsilon_{\alpha} n_{\alpha} \frac{q_{\alpha}}{m_{\alpha}} [\mathbf{v}_0 \times \mathbf{B}] - \varepsilon_{\alpha} n_{\alpha} \mathbf{F}_{\alpha}^{(1)} \right] \right\} - \mathbf{v}_0 \cdot \sum_{\alpha} \rho_{\alpha} \mathbf{F}_{\alpha}^{(1)} + \\
& \sum_{\alpha} \tau_{\alpha} \mathbf{F}_{\alpha}^{(1)} \cdot \left[\frac{\partial}{\partial t} (\rho_{\alpha} \mathbf{v}_0) + \frac{\partial}{\partial \mathbf{r}} \cdot \rho_{\alpha} \mathbf{v}_0 \mathbf{v}_0 + \frac{\partial}{\partial \mathbf{r}} \cdot p_{\alpha} \tilde{\mathbf{I}} - \rho_{\alpha} \mathbf{F}_{\alpha}^{(1)} - q_{\alpha} n_{\alpha} [\mathbf{v}_0 \times \mathbf{B}] \right] = 0.
\end{aligned}$$

(2.6)

Here $\mathbf{F}_{\alpha}^{(1)}$ are the forces of the non-magnetic origin, \mathbf{B} - magnetic induction, $\tilde{\mathbf{I}}$ - unit tensor, q_{α} - charge of the α -component particle, p_{α} - static pressure for α -component, ε_{α} - internal energy for the particles of α -component, \mathbf{v}_0 - hydrodynamic velocity for mixture. For calculations in the self-consistent electro-magnetic field the system of non-local Maxwell equations should be added (see (1.11), (1.12)).

It is well known that basic Schrödinger equation (SE) of quantum mechanics firstly was introduced as a quantum mechanical postulate. The obvious next step should be done and was realized by E. Madelung in 1927 – the derivation of special hydrodynamic form of SE after introduction wave function Ψ as

$$\Psi(x, y, z, t) = \alpha(x, y, z, t) e^{i\beta(x, y, z, t)}. \quad (2.7)$$

Using (2.7) and separating the real and imagine parts of SE one obtains

$$\frac{\partial \alpha^2}{\partial t} + \frac{\partial}{\partial \mathbf{r}} \cdot \left(\frac{\alpha^2 \hbar}{m} \frac{\partial \beta}{\partial \mathbf{r}} \right) = 0, \quad (2.8)$$

and Eq. (2.8) immediately transforms in continuity equation if the identifications in the Madelung's notations for density ρ and velocity \mathbf{v}

$$\rho = \alpha^2 = \Psi \Psi^*, \quad (2.9)$$

$$\mathbf{v} = \frac{\partial}{\partial \mathbf{r}} (\beta \hbar / m) \quad (2.10)$$

388 introduce in Eq. (2.8). Identification for velocity (2.10) is obvious because for 1D flow
 389

$$390 \quad v = \frac{\partial}{\partial x} (\beta \hbar / m) = \frac{\hbar}{m} \frac{\partial}{\partial x} \left[-\frac{1}{\hbar} (E_k t - px) \right] = \frac{1}{m} \frac{\partial}{\partial x} (px) = v_\phi, \quad (2.11)$$

391 where v_ϕ is phase velocity. The existence of the condition (2.10) means that the
 392 corresponding flow has potential

$$393 \quad \Phi = \beta \hbar / m. \quad (2.12)$$

394 As result two effective hydrodynamic equations take place:

$$395 \quad \frac{\partial \rho}{\partial t} + \frac{\partial}{\partial \mathbf{r}} \cdot (\rho \mathbf{v}) = 0, \quad (2.13)$$

$$396 \quad \frac{\partial \mathbf{v}}{\partial t} + \frac{1}{2} \frac{\partial}{\partial \mathbf{r}} v^2 = -\frac{1}{m} \frac{\partial}{\partial \mathbf{r}} \left(U - \frac{\hbar^2}{2m} \frac{\Delta \alpha}{\alpha} \right). \quad (2.14)$$

397 But

$$398 \quad \frac{\Delta \alpha}{\alpha} = \frac{\Delta \alpha^2}{2\alpha^2} - \frac{1}{\alpha^2} \left(\frac{\partial \alpha}{\partial \mathbf{r}} \right)^2, \quad (2.15)$$

399 and the relation (2.15) transforms (2.14) in particular case of the Euler motion equation

$$400 \quad \frac{\partial \mathbf{v}}{\partial t} + (\mathbf{v} \cdot \frac{\partial}{\partial \mathbf{r}}) \mathbf{v} = -\frac{1}{m} \frac{\partial}{\partial \mathbf{r}} U^*, \quad (2.16)$$

401 where introduced the efficient potential

$$402 \quad U^* = U - \frac{\hbar^2}{4m\rho} \left[\Delta \rho - \frac{1}{2\rho} \left(\frac{\partial \rho}{\partial \mathbf{r}} \right)^2 \right]. \quad (2.17)$$

403 Additive quantum part of potential can be written in the so called Bohm form

$$404 \quad \frac{\hbar^2}{2m\sqrt{\rho}} \Delta \sqrt{\rho} = \frac{\hbar^2}{4m\rho} \left[\Delta \rho - \frac{1}{2\rho} \left(\frac{\partial \rho}{\partial \mathbf{r}} \right)^2 \right]. \quad (2.18)$$

405 Then

$$406 \quad U^* = U + U_{qu} = U - \frac{\hbar^2}{2m\sqrt{\rho}} \Delta \sqrt{\rho} = U - \frac{\hbar^2}{4m\rho} \left[\Delta \rho - \frac{1}{2\rho} \left(\frac{\partial \rho}{\partial \mathbf{r}} \right)^2 \right]. \quad (2.19)$$

407 Some remarks:

- 408 a) SE transforms in hydrodynamic form without additional assumptions. But numerical
 409 methods of hydrodynamics are very good developed. As result at the end of seventieth
 410 of the last century we realized the systematic calculations of quantum problems using
 411 quantum hydrodynamics (see for example [1, 28].
- 412 b) SE reduces to the system of continuity equation and particular case of the Euler
 413 equation with the additional potential proportional to \hbar^2 . The physical sense and the
 414 origin of the Bohm potential are established later in [7, 8, 29].
- 415 c) SE (obtained in the frame of the theory of classical complex variables) cannot contain
 416 the energy equation in principle. As result in many cases the palliative approach is used
 417 when for solution of dissipative quantum problems the classical hydrodynamics is used
 418 with insertion of additional Bohm potential in the system of hydrodynamic equations.
- 419 d) The system of the generalized quantum hydrodynamic equations contains energy
 420 equation written for unknown dependent value which can be specified as quantum
 421 pressure p_α of non-local origin.

422 The transport properties in graphene can be described at low energies by a
 423 massless Dirac-fermion model with chiral quasiparticles [30, 31]. The Boltzmann and
 424 Schrödinger approaches are used also [32], [33]. Applications of these approaches are
 425 directed on the calculation of kinetic coefficients. The non-local kinetic equations also are
 426 used by the authors of this article for calculation of graphene electrical conductivity [34].
 427 Here we intend to investigate the possibilities of non-local quantum hydrodynamics for
 428 modeling of the charge density waves in graphene. In non-local quantum hydrodynamics the
 429 many particles correlations manifest itself in equations in the terms proportional to non-
 430 locality parameter τ .

431 The influence of spin and magnetic moment of particles can be taken into account
 432 by the natural elegant way via the internal energy of particles. Really for example electron
 433 has the internal energy \mathcal{E}

$$434 \quad \mathcal{E} = \mathcal{E}_{el,sp} + \mathcal{E}_{el,m}, \quad (2.20)$$

435 containing the spin and magnetic parts, namely

$$437 \quad \mathcal{E}_{el,sp} = \hbar\omega/2, \quad \mathcal{E}_{el,m} = -\mathbf{p}_m \cdot \mathbf{B}; \quad (2.21)$$

438 \mathbf{p}_m - electron magnetic moment, \mathbf{B} - magnetic induction. But $p_m = -\frac{e}{m_e} \frac{\hbar}{2c}$, then

439 $\mathcal{E}_{el} = \frac{\hbar}{2} \omega_{eff}$. Relation (2.20) can be written as

$$440 \quad \mathcal{E} = \frac{\hbar}{2} \left[\omega \pm \frac{e}{m_e c} B \right], \quad (2.22)$$

441 if \mathbf{B} is directed along the spin direction. On this stage of investigations we omit the influence
 442 of the internal energy of particles, therefore spin waves will be investigated separately.

443
 444

445 3. GENERALIZED QUANTUM HYDRODYNAMIC EQUATIONS DESCRIBING THE 446 SOLITON MOVEMENT IN THE CRISTAL LATTICE

447

448 Let us consider the charge density waves which are periodic modulation of
 449 conduction electron density. From direct observations of charge density waves follow that
 450 CDW develop at zero external fields. For our aims is sufficient in the following to suppose
 451 that the effective charge movement was created in graphene lattice as result of an initial
 452 fluctuation.

453 The movement of the soliton waves at the presence of the external electrical
 454 potential difference will be considered also in this article.

455 The effective charge is created due to interference of the induced electron waves
 456 and correlating potentials as result of the polarized modulation of atomic positions. Therefore
 457 in this approach the conduction in graphene convoys the transfer of the positive (+e, m_p)

458 and negative (-e, m_e) charges. Let us formulate the problem in detail. The non-stationary 1D
 459 motion of the combined soliton is considered under influence of the self-consistent electric
 460 forces of the potential and non-potential origin. It was shown [22 - 24] that mentioned soliton
 461 can exists without a chemical bond formation. First of all for better understanding of the
 462 situation let us investigate the situation for the case when the external forces are absent.
 463 Introduce the coordinate system ($\xi = x - Ct$) moving along the positive direction of the x
 464 axis with the velocity $C = u_0$, which is equal to the phase velocity of this quantum object.

Let us find the soliton type solutions for the system of the generalized quantum equations for two species mixture. The graphene crystal lattice is 2D flat structure which is considered in the moving coordinate system ($\xi = x - u_0 t$, y). In the following we intend (without taking into account the component's internal energy) to apply generalized non-local quantum hydrodynamic equations (2.1) – (2.6) to the investigation of the charge density waves (CDW) in the frame of two species model which led to the following dimensional equations [6, 8]:

Poisson equation for the self-consistent electric field:

$$\frac{\partial^2 \phi}{\partial \xi^2} + \frac{\partial^2 \phi}{\partial y^2} = -4\pi e \left\{ \left[n_p - \tau_p \frac{\partial}{\partial \xi} (n_p (u - u_0)) \right] - \left[n_e - \tau_e \frac{\partial}{\partial \xi} (n_e (u - u_0)) \right] \right\} \quad (3.1)$$

Continuity equation for the positive particles:

$$\begin{aligned} & \frac{\partial}{\partial \xi} [\rho_p (u_0 - u)] + \frac{\partial}{\partial \xi} \left\{ \tau_p \frac{\partial}{\partial \xi} [\rho_p (u - u_0)^2] \right\} + \\ & \frac{\partial}{\partial \xi} \left\{ \tau_p \left[\frac{\partial}{\partial \xi} p_p - \rho_p F_{p\xi} \right] \right\} + \frac{\partial}{\partial y} \left\{ \tau_p \left[\frac{\partial}{\partial y} p_p - \rho_p F_{py} \right] \right\} = 0 \end{aligned} \quad (3.2)$$

Continuity equation for electrons:

$$\begin{aligned} & \frac{\partial}{\partial \xi} [\rho_e (u_0 - u)] + \frac{\partial}{\partial \xi} \left\{ \tau_e \frac{\partial}{\partial \xi} [\rho_e (u - u_0)^2] \right\} + \\ & \frac{\partial}{\partial \xi} \left\{ \tau_e \left[\frac{\partial}{\partial \xi} p_e - \rho_e F_{e\xi} \right] \right\} + \frac{\partial}{\partial y} \left\{ \tau_e \left[\frac{\partial}{\partial y} p_e - \rho_e F_{ey} \right] \right\} = 0 \end{aligned} \quad (3.3)$$

Momentum equation for the x direction:

$$\begin{aligned} & \frac{\partial}{\partial \xi} \{ \rho u (u - u_0) + p \} - \rho_p F_{p\xi} - \rho_e F_{e\xi} + \\ & \frac{\partial}{\partial \xi} \left\{ \tau_p \left[\frac{\partial}{\partial \xi} (2 p_p (u_0 - u) - \rho_p u (u_0 - u)^2) - \rho_p F_{p\xi} (u_0 - u) \right] \right\} + \\ & \frac{\partial}{\partial \xi} \left\{ \tau_e \left[\frac{\partial}{\partial \xi} (2 p_e (u_0 - u) - \rho_e u (u_0 - u)^2) - \rho_e F_{e\xi} (u_0 - u) \right] \right\} + \\ & \tau_p F_{p\xi} \left(\frac{\partial}{\partial \xi} (\rho_p (u - u_0)) \right) + \tau_e F_{e\xi} \left(\frac{\partial}{\partial \xi} (\rho_e (u - u_0)) \right) - \\ & \frac{\partial}{\partial \xi} \left\{ \tau_p \frac{\partial}{\partial \xi} (p_p u) \right\} - \frac{\partial}{\partial \xi} \left\{ \tau_e \frac{\partial}{\partial \xi} (p_e u) \right\} - \frac{\partial}{\partial y} \left\{ \tau_p \frac{\partial}{\partial y} (p_p u) \right\} - \frac{\partial}{\partial y} \left\{ \tau_e \frac{\partial}{\partial y} (p_e u) \right\} + \\ & \frac{\partial}{\partial \xi} \{ \tau_p [F_{p\xi} \rho_p u] \} + \frac{\partial}{\partial \xi} \{ \tau_e [F_{e\xi} \rho_e u] \} + \frac{\partial}{\partial y} \{ \tau_p [F_{py} \rho_p u] \} + \frac{\partial}{\partial y} \{ \tau_e [F_{ey} \rho_e u] \} = 0 \end{aligned} \quad (3.4)$$

Energy equation for the positive particles:

$$\begin{aligned}
& \frac{\partial}{\partial \xi} \left[\rho_p u^2 (u - u_0) + 5 p_p u - 3 p_p u_0 \right] - 2 \rho_p F_{p\xi} u + \\
& \frac{\partial}{\partial \xi} \left\{ \tau_p \left[\frac{\partial}{\partial \xi} \left(-\rho_p u^2 (u_0 - u)^2 + 7 p_p u (u_0 - u) + 3 p_p u_0 (u - u_0) - p_p u^2 - 5 \frac{p_p^2}{\rho_p} \right) - \right. \right. \\
& \quad \left. \left. - 2 F_{p\xi} \rho_p u (u_0 - u) + \rho_p u^2 F_{p\xi} + 5 p_p F_{p\xi} \right] \right\} - \\
& \frac{\partial}{\partial y} \left\{ \tau_p \left[\frac{\partial}{\partial y} \left(p_p u^2 + 5 \frac{p_p^2}{\rho_p} \right) - \rho_p F_{py} u^2 - 5 p_p F_{py} \right] \right\} - \\
& 2 \tau_p F_{p\xi} \left[\frac{\partial}{\partial \xi} (\rho_p u (u_0 - u)) \right] - 2 \tau_p \rho_p \left[(F_{p\xi})^2 + (F_{py})^2 \right] + \\
& 2 \tau_p F_{p\xi} \left[\frac{\partial}{\partial \xi} p_p \right] + 2 \tau_p F_{py} \left[\frac{\partial}{\partial y} p_p \right] = - \frac{p_p - p_e}{\tau_{ep}} \quad (3.5)
\end{aligned}$$

488
489
490

Energy equation for electrons:

$$\begin{aligned}
& \frac{\partial}{\partial \xi} \left[\rho_e u^2 (u - u_0) + 5 p_e u - 3 p_e u_0 \right] - 2 \rho_e F_{e\xi} u + \\
& \frac{\partial}{\partial \xi} \left\{ \tau_e \left[\frac{\partial}{\partial \xi} \left(-\rho_e u^2 (u_0 - u)^2 + 7 p_e u (u_0 - u) + 3 p_e u_0 (u - u_0) - p_e u^2 - 5 \frac{p_e^2}{\rho_e} \right) - \right. \right. \\
& \quad \left. \left. - 2 F_{e\xi} \rho_e u (u_0 - u) + \rho_e u^2 F_{e\xi} + 5 p_e F_{e\xi} \right] \right\} - \\
& \frac{\partial}{\partial y} \left\{ \tau_e \left[\frac{\partial}{\partial y} \left(p_e u^2 + 5 \frac{p_e^2}{\rho_e} \right) - \rho_e F_{ey} u^2 - 5 p_e F_{ey} \right] \right\} - \\
& 2 \tau_e F_{e\xi} \left[\frac{\partial}{\partial \xi} (\rho_e u (u_0 - u)) \right] - 2 \tau_e \rho_e \left[(F_{e\xi})^2 + (F_{ey})^2 \right] + \\
& 2 \tau_e F_{e\xi} \left[\frac{\partial}{\partial \xi} p_e \right] + 2 \tau_e F_{ey} \left[\frac{\partial}{\partial y} p_e \right] = - \frac{p_e - p_p}{\tau_{ep}} \quad (3.6)
\end{aligned}$$

492
493
494
495
496
497
498
499

Here u - hydrodynamic velocity; φ - self-consistent electric potential; ρ_e , ρ_p - densities for the electron and positive species; p_e , p_p - quantum electron pressure and the pressure of positive species; F_e , F_p - the forces acting on the mass unit of electrons and the positive particles.

The right hand sides of the energy equations are written in the relaxation forms following from BGK kinetic approximation

Non-local parameters can be written in the form (see (1.14))

500

$$\tau_p = \frac{N_R \hbar}{m_p u^2}, \quad \tau_e = \frac{N_R \hbar}{m_e u^2}, \quad \frac{1}{\tau_{ep}} = \frac{1}{\tau_e} + \frac{1}{\tau_p} \quad (3.7)$$

501

where N_R - integer.

502

503

504

505

506

507

Acting forces are the sum of three terms: the self-consistent potential force (scalar potential φ), connected with the displacement of positive and negative charges, potential forces originated by the grapheme crystal lattice (potential U) and the external electrical field creating the intensity \mathbf{E} . As result the following relations are valid

508

$$F_{pz} = \frac{e}{m_p} \left(-\frac{\partial \varphi}{\partial \xi} - \frac{\partial U}{\partial \xi} + E_{0z} \right), \quad F_{ez} = \frac{e}{m_e} \left(\frac{\partial \varphi}{\partial \xi} + \frac{\partial U}{\partial \xi} - E_{0z} \right),$$

509

510

$$F_{py} = \frac{e}{m_p} \left(-\frac{\partial \varphi}{\partial y} - \frac{\partial U}{\partial y} + E_{0y} \right), \quad F_{ey} = \frac{e}{m_e} \left(\frac{\partial \varphi}{\partial y} + \frac{\partial U}{\partial y} - E_{0y} \right). \quad (3.8)$$

511

512

Let write down these equations in the dimensionless form, where dimensionless symbols are marked by tildes; introduce the scales:

513

$$u = u_0 \tilde{u}, \quad \xi = x_0 \tilde{\xi}, \quad y = x_0 \tilde{y}, \quad \varphi = \varphi_0 \tilde{\varphi}, \quad \rho_e = \rho_0 \tilde{\rho}_e, \quad \rho_p = \rho_0 \tilde{\rho}_p,$$

514

515

where u_0 , x_0 , φ_0 , ρ_0 - scales for velocity, distance, potential and density. Let there be also

516

$p_p = \rho_0 V_{0p}^2 \tilde{p}_p$, $p_e = \rho_0 V_{0e}^2 \tilde{p}_e$, where V_{0p} и V_{0e} - the scales for thermal velocities for the

517

electron and positive species; $F_p = \tilde{F}_p \frac{e \varphi_0}{m_p x_0}$, $F_e = \tilde{F}_e \frac{e \varphi_0}{m_e x_0}$; $\tau_p = \frac{m_e x_0 H}{m_p u_0 \tilde{u}^2}$,

518

$\tau_e = \frac{x_0 H}{u_0 \tilde{u}^2}$, where dimensionless parameter $H = \frac{N_R \hbar}{m_e x_0 u_0}$ is introduced. Then

519

$$\frac{1}{\tau_{ep}} = \frac{u_0}{x_0} \frac{\tilde{u}^2}{H} \left(1 + \frac{m_p}{m_e} \right).$$

520

Let us introduce also the following dimensionless parameters

521

$$R = \frac{e \rho_0 x_0^2}{m_e \varphi_0}, \quad E = \frac{e \varphi_0}{m_e u_0^2}. \quad (3.9)$$

522

523

524

Taking into account the introduced values the following system of dimensionless non-local hydrodynamic equations for the 2D soliton description can be written: Poisson equation for the self-consistent electric field:

525

$$\frac{\partial^2 \tilde{\varphi}}{\partial \tilde{\xi}^2} + \frac{\partial^2 \tilde{\varphi}}{\partial \tilde{y}^2} = -4\pi R \left\{ \frac{m_e}{m_p} \left[\tilde{\rho}_p - \frac{m_e H}{m_p \tilde{u}^2} \frac{\partial}{\partial \tilde{\xi}} (\tilde{\rho}_p (\tilde{u} - 1)) \right] - \left[\tilde{\rho}_e - \frac{H}{\tilde{u}^2} \frac{\partial}{\partial \tilde{\xi}} (\tilde{\rho}_e (\tilde{u} - 1)) \right] \right\}.$$

526

527

Continuity equation for the positive particles:

$$\begin{aligned}
& \frac{\partial}{\partial \tilde{\xi}} [\tilde{\rho}_p (1 - \tilde{u})] + \frac{m_e}{m_p} \frac{\partial}{\partial \tilde{\xi}} \left\{ \frac{H}{\tilde{u}^2} \frac{\partial}{\partial \tilde{\xi}} [\tilde{\rho}_p (\tilde{u} - 1)^2] \right\} + \\
& \frac{m_e}{m_p} \frac{\partial}{\partial \tilde{\xi}} \left\{ \frac{H}{\tilde{u}^2} \left[\frac{V_{0p}^2}{u_0^2} \frac{\partial}{\partial \tilde{\xi}} \tilde{p}_p - \frac{m_e}{m_p} E \tilde{\rho}_p \tilde{F}_{p\tilde{\xi}} \right] \right\} + \\
& \frac{m_e}{m_p} \frac{\partial}{\partial \tilde{y}} \left\{ \frac{H}{\tilde{u}^2} \left[\frac{V_{0p}^2}{u_0^2} \frac{\partial}{\partial \tilde{y}} \tilde{p}_p - \frac{m_e}{m_p} E \tilde{\rho}_p \tilde{F}_{py} \right] \right\} = 0
\end{aligned} \tag{3.11}$$

Continuity equation for electrons:

$$\begin{aligned}
& \frac{\partial}{\partial \tilde{\xi}} [\tilde{\rho}_e (1 - \tilde{u})] + \frac{\partial}{\partial \tilde{\xi}} \left\{ \frac{H}{\tilde{u}^2} \frac{\partial}{\partial \tilde{\xi}} [\tilde{\rho}_e (\tilde{u} - 1)^2] \right\} + \\
& \frac{\partial}{\partial \tilde{\xi}} \left\{ \frac{H}{\tilde{u}^2} \left[\frac{V_{0e}^2}{u_0^2} \frac{\partial}{\partial \tilde{\xi}} \tilde{p}_e - \tilde{\rho}_e E \tilde{F}_{e\tilde{\xi}} \right] \right\} + \frac{\partial}{\partial \tilde{y}} \left\{ \frac{H}{\tilde{u}^2} \left[\frac{V_{0e}^2}{u_0^2} \frac{\partial}{\partial \tilde{y}} \tilde{p}_e - \tilde{\rho}_e E \tilde{F}_{ey} \right] \right\} = 0
\end{aligned} \tag{3.12}$$

Momentum equation for the x direction:

$$\begin{aligned}
& \frac{\partial}{\partial \tilde{\xi}} \left\{ (\tilde{\rho}_p + \tilde{\rho}_e) \tilde{u} (\tilde{u} - 1) + \frac{V_{0p}^2}{u_0^2} \tilde{p}_p + \frac{V_{0e}^2}{u_0^2} \tilde{p}_e \right\} - \frac{m_e}{m_p} \tilde{\rho}_p E \tilde{F}_{p\tilde{\xi}} - \tilde{\rho}_e E \tilde{F}_{e\tilde{\xi}} + \\
& \frac{m_e}{m_p} \frac{\partial}{\partial \tilde{\xi}} \left\{ \frac{H}{\tilde{u}^2} \left[\frac{\partial}{\partial \tilde{\xi}} \left(2 \frac{V_{0p}^2}{u_0^2} \tilde{p}_p (1 - \tilde{u}) - \tilde{\rho}_p \tilde{u} (1 - \tilde{u})^2 \right) - \frac{m_e}{m_p} \tilde{\rho}_p E \tilde{F}_{p\tilde{\xi}} (1 - \tilde{u}) \right] \right\} + \\
& \frac{\partial}{\partial \tilde{\xi}} \left\{ \frac{H}{\tilde{u}^2} \left[\frac{\partial}{\partial \tilde{\xi}} \left(2 \frac{V_{0e}^2}{u_0^2} \tilde{p}_e (1 - \tilde{u}) - \tilde{\rho}_e \tilde{u} (1 - \tilde{u})^2 \right) - \tilde{\rho}_e E \tilde{F}_{e\tilde{\xi}} (1 - \tilde{u}) \right] \right\} + \\
& \frac{H}{\tilde{u}^2} E \left(\frac{m_e}{m_p} \right)^2 \tilde{F}_{p\tilde{\xi}} \left(\frac{\partial}{\partial \tilde{\xi}} (\tilde{\rho}_p (\tilde{u} - 1)) \right) + \frac{H}{\tilde{u}^2} E \tilde{F}_{e\tilde{\xi}} \left(\frac{\partial}{\partial \tilde{\xi}} (\tilde{\rho}_e (\tilde{u} - 1)) \right) - \\
& \frac{m_e}{m_p} \frac{\partial}{\partial \tilde{\xi}} \left\{ \frac{H}{\tilde{u}^2} \frac{V_{0p}^2}{u_0^2} \frac{\partial}{\partial \tilde{\xi}} (\tilde{p}_p \tilde{u}) \right\} - \frac{\partial}{\partial \tilde{\xi}} \left\{ \frac{H}{\tilde{u}^2} \frac{V_{0e}^2}{u_0^2} \frac{\partial}{\partial \tilde{\xi}} (\tilde{p}_e \tilde{u}) \right\} - \\
& \frac{m_e}{m_p} \frac{\partial}{\partial \tilde{y}} \left\{ \frac{H}{\tilde{u}^2} \frac{V_{0p}^2}{u_0^2} \frac{\partial}{\partial \tilde{y}} (\tilde{p}_p \tilde{u}) \right\} - \frac{\partial}{\partial \tilde{y}} \left\{ \frac{H}{\tilde{u}^2} \frac{V_{0e}^2}{u_0^2} \frac{\partial}{\partial \tilde{y}} (\tilde{p}_e \tilde{u}) \right\} + \\
& \left(\frac{m_e}{m_p} \right)^2 \frac{\partial}{\partial \tilde{\xi}} \left\{ \frac{H}{\tilde{u}^2} E [\tilde{F}_{p\tilde{\xi}} \tilde{\rho}_p \tilde{u}] \right\} + \frac{\partial}{\partial \tilde{\xi}} \left\{ \frac{H}{\tilde{u}^2} E [\tilde{F}_{e\tilde{\xi}} \tilde{\rho}_e \tilde{u}] \right\} + \\
& \left(\frac{m_e}{m_p} \right)^2 \frac{\partial}{\partial \tilde{y}} \left\{ \frac{H}{\tilde{u}^2} E [\tilde{F}_{py} \tilde{\rho}_p \tilde{u}] \right\} + \frac{\partial}{\partial \tilde{y}} \left\{ \frac{H}{\tilde{u}^2} E [\tilde{F}_{ey} \tilde{\rho}_e \tilde{u}] \right\} = 0
\end{aligned} \tag{3.13}$$

Energy equation for the positive particles:

$$\begin{aligned}
& \frac{\partial}{\partial \tilde{\xi}} \left[\tilde{\rho}_p \tilde{u}^2 (\tilde{u} - 1) + 5 \frac{V_{0p}^2}{u_0^2} \tilde{p}_p \tilde{u} - 3 \frac{V_{0p}^2}{u_0^2} \tilde{p}_p \right] - 2 \frac{m_e}{m_p} \tilde{\rho}_p E \tilde{F}_{p\tilde{\xi}} \tilde{u} + \\
& \frac{\partial}{\partial \tilde{\xi}} \left\{ \frac{H}{\tilde{u}^2} \frac{m_e}{m_p} \left[\frac{\partial}{\partial \tilde{\xi}} \left(-\tilde{\rho}_p \tilde{u}^2 (1 - \tilde{u})^2 + 7 \frac{V_{0p}^2}{u_0^2} \tilde{p}_p \tilde{u} (1 - \tilde{u}) + 3 \frac{V_{0p}^2}{u_0^2} \tilde{p}_p (\tilde{u} - 1) - \frac{V_{0p}^2}{u_0^2} \tilde{p}_p \tilde{u}^2 - \right. \right. \right. \\
& \left. \left. \left. 5 \frac{V_{0p}^4}{u_0^4} \frac{\tilde{p}_p^2}{\tilde{\rho}_p} \right) - 2 \frac{m_e}{m_p} E \tilde{F}_{p\tilde{\xi}} \tilde{\rho}_p \tilde{u} (1 - \tilde{u}) + \frac{m_e}{m_p} \tilde{\rho}_p \tilde{u}^2 E \tilde{F}_{p\tilde{\xi}} + 5 \frac{m_e}{m_p} \frac{V_{0p}^2}{u_0^2} \tilde{p}_p E \tilde{F}_{p\tilde{\xi}} \right] \right\} - \\
& \frac{\partial}{\partial \tilde{y}} \left\{ \frac{H}{\tilde{u}^2} \frac{m_e}{m_p} \left[\frac{\partial}{\partial \tilde{y}} \left(\frac{V_{0p}^2}{u_0^2} \tilde{p}_p \tilde{u}^2 + 5 \frac{V_{0p}^4}{u_0^4} \frac{\tilde{p}_p^2}{\tilde{\rho}_p} \right) - \frac{m_e}{m_p} \tilde{\rho}_p E \tilde{F}_{py} \tilde{u}^2 - 5 \frac{m_e}{m_p} \frac{V_{0p}^2}{u_0^2} \tilde{p}_p E \tilde{F}_{py} \right] \right\} - \\
& 2 \frac{H}{\tilde{u}^2} \left(\frac{m_e}{m_p} \right)^2 E \tilde{F}_{p\tilde{\xi}} \left[\frac{\partial}{\partial \tilde{\xi}} (\tilde{\rho}_p \tilde{u} (1 - \tilde{u})) \right] - 2 \frac{H}{\tilde{u}^2} \left(\frac{m_e}{m_p} \right)^3 \tilde{\rho}_p E^2 \left[(\tilde{F}_{p\tilde{\xi}})^2 + (\tilde{F}_{py})^2 \right] + \\
& 2 \frac{H}{\tilde{u}^2} \left(\frac{m_e}{m_p} \right)^2 E \tilde{F}_{p\tilde{\xi}} \left[\frac{V_{0p}^2}{u_0^2} \frac{\partial}{\partial \tilde{\xi}} \tilde{p}_p \right] + 2 \frac{H}{\tilde{u}^2} \left(\frac{m_e}{m_p} \right)^2 E \tilde{F}_{py} \left[\frac{V_{0p}^2}{u_0^2} \frac{\partial}{\partial \tilde{y}} \tilde{p}_p \right] = \\
& - \frac{\tilde{u}^2}{Hu_0^2} (V_{0p}^2 \tilde{p}_p - \tilde{p}_e V_{0e}^2) \left(1 + \frac{m_p}{m_e} \right)
\end{aligned}
\tag{3.14}$$

542 Energy equation for electrons:
543

$$\begin{aligned}
& \frac{\partial}{\partial \tilde{\xi}} \left[\tilde{\rho}_e \tilde{u}^2 (\tilde{u} - 1) + 5 \frac{V_{0e}^2}{u_0^2} \tilde{p}_e \tilde{u} - 3 \frac{V_{0e}^2}{u_0^2} \tilde{p}_e \right] - 2 \tilde{\rho}_e E \tilde{F}_{e\tilde{\xi}} \tilde{u} + \\
& \frac{\partial}{\partial \tilde{\xi}} \left\{ \frac{H}{\tilde{u}^2} \left[\frac{\partial}{\partial \tilde{\xi}} \left(-\tilde{\rho}_e \tilde{u}^2 (1 - \tilde{u})^2 + 7 \frac{V_{0e}^2}{u_0^2} \tilde{p}_e \tilde{u} (1 - \tilde{u}) + 3 \frac{V_{0e}^2}{u_0^2} \tilde{p}_e (\tilde{u} - 1) - \frac{V_{0e}^2}{u_0^2} \tilde{p}_e \tilde{u}^2 - \right. \right. \right. \\
& \left. \left. \left. 5 \frac{V_{0e}^4}{u_0^4} \frac{\tilde{p}_e^2}{\tilde{\rho}_e} \right) - 2 E \tilde{F}_{e\tilde{\xi}} \tilde{\rho}_e \tilde{u} (1 - \tilde{u}) + \tilde{\rho}_e \tilde{u}^2 E \tilde{F}_{e\tilde{\xi}} + 5 \frac{V_{0e}^2}{u_0^2} \tilde{p}_e E \tilde{F}_{e\tilde{\xi}} \right] \right\} - \\
& \frac{\partial}{\partial \tilde{y}} \left\{ \frac{H}{\tilde{u}^2} \left[\frac{\partial}{\partial \tilde{y}} \left(\frac{V_{0e}^2}{u_0^2} \tilde{p}_e \tilde{u}^2 + 5 \frac{V_{0e}^4}{u_0^4} \frac{\tilde{p}_e^2}{\tilde{\rho}_e} \right) - \tilde{\rho}_e E \tilde{F}_{ey} \tilde{u}^2 - 5 \frac{V_{0e}^2}{u_0^2} \tilde{p}_e E \tilde{F}_{ey} \right] \right\} - \\
& 2 \frac{H}{\tilde{u}^2} E \tilde{F}_{e\tilde{\xi}} \left[\frac{\partial}{\partial \tilde{\xi}} (\tilde{\rho}_e \tilde{u} (1 - \tilde{u})) \right] - 2 \frac{H}{\tilde{u}^2} \tilde{\rho}_e E^2 \left[(\tilde{F}_{e\tilde{\xi}})^2 + (\tilde{F}_{ey})^2 \right] + \\
& 2 \frac{H}{\tilde{u}^2} E \tilde{F}_{e\tilde{\xi}} \left[\frac{V_{0e}^2}{u_0^2} \frac{\partial}{\partial \tilde{\xi}} \tilde{p}_e \right] + 2 \frac{H}{\tilde{u}^2} E \tilde{F}_{ey} \left[\frac{V_{0e}^2}{u_0^2} \frac{\partial}{\partial \tilde{y}} \tilde{p}_e \right] = \\
& - \frac{\tilde{u}^2}{Hu_0^2} (V_{0e}^2 \tilde{p}_e - V_{0p}^2 \tilde{p}_p) \left(1 + \frac{m_p}{m_e} \right)
\end{aligned}
\tag{3.15}$$

546 We have the following dimensionless relations for forces:

$$\begin{aligned}
 547 \quad \tilde{F}_{p\xi} &= -\frac{\partial \tilde{\varphi}}{\partial \tilde{\xi}} - \frac{\partial \tilde{U}}{\partial \tilde{\xi}} + \tilde{E}_{\xi}, \quad \tilde{F}_{e\xi} = \frac{\partial \tilde{\varphi}}{\partial \tilde{\xi}} + \frac{\partial \tilde{U}}{\partial \tilde{\xi}} - \tilde{E}_{\xi}, \\
 548 \quad \tilde{F}_{py} &= -\frac{\partial \tilde{\varphi}}{\partial \tilde{y}} - \frac{\partial \tilde{U}}{\partial \tilde{y}} + \tilde{E}_y, \quad \tilde{F}_{ey} = \frac{\partial \tilde{\varphi}}{\partial \tilde{y}} + \frac{\partial \tilde{U}}{\partial \tilde{y}} - \tilde{E}_y. \quad (3.16)
 \end{aligned}$$

549
 550 Graphene is a single layer of carbon atoms densely packed in a honeycomb lattice. Figure 1
 551 reflects the structure of grapheme as the 2D hexagonal carbon crystal, the distance a
 552 between the nearest atoms is equal to $a = 0.142 \text{ nm}$.

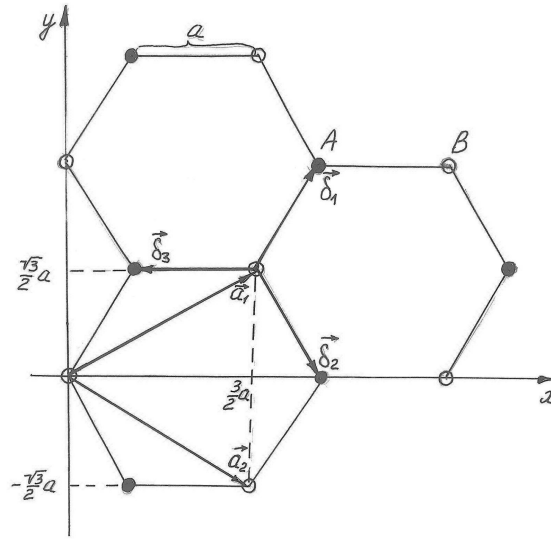


Figure 1. Crystal graphene lattice.

553
 554
 555 Elementary cell contains two atoms (for example A and B, figure 1) and the primitive
 556 lattice vectors are given by
 557

$$558 \quad \mathbf{a}_1 = \frac{a}{2}(3; \sqrt{3}), \quad \mathbf{a}_2 = \frac{a}{2}(3; -\sqrt{3}).$$

559 Coordinates of the nearest atoms to the given atom define by vectors

$$560 \quad \delta_1 = \frac{a}{2}(1; \sqrt{3}), \quad \delta_2 = \frac{a}{2}(1; -\sqrt{3}), \quad \delta_3 = -a(1; 0).$$

561 Six neighboring atoms of the second order are placed in knots defined by vectors

$$562 \quad \delta'_1 = \pm \mathbf{a}_1, \quad \delta'_2 = \pm \mathbf{a}_2, \quad \delta'_3 = \pm(\mathbf{a}_2 - \mathbf{a}_1).$$

563 Let us take the first atom of the elementary cell in the origin of the coordinate system
 564 (figure 1) and compose the radii-vector of the second atom with respect to the basis \mathbf{a}_1 и
 565 \mathbf{a}_2 :

$$566 \quad \mathbf{r}_1 = u\mathbf{a}_1 + v\mathbf{a}_2 = u\left(3\frac{a}{2}\mathbf{e}_x + \sqrt{3}\frac{a}{2}\mathbf{e}_y\right) + v\left(3\frac{a}{2}\mathbf{e}_x - \sqrt{3}\frac{a}{2}\mathbf{e}_y\right). \quad (3.17)$$

567 Let us find u и v , taking into account that

$$568 \quad \mathbf{r}_1 = \delta_1 = \frac{a}{2}(1; \sqrt{3}) = \frac{a}{2}\mathbf{e}_x + \frac{a}{2}\sqrt{3}\mathbf{e}_y. \quad (3.18)$$

569 Equalizing (3.17) и (3.18), we have $u = \frac{2}{3}$, $v = -\frac{1}{3}$, then

570
$$\mathbf{r}_1 = \frac{2}{3}\mathbf{a}_1 - \frac{1}{3}\mathbf{a}_2. \quad (3.19)$$

571 Assume that $V_1(\mathbf{r})$ is the periodical potential created by one sublattice. Then
572 potential of crystal is

573
$$V(\mathbf{r}) = V_1(\mathbf{r}) + V_1(\mathbf{r} - \mathbf{r}_1) = \sum_{n=0}^1 V_1(\mathbf{r} - \mathbf{r}_n). \quad (3.20)$$

574 Atoms in crystal form the periodic structure and as the consequence the corresponding
575 potential is periodic function

576
$$V_1(\mathbf{r}) = V_1(\mathbf{r} + \mathbf{a}_m),$$

577 where for 2D structure

578
$$\mathbf{a}_m = m_1\mathbf{a}_1 + m_2\mathbf{a}_2,$$

579 and m_1 и m_2 are arbitrary entire numbers. Expanding $V_1(\mathbf{r})$ in the Fourier series one
580 obtains

581
$$V_1(\mathbf{r} - \mathbf{r}_n) = \sum_{\mathbf{b}} V_{\mathbf{b}} e^{i\mathbf{b} \cdot (\mathbf{r} - \mathbf{r}_n)}. \quad (3.21)$$

582 In our case the both basis atoms ($n=0,1$) are the same. Here

583
$$\mathbf{b} = g_1\mathbf{b}_1 + g_2\mathbf{b}_2,$$

584 \mathbf{b}_1 и \mathbf{b}_2 are the translational vectors of the reciprocal lattice. For graphene
585

586
$$\mathbf{b}_1 = \frac{2\pi}{3a}(1; \sqrt{3}), \quad \mathbf{b}_2 = \frac{2\pi}{3a}(1; -\sqrt{3}). \quad (3.22)$$

587 Then

588
$$V(\mathbf{r}) = \sum_{\mathbf{b}} \sum_{n=0}^1 V_{1\mathbf{b}} e^{i\mathbf{b} \cdot (\mathbf{r} - \mathbf{r}_n)} = \sum_{\mathbf{b}} V_{\mathbf{b}} e^{i\mathbf{b} \cdot \mathbf{r}}, \quad (3.23)$$

589 where $V_{\mathbf{b}} = V_{1\mathbf{b}} \cdot \sum_n e^{-i\mathbf{b} \cdot \mathbf{r}_n} = V_{1\mathbf{b}} \cdot S_{\mathbf{b}}$. The structure factor $S_{\mathbf{b}}$ for graphene:

590
$$S_{\mathbf{b}} = e^{-i\mathbf{b} \cdot 0} + e^{-i\mathbf{b} \cdot \left(\frac{2}{3}\mathbf{a}_1 - \frac{1}{3}\mathbf{a}_2\right)} = 1 + e^{i\frac{2\pi}{3}(g_2 - 2g_1)}. \quad (3.24)$$

591

592
$$V(\mathbf{r}) = \sum_{g_1, g_2} V_{1g_1, g_2} e^{i(g_1\mathbf{b}_1 + g_2\mathbf{b}_2) \cdot \mathbf{r}} \left(1 + e^{i\frac{2\pi}{3}(g_2 - 2g_1)} \right). \quad (3.25)$$

593

594 For the approximate calculation we use the terms of the series with $|g_1| \leq 2$, $|g_2| \leq 2$.

595 Therefore

$$\begin{aligned}
V(\mathbf{r}) = & 2V_{1,(00)} + 4V_{1,(10)} \left(\cos\left(\frac{1}{2}(\mathbf{b}_1 + \mathbf{b}_2) \cdot \mathbf{r}\right) \cos\left(\frac{1}{2}(\mathbf{b}_1 - \mathbf{b}_2) \cdot \mathbf{r}\right) + \right. \\
& \cos\left(\frac{1}{2}(\mathbf{b}_1 + \mathbf{b}_2) \cdot \mathbf{r} + \frac{2\pi}{3}\right) \cos\left(\frac{1}{2}(\mathbf{b}_1 - \mathbf{b}_2) \cdot \mathbf{r}\right) \Bigg) + \\
& 2V_{1,(11)} \left(\cos((\mathbf{b}_1 + \mathbf{b}_2) \cdot \mathbf{r}) + \cos\left((\mathbf{b}_1 + \mathbf{b}_2) \cdot \mathbf{r} - \frac{2\pi}{3}\right) + 2 \cos((\mathbf{b}_1 - \mathbf{b}_2) \cdot \mathbf{r}) \right) - \\
& 4V_{1,(20)} \cos((\mathbf{b}_2 - \mathbf{b}_1) \cdot \mathbf{r}) \cos\left((\mathbf{b}_2 + \mathbf{b}_1) \cdot \mathbf{r} + \frac{2\pi}{3}\right) + \\
& 2V_{1,(12)} \left(2 \cos((\mathbf{b}_1 + 2\mathbf{b}_2) \cdot \mathbf{r}) + 2 \cos((2\mathbf{b}_1 + \mathbf{b}_2) \cdot \mathbf{r}) + \right. \\
& \cos((\mathbf{b}_1 - 2\mathbf{b}_2) \cdot \mathbf{r} - \frac{\pi}{3}) - \cos\left((2\mathbf{b}_1 - \mathbf{b}_2) \cdot \mathbf{r} - \frac{2\pi}{3}\right) \Bigg) + \\
& 2V_{1,(22)} \left(2 \cos(2(\mathbf{b}_1 - \mathbf{b}_2) \cdot \mathbf{r}) - \cos\left(2(\mathbf{b}_1 + \mathbf{b}_2) \cdot \mathbf{r} - \frac{2\pi}{3}\right) \right). \tag{3.26}
\end{aligned}$$

Using the vectors \mathbf{b}_1 and \mathbf{b}_2 of the reciprocal lattice from (3.22) and coordinates x and y one obtains from (3.26):

$$\begin{aligned}
V(x, y) = & 2V_{1,(00)} + 4V_{1,(10)} \cos\left(\frac{2\pi}{3a}x + \frac{\pi}{3}\right) \cos\left(\frac{2\pi}{3a}\sqrt{3}y\right) + \\
& 2V_{1,(11)} \left(\cos\left(\frac{4\pi}{3a}x - \frac{\pi}{3}\right) + 2 \cos\left(\frac{4\pi}{3a}\sqrt{3}y\right) \right) - 4V_{1,(20)} \cos\left(\frac{4\pi}{3a}\sqrt{3}y\right) \cos\left(\frac{4\pi}{3a}x + \frac{2\pi}{3}\right) + \\
& 4V_{1,(12)} \left(2 \cos\left(\frac{2\pi}{a}x\right) \cos\left(\frac{2\pi}{3a}\sqrt{3}y\right) - \sin\left(\frac{2\pi}{3a}x - \frac{\pi}{6}\right) \cos\left(\frac{2\pi}{a}\sqrt{3}y\right) \right) + \\
& 2V_{1,(22)} \left(2 \cos\left(\frac{8\pi}{3a}\sqrt{3}y\right) - \cos\left(\frac{8\pi}{3a}x - \frac{2\pi}{3}\right) \right). \tag{3.27}
\end{aligned}$$

We need the derivatives for the forces components in dimensionless form

$$\begin{aligned}
-\frac{\partial \tilde{U}}{\partial \tilde{\xi}} = & \tilde{U}'_{10} \sin\left(\frac{2\pi}{3\tilde{a}}\tilde{x} + \frac{\pi}{3}\right) \cos\left(\frac{2\pi}{3\tilde{a}}\sqrt{3}\tilde{y}\right) + \tilde{U}'_{11} \sin\left(\frac{4\pi}{3\tilde{a}}\tilde{x} - \frac{\pi}{3}\right) - \\
& \tilde{U}'_{20} \cos\left(\frac{4\pi}{3\tilde{a}}\sqrt{3}\tilde{y}\right) \sin\left(\frac{4\pi}{3\tilde{a}}x + \frac{2\pi}{3}\right) + \tilde{U}'_{12} \left(6 \sin\left(\frac{2\pi}{\tilde{a}}\tilde{x}\right) \cos\left(\frac{2\pi}{3\tilde{a}}\sqrt{3}\tilde{y}\right) + \right. \\
& \cos\left(\frac{2\pi}{3\tilde{a}}\tilde{x} - \frac{\pi}{6}\right) \cos\left(\frac{2\pi}{\tilde{a}}\sqrt{3}\tilde{y}\right) \Bigg) - \tilde{U}'_{22} \sin\left(\frac{8\pi}{3\tilde{a}}\tilde{x} - \frac{2\pi}{3}\right), \tag{3.28}
\end{aligned}$$

$$\begin{aligned}
612 \quad & -\frac{\partial \tilde{U}}{\partial \tilde{y}} = \tilde{U}'_{10} \sqrt{3} \cos\left(\frac{2\pi}{3\tilde{a}} \tilde{x} + \frac{\pi}{3}\right) \sin\left(\frac{2\pi}{3\tilde{a}} \sqrt{3}\tilde{y}\right) + \tilde{U}'_{11} 2\sqrt{3} \sin\left(\frac{4\pi}{3\tilde{a}} \sqrt{3}\tilde{y}\right) - \\
613 \quad & \sqrt{3}\tilde{U}'_{20} \sin\left(\frac{4\pi}{3\tilde{a}} \sqrt{3}\tilde{y}\right) \cos\left(\frac{4\pi}{3\tilde{a}} \tilde{x} + \frac{2\pi}{3}\right) + \tilde{U}'_{12} \left(2\sqrt{3} \cos\left(\frac{2\pi}{\tilde{a}} \tilde{x}\right) \sin\left(\frac{2\pi}{3\tilde{a}} \sqrt{3}\tilde{y}\right) - \right. \\
614 \quad & \left. 3\sqrt{3} \sin\left(\frac{2\pi}{3\tilde{a}} \tilde{x} - \frac{\pi}{6}\right) \sin\left(\frac{2\pi}{\tilde{a}} \sqrt{3}\tilde{y}\right)\right) + 2\sqrt{3}\tilde{U}'_{22} \sin\left(\frac{8\pi}{3\tilde{a}} \sqrt{3}\tilde{y}\right), \quad (3.29)
\end{aligned}$$

615 where the notations are introduced:
616

$$617 \quad \tilde{U}'_{10} = \frac{8\pi}{3\tilde{a}} \tilde{V}_{1,(10)}, \quad \tilde{U}'_{11} = \frac{8\pi}{3\tilde{a}} \tilde{V}_{1,(11)}, \quad \tilde{U}'_{20} = \frac{16\pi}{3\tilde{a}} \tilde{V}_{1,(20)}, \quad \tilde{U}'_{12} = \frac{8\pi}{3\tilde{a}} \tilde{V}_{1,(12)}, \quad \tilde{U}'_{22} = \frac{16\pi}{3\tilde{a}} \tilde{V}_{1,(22)}. \quad (3.30)$$

620 Consider as the approximation the acting forces by $\tilde{t} = 0$, when $\tilde{\xi} = \tilde{x}$. After substitution
621 of (3.28) and (3.29) in (3.16), one obtains the expressions for the dimensionless forces
622 acting on the unit of mass of particles:

$$\begin{aligned}
623 \quad & \tilde{F}_{p\xi} = -\frac{\partial \tilde{\Phi}}{\partial \tilde{\xi}} + \tilde{U}'_{10} \sin\left(\frac{2\pi}{3\tilde{a}} \tilde{\xi} + \frac{\pi}{3}\right) \cos\left(\frac{2\pi}{3\tilde{a}} \sqrt{3}\tilde{y}\right) + \tilde{U}'_{11} \sin\left(\frac{4\pi}{3\tilde{a}} \tilde{\xi} - \frac{\pi}{3}\right) - \\
& \tilde{U}'_{20} \cos\left(\frac{4\pi}{3\tilde{a}} \sqrt{3}\tilde{y}\right) \sin\left(\frac{4\pi}{3\tilde{a}} \tilde{\xi} + \frac{2\pi}{3}\right) + \tilde{U}'_{12} \left(6 \sin\left(\frac{2\pi}{\tilde{a}} \tilde{\xi}\right) \cos\left(\frac{2\pi}{3\tilde{a}} \sqrt{3}\tilde{y}\right) + \right. \\
& \left. \cos\left(\frac{2\pi}{3\tilde{a}} \tilde{\xi} - \frac{\pi}{6}\right) \cos\left(\frac{2\pi}{\tilde{a}} \sqrt{3}\tilde{y}\right)\right) - \tilde{U}'_{22} \sin\left(\frac{8\pi}{3\tilde{a}} \tilde{\xi} - \frac{2\pi}{3}\right) + \tilde{E}_{\xi}, \quad (3.31)
\end{aligned}$$

$$\begin{aligned}
& \tilde{F}_{py} = -\frac{\partial \tilde{\Phi}}{\partial \tilde{y}} + \tilde{U}'_{10} \sqrt{3} \cos\left(\frac{2\pi}{3\tilde{a}} \tilde{\xi} + \frac{\pi}{3}\right) \sin\left(\frac{2\pi}{3\tilde{a}} \sqrt{3}\tilde{y}\right) + \tilde{U}'_{11} 2\sqrt{3} \sin\left(\frac{4\pi}{3\tilde{a}} \sqrt{3}\tilde{y}\right) - \\
624 \quad & \sqrt{3}\tilde{U}'_{20} \sin\left(\frac{4\pi}{3\tilde{a}} \sqrt{3}\tilde{y}\right) \cos\left(\frac{4\pi}{3\tilde{a}} \tilde{\xi} + \frac{2\pi}{3}\right) + \tilde{U}'_{12} \left(2\sqrt{3} \cos\left(\frac{2\pi}{\tilde{a}} \tilde{\xi}\right) \sin\left(\frac{2\pi}{3\tilde{a}} \sqrt{3}\tilde{y}\right) - \right. \\
& \left. 3\sqrt{3} \sin\left(\frac{2\pi}{3\tilde{a}} \tilde{\xi} - \frac{\pi}{6}\right) \sin\left(\frac{2\pi}{\tilde{a}} \sqrt{3}\tilde{y}\right)\right) + 2\sqrt{3}\tilde{U}'_{22} \sin\left(\frac{8\pi}{3\tilde{a}} \sqrt{3}\tilde{y}\right) + \tilde{E}_y. \quad (3.32)
\end{aligned}$$

625 Analogically

$$626 \quad \tilde{F}_{e\xi} = -\tilde{F}_{p\xi}, \quad \tilde{F}_{ey} = -\tilde{F}_{py}. \quad (3.33)$$

627 The forces (3.31)-(3.33) should be introduced in the system of the hydrodynamic equations
628 (3.10)-(3.15).

629 Suppose that the external field intensity \mathbf{E} is equal to zero. The effective
630 hydrodynamic velocity is directed along x axis. This fact can be used by averaging over \tilde{y}
631 of the obtained system of quantum hydrodynamic equations. The averaging will be realized
632 in the limit of one hexagonal crystal cell. Carry out the integration of the left and right hand

633 sides of the hydrodynamic equations calculating the integral $\frac{1}{\sqrt{3}\tilde{a}} \int_{-\frac{\sqrt{3}}{2}\tilde{a}}^{\frac{\sqrt{3}}{2}\tilde{a}} d\tilde{y}$ (see figure 1) and

634 taking into account that $\frac{1}{\sqrt{3\tilde{a}}} \int_{-\frac{\sqrt{3}\tilde{a}}{2}}^{\frac{\sqrt{3}\tilde{a}}{2}} \frac{\partial \psi}{\partial \tilde{y}} d\tilde{y} = 0$ because of system symmetry for arbitrary

635 function ψ , characterizing the state of the physical system. We suppose also that by
636 averaging all physical values (characterizing the state of the physical system) do not depend
637 on \tilde{y} .

638 As result we have the following system of equations:

639 Dimensionless Poisson equation for the self-consistent potential $\tilde{\phi}$ of the electric field:

$$640 \quad \frac{\partial^2 \tilde{\phi}}{\partial \tilde{\xi}^2} = -4\pi R \left\{ \frac{m_e}{m_p} \left[\tilde{\rho}_p - \frac{m_e H}{m_p \tilde{u}^2} \frac{\partial}{\partial \tilde{\xi}} (\tilde{\rho}_p (\tilde{u} - 1)) \right] - \left[\tilde{\rho}_e - \frac{H}{\tilde{u}^2} \frac{\partial}{\partial \tilde{\xi}} (\tilde{\rho}_e (\tilde{u} - 1)) \right] \right\}. \quad (3.34)$$

641

642 Continuity equation for the positive particles:

643

$$644 \quad \frac{\partial}{\partial \tilde{\xi}} [\tilde{\rho}_p (1 - \tilde{u})] + \frac{m_e}{m_p} \frac{\partial}{\partial \tilde{\xi}} \left\{ \frac{H}{\tilde{u}^2} \frac{\partial}{\partial \tilde{\xi}} [\tilde{\rho}_p (\tilde{u} - 1)^2] \right\} + \frac{m_e}{m_p} \frac{\partial}{\partial \tilde{\xi}} \left\{ \frac{H}{\tilde{u}^2} \left[\frac{V_{0p}^2}{u_0^2} \frac{\partial}{\partial \tilde{\xi}} \tilde{p}_p - \right. \right. \\ \left. \left. \frac{m_e}{m_p} \tilde{\rho}_p E \left(-\frac{\partial \tilde{\phi}}{\partial \tilde{\xi}} + \tilde{U}'_{11} \sin \left(\frac{4\pi}{3\tilde{a}} \tilde{\xi} - \frac{\pi}{3} \right) - \tilde{U}'_{22} \sin \left(\frac{8\pi}{3\tilde{a}} \tilde{\xi} - \frac{2\pi}{3} \right) \right) \right] \right\} = 0 \quad (3.35)$$

645 Continuity equation for electrons:

646

$$647 \quad \frac{\partial}{\partial \tilde{\xi}} [\tilde{\rho}_e (1 - \tilde{u})] + \frac{\partial}{\partial \tilde{\xi}} \left\{ \frac{H}{\tilde{u}^2} \frac{\partial}{\partial \tilde{\xi}} [\tilde{\rho}_e (\tilde{u} - 1)^2] \right\} + \frac{\partial}{\partial \tilde{\xi}} \left\{ \frac{H}{\tilde{u}^2} \left[\frac{V_{0e}^2}{u_0^2} \frac{\partial}{\partial \tilde{\xi}} \tilde{p}_e - \right. \right. \\ \left. \left. \tilde{\rho}_e E \left(\frac{\partial \tilde{\phi}}{\partial \tilde{\xi}} - \tilde{U}'_{11} \sin \left(\frac{4\pi}{3\tilde{a}} \tilde{\xi} - \frac{\pi}{3} \right) + \tilde{U}'_{22} \sin \left(\frac{8\pi}{3\tilde{a}} \tilde{\xi} - \frac{2\pi}{3} \right) \right) \right] \right\} = 0 \quad (3.36)$$

648 Momentum equation for the movement along the x direction:

649

$$650 \quad \frac{\partial}{\partial \tilde{\xi}} \left\{ (\tilde{\rho}_p + \tilde{\rho}_e) \tilde{u} (\tilde{u} - 1) + \frac{V_{0p}^2}{u_0^2} \tilde{p}_p + \frac{V_{0e}^2}{u_0^2} \tilde{p}_e \right\} - \\ \frac{m_e}{m_p} \tilde{\rho}_p E \left(-\frac{\partial \tilde{\phi}}{\partial \tilde{\xi}} + \tilde{U}'_{11} \sin \left(\frac{4\pi}{3\tilde{a}} \tilde{\xi} - \frac{\pi}{3} \right) - \tilde{U}'_{22} \sin \left(\frac{8\pi}{3\tilde{a}} \tilde{\xi} - \frac{2\pi}{3} \right) \right) - \\ \tilde{\rho}_e E \left(\frac{\partial \tilde{\phi}}{\partial \tilde{\xi}} - \tilde{U}'_{11} \sin \left(\frac{4\pi}{3\tilde{a}} \tilde{\xi} - \frac{\pi}{3} \right) + \tilde{U}'_{22} \sin \left(\frac{8\pi}{3\tilde{a}} \tilde{\xi} - \frac{2\pi}{3} \right) \right) +$$

$$\begin{aligned}
& \frac{m_e}{m_p} \frac{\partial}{\partial \tilde{\xi}} \left\{ \frac{H}{\tilde{u}^2} \left[\frac{\partial}{\partial \tilde{\xi}} \left(2 \frac{V_{0p}^2}{u_0^2} \tilde{p}_p (1 - \tilde{u}) - \tilde{\rho}_p \tilde{u} (1 - \tilde{u})^2 \right) - \right. \right. \\
& \left. \left. \frac{m_e}{m_p} \tilde{\rho}_p (1 - \tilde{u}) E \left(-\frac{\partial \tilde{\Phi}}{\partial \tilde{\xi}} + \tilde{U}'_{11} \sin \left(\frac{4\pi}{3\tilde{a}} \tilde{\xi} - \frac{\pi}{3} \right) - \tilde{U}'_{22} \sin \left(\frac{8\pi}{3\tilde{a}} \tilde{\xi} - \frac{2\pi}{3} \right) \right) \right] \right\} + \\
& \frac{\partial}{\partial \tilde{\xi}} \left\{ \frac{H}{\tilde{u}^2} \left[\frac{\partial}{\partial \tilde{\xi}} \left(2 \frac{V_{0e}^2}{u_0^2} \tilde{p}_e (1 - \tilde{u}) - \tilde{\rho}_e \tilde{u} (1 - \tilde{u})^2 \right) - \right. \right. \\
& \left. \left. \tilde{\rho}_e (1 - \tilde{u}) E \left(\frac{\partial \tilde{\Phi}}{\partial \tilde{\xi}} - \tilde{U}'_{11} \sin \left(\frac{4\pi}{3\tilde{a}} \tilde{\xi} - \frac{\pi}{3} \right) + \tilde{U}'_{22} \sin \left(\frac{8\pi}{3\tilde{a}} \tilde{\xi} - \frac{2\pi}{3} \right) \right) \right] \right\} + \\
& \frac{H}{\tilde{u}^2} E \left(\frac{m_e}{m_p} \right)^2 \left(-\frac{\partial \tilde{\Phi}}{\partial \tilde{\xi}} + \tilde{U}'_{11} \sin \left(\frac{4\pi}{3\tilde{a}} \tilde{\xi} - \frac{\pi}{3} \right) - \tilde{U}'_{22} \sin \left(\frac{8\pi}{3\tilde{a}} \tilde{\xi} - \frac{2\pi}{3} \right) \right) \left(\frac{\partial}{\partial \tilde{\xi}} (\tilde{\rho}_p (\tilde{u} - 1)) \right) + \\
& \frac{H}{\tilde{u}^2} E \left(\frac{\partial \tilde{\Phi}}{\partial \tilde{\xi}} - \tilde{U}'_{11} \sin \left(\frac{4\pi}{3\tilde{a}} \tilde{\xi} - \frac{\pi}{3} \right) + \tilde{U}'_{22} \sin \left(\frac{8\pi}{3\tilde{a}} \tilde{\xi} - \frac{2\pi}{3} \right) \right) \left(\frac{\partial}{\partial \tilde{\xi}} (\tilde{\rho}_e (\tilde{u} - 1)) \right) - \\
& \frac{m_e}{m_p} \frac{\partial}{\partial \tilde{\xi}} \left\{ \frac{H}{\tilde{u}^2} \frac{V_{0p}^2}{u_0^2} \frac{\partial}{\partial \tilde{\xi}} (\tilde{p}_p \tilde{u}) \right\} - \frac{\partial}{\partial \tilde{\xi}} \left\{ \frac{H}{\tilde{u}^2} \frac{V_{0e}^2}{u_0^2} \frac{\partial}{\partial \tilde{\xi}} (\tilde{p}_e \tilde{u}) \right\} + \\
& \left(\frac{m_e}{m_p} \right)^2 E \frac{\partial}{\partial \tilde{\xi}} \left\{ \frac{H}{\tilde{u}^2} \left[\left(-\frac{\partial \tilde{\Phi}}{\partial \tilde{\xi}} + \tilde{U}'_{11} \sin \left(\frac{4\pi}{3\tilde{a}} \tilde{\xi} - \frac{\pi}{3} \right) - \tilde{U}'_{22} \sin \left(\frac{8\pi}{3\tilde{a}} \tilde{\xi} - \frac{2\pi}{3} \right) \right) \tilde{\rho}_p \tilde{u} \right] \right\} + \\
& E \frac{\partial}{\partial \tilde{\xi}} \left\{ \frac{H}{\tilde{u}^2} \left[\left(\frac{\partial \tilde{\Phi}}{\partial \tilde{\xi}} - \tilde{U}'_{11} \sin \left(\frac{4\pi}{3\tilde{a}} \tilde{\xi} - \frac{\pi}{3} \right) + \tilde{U}'_{22} \sin \left(\frac{8\pi}{3\tilde{a}} \tilde{\xi} - \frac{2\pi}{3} \right) \right) \tilde{\rho}_e \tilde{u} \right] \right\} = 0 \tag{3.37}
\end{aligned}$$

655
656
657

Energy equation for the positive particles:

$$\begin{aligned}
& \frac{\partial}{\partial \tilde{\xi}} \left[\tilde{\rho}_p \tilde{u}^2 (\tilde{u} - 1) + 5 \frac{V_{0p}^2}{u_0^2} \tilde{p}_p \tilde{u} - 3 \frac{V_{0p}^2}{u_0^2} \tilde{p}_p \right] - \\
& 2 \frac{m_e}{m_p} \tilde{\rho}_p E \left(-\frac{\partial \tilde{\Phi}}{\partial \tilde{\xi}} + \tilde{U}'_{11} \sin \left(\frac{4\pi}{3\tilde{a}} \tilde{\xi} - \frac{\pi}{3} \right) - \tilde{U}'_{22} \sin \left(\frac{8\pi}{3\tilde{a}} \tilde{\xi} - \frac{2\pi}{3} \right) \right) \tilde{u} +
\end{aligned}$$

658

$$\begin{aligned}
& \frac{\partial}{\partial \tilde{\xi}} \left\{ \frac{H}{\tilde{u}^2} \frac{m_e}{m_p} \left[\frac{\partial}{\partial \tilde{\xi}} \left(-\tilde{\rho}_p \tilde{u}^2 (1-\tilde{u})^2 + 7 \frac{V_{0p}^2}{u_0^2} \tilde{p}_p \tilde{u} (1-\tilde{u}) + 3 \frac{V_{0p}^2}{u_0^2} \tilde{p}_p (\tilde{u}-1) - \frac{V_{0p}^2}{u_0^2} \tilde{p}_p \tilde{u}^2 - \right. \right. \right. \\
659 & \left. \left. \left. 5 \frac{V_{0p}^4}{u_0^4} \frac{\tilde{p}_p^2}{\tilde{\rho}_p} \right) + E \left(-2 \frac{m_e}{m_p} \tilde{\rho}_p \tilde{u} (1-\tilde{u}) + \frac{m_e}{m_p} \tilde{\rho}_p \tilde{u}^2 + 5 \frac{m_e}{m_p} \frac{V_{0p}^2}{u_0^2} \tilde{p}_p \right) \left(-\frac{\partial \tilde{\phi}}{\partial \tilde{\xi}} + \right. \right. \\
& \left. \left. \tilde{U}'_{11} \sin \left(\frac{4\pi}{3\tilde{a}} \tilde{\xi} - \frac{\pi}{3} \right) - \tilde{U}'_{22} \sin \left(\frac{8\pi}{3\tilde{a}} \tilde{\xi} - \frac{2\pi}{3} \right) \right) \right] \left. \right\} + 2 \frac{H}{\tilde{u}^2} E \left(\frac{m_e}{m_p} \right)^2 \left[-\frac{\partial}{\partial \tilde{\xi}} (\tilde{\rho}_p \tilde{u} (1-\tilde{u})) + \right. \\
660 & \left. \frac{V_{0p}^2}{u_0^2} \frac{\partial}{\partial \tilde{\xi}} \tilde{p}_p \right] \left[-\frac{\partial \tilde{\phi}}{\partial \tilde{\xi}} + \tilde{U}'_{11} \sin \left(\frac{4\pi}{3\tilde{a}} \tilde{\xi} - \frac{\pi}{3} \right) - \tilde{U}'_{22} \sin \left(\frac{8\pi}{3\tilde{a}} \tilde{\xi} - \frac{2\pi}{3} \right) \right] - \\
& 2 \frac{H}{\tilde{u}^2} E^2 \left(\frac{m_e}{m_p} \right)^3 \tilde{\rho}_p \left[\left(-\frac{\partial \tilde{\phi}}{\partial \tilde{\xi}} + \tilde{U}'_{11} \sin \left(\frac{4\pi}{3\tilde{a}} \tilde{\xi} - \frac{\pi}{3} \right) - \tilde{U}'_{22} \sin \left(\frac{8\pi}{3\tilde{a}} \tilde{\xi} - \frac{2\pi}{3} \right) \right)^2 + \right. \\
& \frac{1}{2} \left(\tilde{U}'_{10} \sin \left(\frac{2\pi}{3\tilde{a}} \tilde{\xi} + \frac{\pi}{3} \right) + 6 \tilde{U}'_{12} \sin \left(\frac{2\pi}{\tilde{a}} \tilde{\xi} \right) \right)^2 + \frac{1}{2} (\tilde{U}'_{12})^2 \cos^2 \left(\frac{2\pi}{3\tilde{a}} \tilde{\xi} - \frac{\pi}{6} \right) + \\
& \frac{1}{2} (\tilde{U}'_{02})^2 \sin^2 \left(\frac{4\pi}{3\tilde{a}} \tilde{\xi} + \frac{2\pi}{3} \right) - \frac{4}{3\pi} \tilde{U}'_{02} \sin \left(\frac{4\pi}{3\tilde{a}} \tilde{\xi} + \frac{2\pi}{3} \right) \left(\tilde{U}'_{10} \sin \left(\frac{2\pi}{3\tilde{a}} \tilde{\xi} + \frac{\pi}{3} \right) - \right. \\
& 6 \tilde{U}'_{12} \sin \left(\frac{2\pi}{\tilde{a}} \tilde{\xi} \right) \left. \right) - \frac{12}{5\pi} \tilde{U}'_{02} \tilde{U}'_{12} \sin \left(\frac{4\pi}{3\tilde{a}} \tilde{\xi} + \frac{2\pi}{3} \right) \cos \left(\frac{2\pi}{3\tilde{a}} \tilde{\xi} - \frac{\pi}{6} \right) + \\
& \frac{3}{2} \left(\tilde{U}'_{10} \cos \left(\frac{2\pi}{3\tilde{a}} \tilde{\xi} + \frac{\pi}{3} \right) + 2 \tilde{U}'_{12} \cos \left(\frac{2\pi}{\tilde{a}} \tilde{\xi} \right) \right)^2 + \\
& \frac{3}{2} \left(2 \tilde{U}'_{11} - \tilde{U}'_{02} \cos \left(\frac{4\pi}{3\tilde{a}} \tilde{\xi} + \frac{2\pi}{3} \right) \right)^2 + \frac{27}{2} (\tilde{U}'_{12})^2 \sin^2 \left(\frac{2\pi}{3\tilde{a}} \tilde{\xi} - \frac{\pi}{6} \right) + 6 (\tilde{U}'_{22})^2 + \\
& \frac{8}{\pi} \left(\tilde{U}'_{10} \cos \left(\frac{2\pi}{3\tilde{a}} \tilde{\xi} + \frac{\pi}{3} \right) + 2 \tilde{U}'_{12} \cos \left(\frac{2\pi}{\tilde{a}} \tilde{\xi} \right) \right) \left(2 \tilde{U}'_{11} - \tilde{U}'_{02} \cos \left(\frac{4\pi}{3\tilde{a}} \tilde{\xi} + \frac{2\pi}{3} \right) \right) - \\
& \frac{96}{15\pi} \left(\tilde{U}'_{10} \cos \left(\frac{2\pi}{3\tilde{a}} \tilde{\xi} + \frac{\pi}{3} \right) + 2 \tilde{U}'_{12} \cos \left(\frac{2\pi}{\tilde{a}} \tilde{\xi} \right) \right) \tilde{U}'_{22} - \\
661 & \left. \frac{72}{5\pi} \tilde{U}'_{12} \left(2 \tilde{U}'_{11} - \tilde{U}'_{02} \cos \left(\frac{4\pi}{3\tilde{a}} \tilde{\xi} + \frac{2\pi}{3} \right) \right) \sin \left(\frac{2\pi}{3\tilde{a}} \tilde{\xi} - \frac{\pi}{6} \right) - \frac{288}{7\pi} \tilde{U}'_{12} \tilde{U}'_{22} \sin \left(\frac{2\pi}{3\tilde{a}} \tilde{\xi} - \frac{\pi}{6} \right) \right] = \\
662 & - \frac{\tilde{u}^2}{Hu_0^2} (V_{0p}^2 \tilde{p}_p - \tilde{p}_e V_{0e}^2) \left(1 + \frac{m_p}{m_e} \right) \tag{3.38}
\end{aligned}$$

663
664
665

Energy equation for electrons:

$$\begin{aligned}
& \frac{\partial}{\partial \tilde{\xi}} \left[\tilde{\rho}_e \tilde{u}^2 (\tilde{u} - 1) + 5 \frac{V_{0e}^2}{u_0^2} \tilde{p}_e \tilde{u} - 3 \frac{V_{0e}^2}{u_0^2} \tilde{p}_e \right] - \\
& 2 \tilde{\rho}_e \tilde{u} E \left(\frac{\partial \tilde{\varphi}}{\partial \tilde{\xi}} - \tilde{U}'_{11} \sin \left(\frac{4\pi}{3\tilde{a}} \tilde{\xi} - \frac{\pi}{3} \right) + \tilde{U}'_{22} \sin \left(\frac{8\pi}{3\tilde{a}} \tilde{\xi} - \frac{2\pi}{3} \right) \right) + \\
& \frac{\partial}{\partial \tilde{\xi}} \left\{ \frac{H}{\tilde{u}^2} \left[\frac{\partial}{\partial \tilde{\xi}} \left(-\tilde{\rho}_e \tilde{u}^2 (1 - \tilde{u})^2 + 7 \frac{V_{0e}^2}{u_0^2} \tilde{p}_e \tilde{u} (1 - \tilde{u}) + 3 \frac{V_{0e}^2}{u_0^2} \tilde{p}_e (\tilde{u} - 1) - \frac{V_{0e}^2}{u_0^2} \tilde{p}_e \tilde{u}^2 - \right. \right. \right. \\
& 5 \frac{V_{0e}^4}{u_0^4} \frac{\tilde{p}_e^2}{\tilde{\rho}_e} \left. \left. \right) + E \left(-2 \tilde{\rho}_e \tilde{u} (1 - \tilde{u}) + \tilde{\rho}_e \tilde{u}^2 + 5 \frac{V_{0e}^2}{u_0^2} \tilde{p}_e \right) \left(\frac{\partial \tilde{\varphi}}{\partial \tilde{\xi}} - \right. \right. \\
& \tilde{U}'_{11} \sin \left(\frac{4\pi}{3\tilde{a}} \tilde{\xi} - \frac{\pi}{3} \right) + \tilde{U}'_{22} \sin \left(\frac{8\pi}{3\tilde{a}} \tilde{\xi} - \frac{2\pi}{3} \right) \left. \left. \right) \right\} + \\
& E \left(-2 \frac{H}{\tilde{u}^2} \frac{\partial}{\partial \tilde{\xi}} (\tilde{\rho}_e \tilde{u} (1 - \tilde{u})) + 2 \frac{H}{\tilde{u}^2} \frac{V_{0e}^2}{u_0^2} \frac{\partial}{\partial \tilde{\xi}} \tilde{p}_e \right) \left(\frac{\partial \tilde{\varphi}}{\partial \tilde{\xi}} - \right. \\
& \tilde{U}'_{11} \sin \left(\frac{4\pi}{3\tilde{a}} \tilde{\xi} - \frac{\pi}{3} \right) + \tilde{U}'_{22} \sin \left(\frac{8\pi}{3\tilde{a}} \tilde{\xi} - \frac{2\pi}{3} \right) \left. \right) - \\
& 2E^2 \frac{H}{\tilde{u}^2} \tilde{\rho}_e \left[\left(-\frac{\partial \tilde{\varphi}}{\partial \tilde{\xi}} + \tilde{U}'_{11} \sin \left(\frac{4\pi}{3\tilde{a}} \tilde{\xi} - \frac{\pi}{3} \right) - \tilde{U}'_{22} \sin \left(\frac{8\pi}{3\tilde{a}} \tilde{\xi} - \frac{2\pi}{3} \right) \right)^2 + \right. \\
& \frac{1}{2} \left(\tilde{U}'_{10} \sin \left(\frac{2\pi}{3\tilde{a}} \tilde{\xi} + \frac{\pi}{3} \right) + 6 \tilde{U}'_{12} \sin \left(\frac{2\pi}{\tilde{a}} \tilde{\xi} \right) \right)^2 + \frac{1}{2} (\tilde{U}'_{12})^2 \cos^2 \left(\frac{2\pi}{3\tilde{a}} \tilde{\xi} - \frac{\pi}{6} \right) + \\
& \frac{1}{2} (\tilde{U}'_{02})^2 \sin^2 \left(\frac{4\pi}{3\tilde{a}} \tilde{\xi} + \frac{2\pi}{3} \right) - \frac{4}{3\pi} \tilde{U}'_{02} \sin \left(\frac{4\pi}{3\tilde{a}} \tilde{\xi} + \frac{2\pi}{3} \right) \left(\tilde{U}'_{10} \sin \left(\frac{2\pi}{3\tilde{a}} \tilde{\xi} + \frac{\pi}{3} \right) + \right. \\
& 6 \tilde{U}'_{12} \sin \left(\frac{2\pi}{\tilde{a}} \tilde{\xi} \right) \left. \right) - \frac{12}{5\pi} \tilde{U}'_{02} \tilde{U}'_{12} \sin \left(\frac{4\pi}{3\tilde{a}} \tilde{\xi} + \frac{2\pi}{3} \right) \cos \left(\frac{2\pi}{3\tilde{a}} \tilde{\xi} - \frac{\pi}{6} \right) + \\
& \frac{3}{2} \left(\tilde{U}'_{10} \cos \left(\frac{2\pi}{3\tilde{a}} \tilde{\xi} + \frac{\pi}{3} \right) + 2 \tilde{U}'_{12} \cos \left(\frac{2\pi}{\tilde{a}} \tilde{\xi} \right) \right)^2 + \\
& \frac{3}{2} \left(2 \tilde{U}'_{11} - \tilde{U}'_{02} \cos \left(\frac{4\pi}{3\tilde{a}} \tilde{\xi} + \frac{2\pi}{3} \right) \right)^2 + \frac{27}{2} (\tilde{U}'_{12})^2 \sin^2 \left(\frac{2\pi}{3\tilde{a}} \tilde{\xi} - \frac{\pi}{6} \right) + 6 (\tilde{U}'_{22})^2 + \\
& \frac{8}{\pi} \left(\tilde{U}'_{10} \cos \left(\frac{2\pi}{3\tilde{a}} \tilde{\xi} + \frac{\pi}{3} \right) + 2 \tilde{U}'_{12} \cos \left(\frac{2\pi}{\tilde{a}} \tilde{\xi} \right) \right) \left(2 \tilde{U}'_{11} - \tilde{U}'_{02} \cos \left(\frac{4\pi}{3\tilde{a}} \tilde{\xi} + \frac{2\pi}{3} \right) \right) - \\
& \frac{96}{15\pi} \left(\tilde{U}'_{10} \cos \left(\frac{2\pi}{3\tilde{a}} \tilde{\xi} + \frac{\pi}{3} \right) + 2 \tilde{U}'_{12} \cos \left(\frac{2\pi}{\tilde{a}} \tilde{\xi} \right) \right) \tilde{U}'_{22} -
\end{aligned}$$

$$\begin{aligned}
& \frac{72}{5\pi} \tilde{U}'_{12} \left(2\tilde{U}'_{11} - \tilde{U}'_{02} \cos \left(\frac{4\pi}{3\tilde{a}} \tilde{\xi} + \frac{2\pi}{3} \right) \right) \sin \left(\frac{2\pi}{3\tilde{a}} \tilde{\xi} - \frac{\pi}{6} \right) - \frac{288}{7\pi} \tilde{U}'_{12} \tilde{U}'_{22} \sin \left(\frac{2\pi}{3\tilde{a}} \tilde{\xi} - \frac{\pi}{6} \right) \Bigg] = \\
& - \frac{\tilde{u}^2}{Hu_0^2} (V_{0e}^2 \tilde{p}_e - V_{0p}^2 \tilde{p}_p) \left(1 + \frac{m_p}{m_e} \right) \quad (3.39)
\end{aligned}$$

4. ESTIMATIONS OF THE NUMERICAL PARAMETERS

We need estimations for the numerical values of dimensionless parameters for solutions of the hydrodynamic equations (3.34) - (3.39). In its turn these parameters depend on choosing of the independent scales of physical values. Analyze the independent scales for the physical problem under consideration. It should be stressed that we choose just scales but not real physical values which may differ significantly from scale values. Real physical values will be obtained as a result of numerical self-consistent calculations.

Assume that the surface electron density in graphene is about $\tilde{n}_e \approx 10^{10} \text{ cm}^{-2}$ (such value is typical for many experiments (see [35-37])), the thickness of the graphene layer is equal to $\sim 1 \text{ nm}$. Then the electron concentration consists $n_e \approx 10^{17} \text{ cm}^{-3}$, and the density for the electron species $\rho_e = m_e n_e \approx 10^{-10} \text{ g/cm}^3$ which leads to the scale $\rho_0 = 10^{-10} \text{ g/cm}^3$. For numerical solutions of the hydrodynamic equations (3.34)-(3.39) we need Cauchy conditions, obviously in the typical for graphene conditions the estimation $\tilde{\rho}_e \sim 1$ is valid which can be used as the condition by $\tilde{\xi} = 0$.

The process of the carbon atoms polarization leads to displacement of the atoms from the regular chain and to the creation of the "effective" positive particles which concentration $n_p \approx n_e$. Masses of these particles is about the mass of the carbon atom

$$m_p \approx 2 \cdot 10^{-23} \text{ g}. \text{ Then, } \frac{L}{T} = \frac{m_e}{m_p} \approx 5 \cdot 10^{-5}; \quad \rho_p = m_p n_p \approx 2 \cdot 10^{-6} \text{ g/cm}^3 \text{ and by the}$$

choosed scale for the density ρ_0 we have $\tilde{\rho}_p \sim 2 \cdot 10^4$.

Going to the scales for thermal velocities for electrons and the positive particles we have by $T=300 \text{ K}$:

$$V_{0e} \sim \sqrt{\frac{k_B T}{m_e}} \approx 6.4 \cdot 10^6 \text{ cm/s}, \text{ take the scale } V_{0e} = 5 \cdot 10^6 \text{ cm/s};$$

$$V_{0p} \sim \sqrt{\frac{k_B T}{m_p}} \approx 4.5 \cdot 10^4 \text{ cm/s}, \text{ take the scale } V_{0p} = 5 \cdot 10^4 \text{ cm/s}.$$

The theoretical mobility in graphene reaches up to $10^6 \text{ cm}^2/\text{V} \cdot \text{s}$ [38]. Let us use the scale

$$u_0 = 5 \cdot 10^6 \text{ cm/s}. \text{ Then } N = \frac{V_{0e}^2}{u_0^2} = 1, \quad P = \frac{V_{0p}^2}{u_0^2} = 10^{-4}.$$

Let us estimate the parameters E and R . For this estimation we need the scale φ_0 .

Admit $\varphi_0 \approx \delta \frac{e}{a}$, where δ is a "shielding coefficient". Naturally to take $x_0 = a = 0.142 \text{ nm}$

(see figure 1) as the length scale, then $\tilde{a} = 1$. In the situation of a uncertainty in φ_0 choosing let us consider two limit cases:
 1) $\delta \sim 1$.

Then $E = \frac{e\varphi_0}{m_e u_0^2} \sim 1000$, $R = \frac{e\rho_0 x_0^2}{m_e \varphi_0} \sim 3 \cdot 10^{-7}$.

2) $\delta = 0.0001$.

Then $E = \frac{e\varphi_0}{m_e u_0^2} \sim 0.1$, $R = \frac{e\rho_0 x_0^2}{m_e \varphi_0} \sim 3 \cdot 10^{-3}$.

Consider the terms describing the lattice influence. We should estimate the coefficients (3.30) using φ_0 as the scale for the potential V , $V = \varphi_0 \tilde{V}$. Three possible cases under consideration:

1) $V \sim \varphi_0$

We choose $U = \tilde{U}'_{10} \sim 10$, $F = \tilde{U}'_{11} \sim 10$, $J = \tilde{U}'_{20} \sim \pm 5$, $B = \tilde{U}'_{12} \sim \pm 2.5$, $G = \tilde{U}'_{22} \sim \pm 5$.

In this case the coefficients of "the second order" are less than the coefficients of "the first order."

2) $V \ll \varphi_0$ (The small influence of the lattice),

We choose $U = \tilde{U}'_{10} \sim 0.1$, $F = \tilde{U}'_{11} \sim 0.1$, $J = \tilde{U}'_{20} \sim 0.05$, $B = \tilde{U}'_{12} \sim 0.025$, $G = \tilde{U}'_{22} \sim 0.05$.

3) $V \gg \varphi_0$ (The great influence of the lattice),

We choose $U = \tilde{U}'_{10} \sim 1000$, $F = \tilde{U}'_{11} \sim 1000$, $J = \tilde{U}'_{20} \sim 500$, $B = \tilde{U}'_{12} \sim 250$, $G = \tilde{U}'_{22} \sim 500$.

Estimate parameter $H = \frac{N_R \hbar}{m_e x_0 u_0}$ for two limit cases:

1) $N_R = 1$, then $H \sim 15$.

2) $N_R = 100$, then $H \sim 1500$.

Initial conditions demand also the estimations for the quantum electron pressure and the pressure for the positive species. For the electron pressure we have $p_e = \rho_0 V_{0e}^2 \tilde{p}_e$ and using for the scale estimation $p_e = n_e k_B T \sim n_e m_e V_{0e}^2 = \rho_e V_{0e}^2 \sim \rho_0 V_{0e}^2$, one obtains $\tilde{p}_e \sim 1$.

Analogically for the positive particles $p_p = \rho_0 V_{0p}^2 \tilde{p}_p$, and using $p_p = n_p k_B T \sim n_p m_p V_{0p}^2 = \rho_p V_{0p}^2$, we have $p_p \sim 2 \cdot 10^4 \rho_0 V_{0p}^2$, $\tilde{p}_p \sim 2 \cdot 10^4$.

Tables 1, 2 contain the initial conditions and parameters which were not varied by the numerical modeling.

Table 1. Initial conditions.

| $\tilde{\rho}_e(0)$ | $\tilde{\rho}_p(0)$ | $\tilde{\varphi}(0)$ | $\tilde{p}_e(0)$ | $\tilde{p}_p(0)$ | $\frac{\partial \tilde{\rho}_e}{\partial \tilde{\xi}}(0)$ | $\frac{\partial \tilde{\rho}_p}{\partial \tilde{\xi}}(0)$ | $\frac{\partial \tilde{\varphi}}{\partial \tilde{\xi}}(0)$ | $\frac{\partial \tilde{p}_e}{\partial \tilde{\xi}}(0)$ | $\frac{\partial \tilde{p}_p}{\partial \tilde{\xi}}(0)$ |
|---------------------|---------------------|----------------------|------------------|------------------|---|---|--|--|--|
| 1 | $2 \cdot 10^4$ | 1 | 1 | $2 \cdot 10^4$ | 0 | 0 | 0 | 0 | 0 |

Table 2. Constant parameters.

| \tilde{a} | L | T | N | P |
|-------------|-----|-------|-----|-----------|
| 1 | 1 | 20000 | 1 | 10^{-4} |

Table 3 contains parameters (for the six different cases) which were varied by the numerical modeling.

Table 3. Varied parameters.

| Variant № | E | R | H | U | F | J | B | G |
|-----------|------|-------------------|------|------|------|------|-------|------|
| 1 | 0.1 | 0.003 | 15 | 10 | 10 | 5 | 2.5 | 5 |
| 2 | 0.1 | 0.003 | 15 | 0.1 | 0.1 | 0.05 | 0.025 | 0.05 |
| 3 | 0.1 | 0.003 | 15 | 10 | 10 | -5 | -2.5 | -5 |
| 4 | 1000 | $3 \cdot 10^{-7}$ | 15 | 10 | 10 | 5 | 2.5 | 5 |
| 5 | 0.1 | 0.003 | 1500 | 10 | 10 | 5 | 2.5 | 5 |
| 6 | 0.1 | 0.003 | 15 | 1000 | 1000 | 500 | 250 | 500 |

In the present time there no the foolproof methods of the calculations of the potential lattice forces in graphene. In the following mathematical modeling the strategy is taken consisting in the vast variation of the parameters defining the evolution of the physical system.

5. RESULTS OF THE MATHEMATICAL MODELING WITHOUT THE EXTERNAL ELECTRIC FIELD

The calculations are realized on the basement of equations (3.34)-(3.39) by the initial conditions and parameters containing in the Tables 1 – 3. Now we are ready to display the results of the mathematical modeling realized with the help of Maple (the versions Maple 9 or more can be used). The system of generalized hydrodynamic equations (3.34) – (3.39) have the great possibilities of mathematical modeling as result of changing of Cauchy conditions and parameters describing the character features of initial perturbations which lead to the soliton formation.

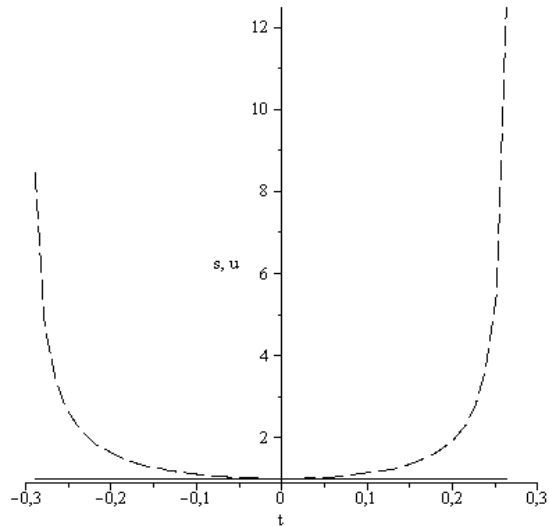
The mathematical software Maple (beginning with the version 9) is applicable; the following Maple notations on figures are used: r- density $\tilde{\rho}_r$, s - density $\tilde{\rho}_s$, u- velocity \tilde{u} (

solid black line), p - pressure \tilde{p}_p (black dashed line), q – pressure \tilde{p}_e and v - self consistent potential $\tilde{\phi}$. Explanations placed under all following figures, Maple program contains Maple's notations – for example, the expression $D(u)(0) = 0$ means in the usual

notations $\frac{\partial \tilde{u}}{\partial \tilde{\xi}}(0) = 0$, independent variable t responds to $\tilde{\xi}$.

Important to underline that no special boundary conditions were used for all following cases. The aim of the numerical investigation consists in the discovery of the soliton waves as a product of the self-organization of matter in graphene. It means that the solution should exist only in the restricted domain of the 1D space and the obtained object in the moving coordinate system ($\tilde{\xi} = \tilde{x} - \tilde{t}$) has the constant velocity $\tilde{u} = 1$ for all parts of the object. In this case the domain of the solution existence defines the character soliton size. The following numerical results demonstrate the realization of mentioned principles.

768 Figures 2 - 9 reflect the result of calculations for Variant 1 (Table 3) in the first and
 769 the second approximations. In the first approximation the terms of series (3.25) with $|g_1| \leq 1$,
 770 $|g_2| \leq 1$ (then coefficients U and F) were taken into account. The second approximation
 771 contains all terms of the series (3.25) with $|g_1| \leq 2$, $|g_2| \leq 2$ (then coefficients U , F , J , B
 772 and G).



773
 774 Figure 2. s – the electron density $\tilde{\rho}_e$,
 775 u – velocity \tilde{u} (solid line).
 776 (first approximation, Variant 1).
 777

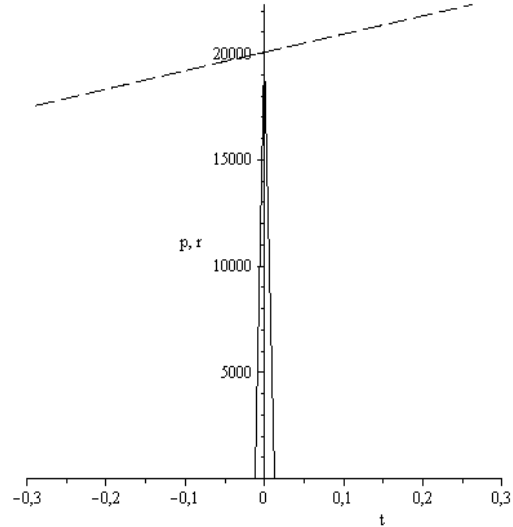
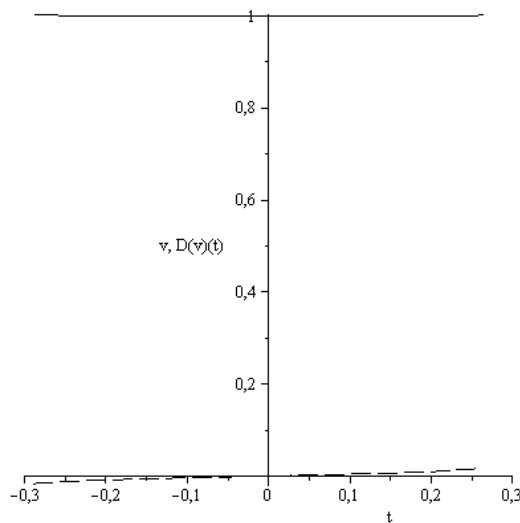


Figure 3. r – the positive particles density,
 (solid line); p – the positive particles pressure
 (first approximation, Variant 1)



778
 779 Figure 4. v – potential $\tilde{\varphi}$ (solid line).
 780 and derivative $D(v)(t)$.
 781 (first approximation, Variant 1).
 782

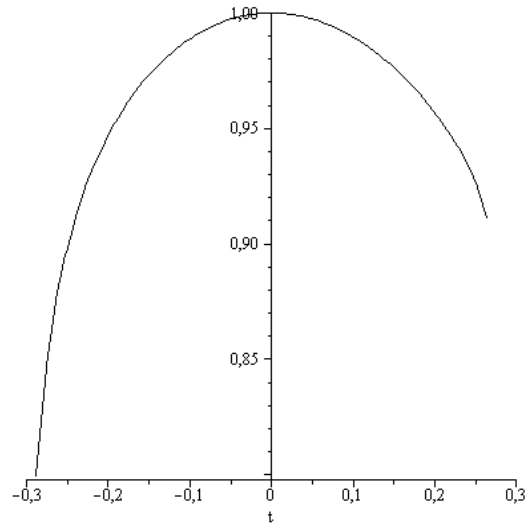
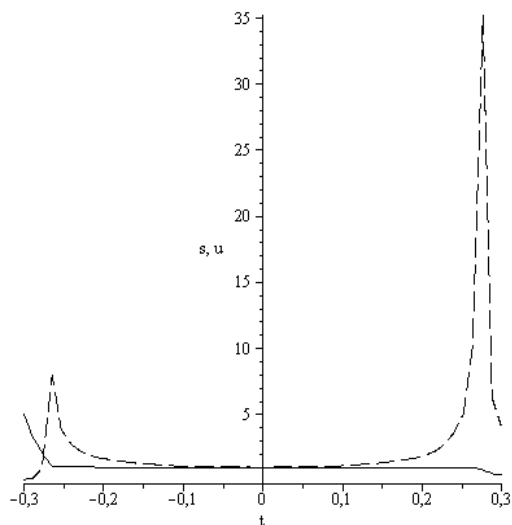


Figure 5. q – electron pressure.
 (first approximation, Variant 1).



783
784 Figure 6. s – electron density $\tilde{\rho}_e$,
785 u – velocity \tilde{u} (solid line),
786 (the second approximation, Variant 1).
787

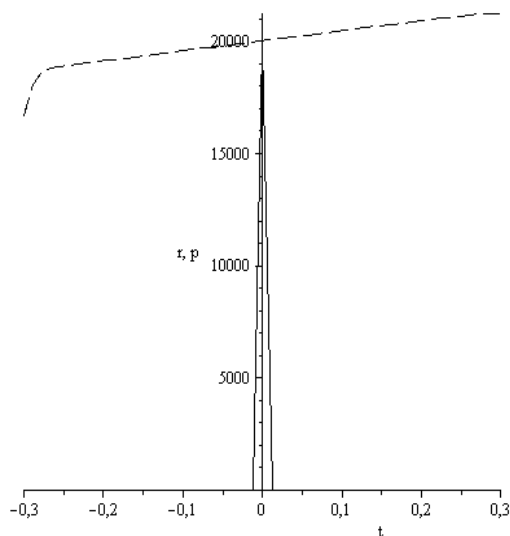
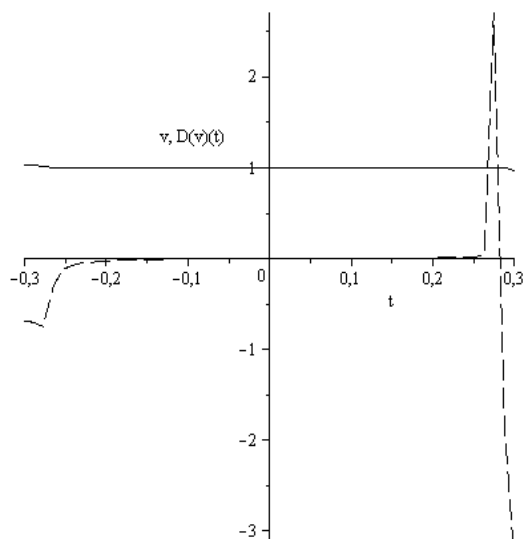


Figure 7. r – the positive particles density (solid line)
 p – the positive particles pressure,
(the second approximation, Variant 1).



788
789 Figure 8. v – potential $\tilde{\varphi}$ (solid line),
790 and derivative $D(v)(t)$.
791 (the second approximation, Variant 1).
792

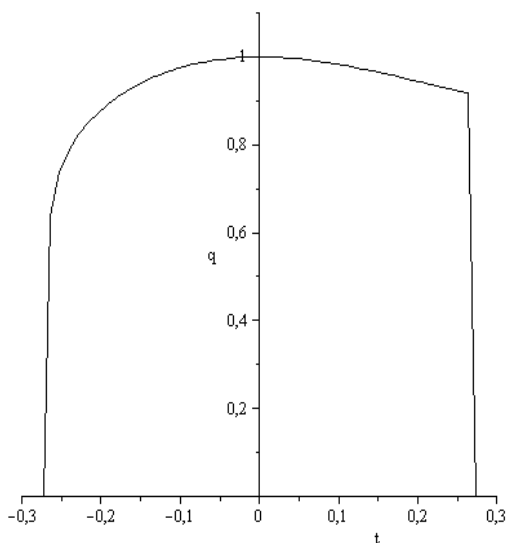


Figure 9. q – electron pressure.
(the second approximation, Variant 1).

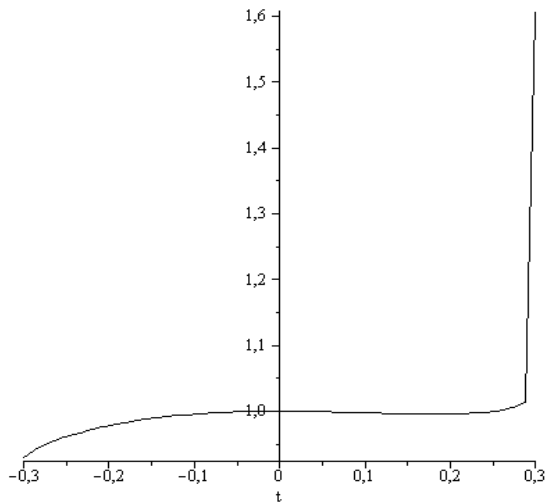
793 From figures 2 - 9 follow that the size of the created soliton is about $0.5a$, where
794 $a=0.142 \text{ nm}$. The domain size occupied by the polarized positive charge is about $0.025a$
795 (see Figs. 3, 7). But the negative charge distributes over the entire soliton domain (Figs. 2,
796 6), but the negative charge density increases to the edges of the soliton. Therefore the
797 soliton structure reminds the 1D atom with the positive nuclei and the negative shell.

798 The self-consistent potential $\tilde{\varphi}$ is practically constant in the soliton boundaries,
799 (Figs. 4, 8). The small grows of the positive particles pressure exists in the x direction. This

800 effect can be connected with the hydrodynamic movement along x and “the reconstruction”
 801 of the polarized particles in the soliton front.

802 Comparing the figures 2 – 5 and 6 – 9 we conclude that the calculation results in the
 803 first and the second approximation do not vary significantly. Seemingly significant difference
 804 of figures 2 and 6 on the edges of the domain has not the physical sense because
 805 corresponds to the regions where $u \neq const$. Then the restriction of two successive
 806 approximations is justified. Along with it the question about the convergence of the series
 807 lives open because the first and the second approximations include only the restricted
 808 quantity of terms of the infinite series with the coefficients known with the small accuracy.

809 Figures 10 - 15 show the results of calculations responding to Variant 3 (Table 3). In
 810 the first approximation Variant 3 is identical to Variant 1 (coefficients $J = B = G = 0$) and
 811 only the results of the second approximation are delivered. These calculations are more
 812 complicated in the numerical realization and all curves are imaged separately, (Figures 10 –
 813 15).



814
 815 Figure 10. u – velocity \tilde{u} .
 816 (the second approximation, Variant 3).

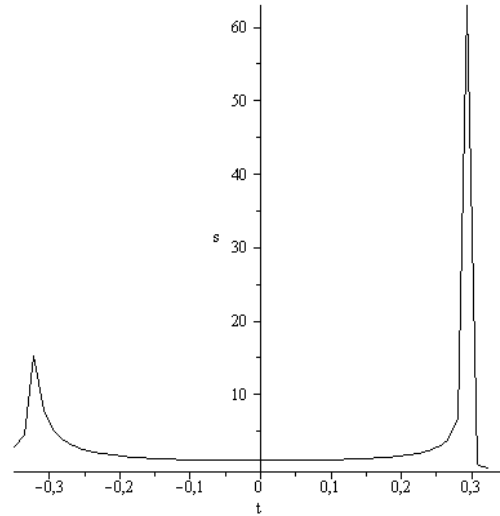
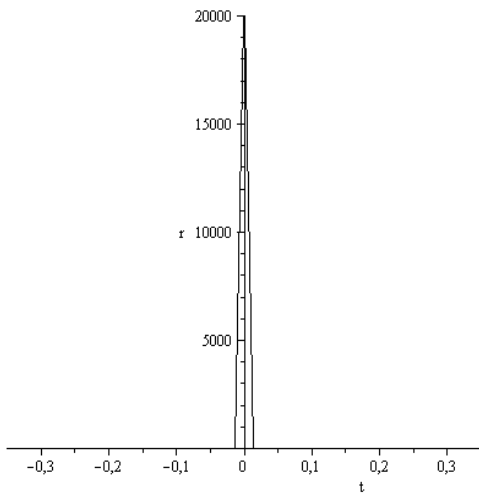


Figure 11. s – electron density $\tilde{\rho}_e$,
 (the second approximation, Variant 3).



817
 818 Figure 12. r – the positive particles density.
 819 (the second approximation, Variant 3).

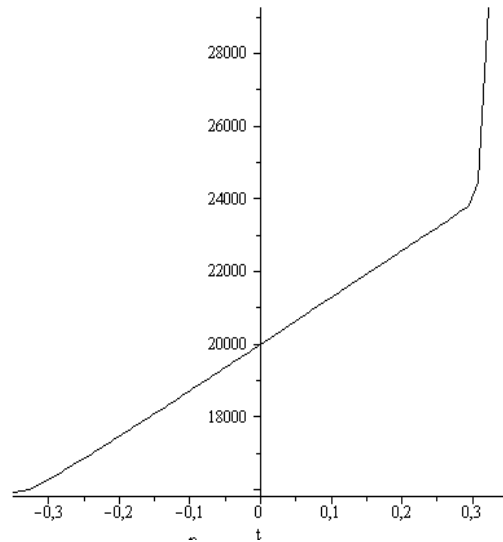


Figure 13. p – the positive particles pressure,
 (the second approximation, Variant 3).

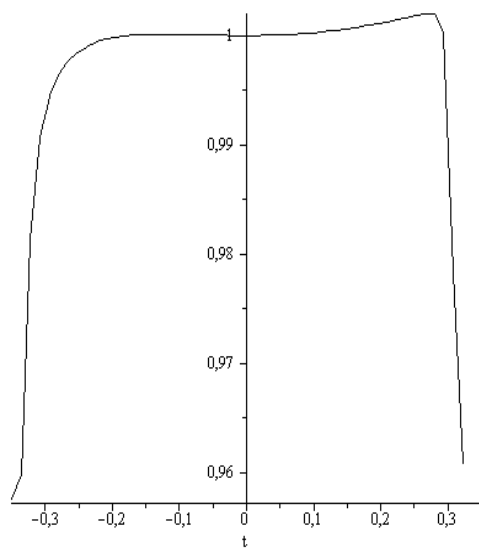


Figure 14. v – potential $\tilde{\varphi}$.
(the second approximation, Variant 3).

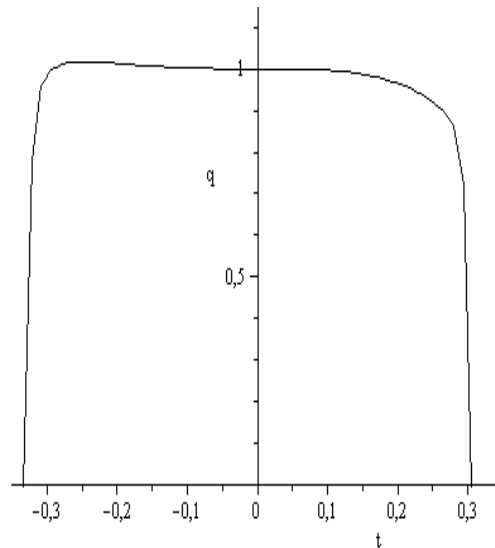


Figure 15. q – electron pressure.
(the second approximation, Variant 3).

In the comparison with Variant 1 the calculations in Variant 3 are realized for the case with opposite signs in front of the coefficients of second order. In this case the distortion of the left side of soliton is observed because by $\tilde{\xi} < 0$ the velocity \tilde{u} is not constant. Then this kind of potential for lattice is not favorable for creation of the superconducting structures.

Variant 2 (Table 3) correspond to diminishing of the lattice potential in 100 times by the same practically self-consistent potential, (see figures 16 – 23).

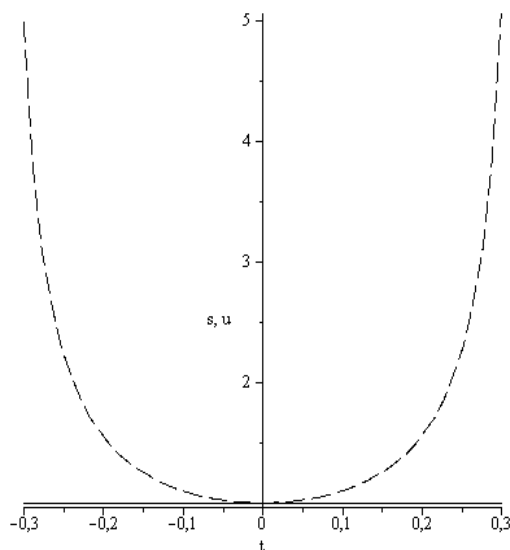


Figure 16. s – electron density $\tilde{\rho}_e$,
 u – velocity \tilde{u} (solid line).
(the first approximation, Variant 2).

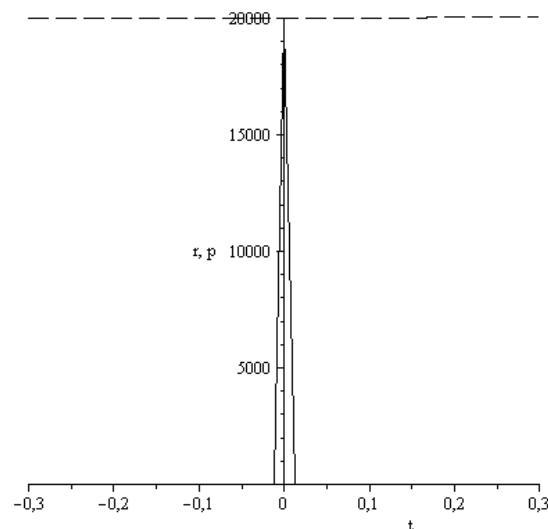
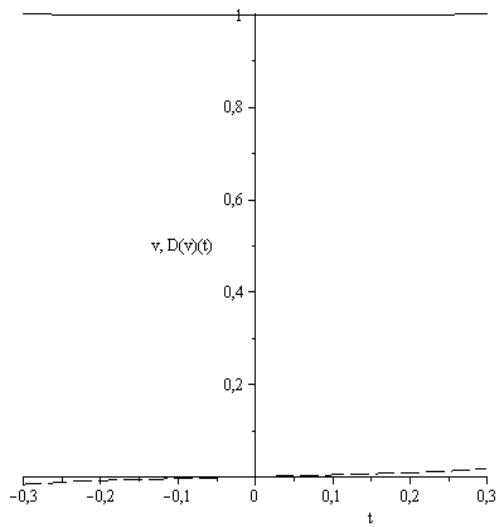


Figure 17. r – the positive particles density,
(solid line); p – the positive particles pressure
(the first approximation, Variant 2).



837
838
839
840
841

Figure 18. v – potential $\tilde{\varphi}$ (solid line),
 $D(v)(t)$, (the first approximation, Variant 2).

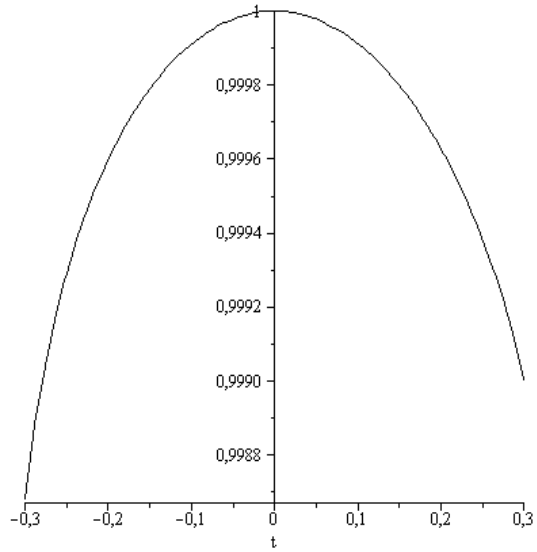
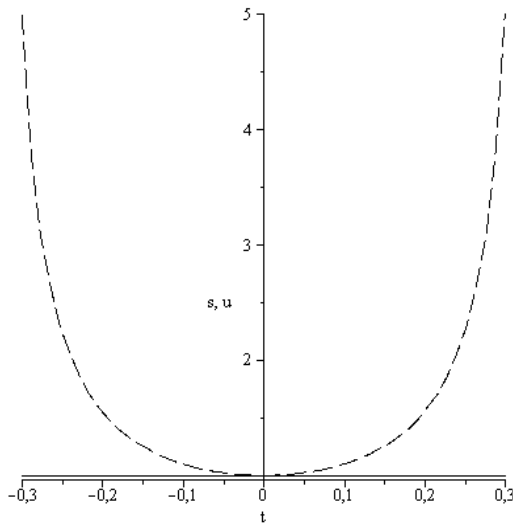


Figure 19. q – electron pressure.
(the first approximation, Variant 2).



842
843
844
845
846

Figure 20. s – electron density $\tilde{\rho}_e$,
 u – velocity \tilde{u} (solid line).
(the second approximation, Variant 2).

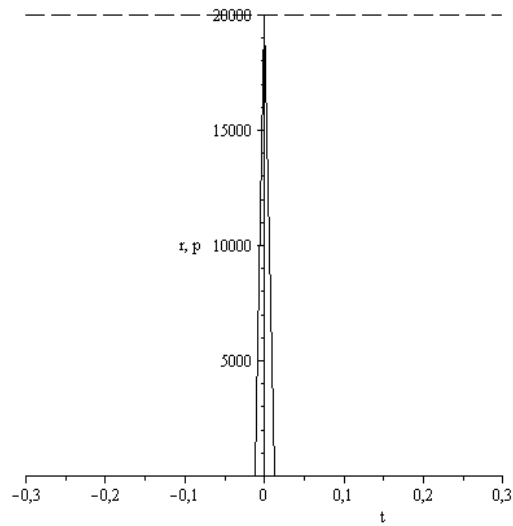


Figure 21. r – the positive particles density,
(solid line); p – the positive particles pressure
(the second approximation, Variant 2).

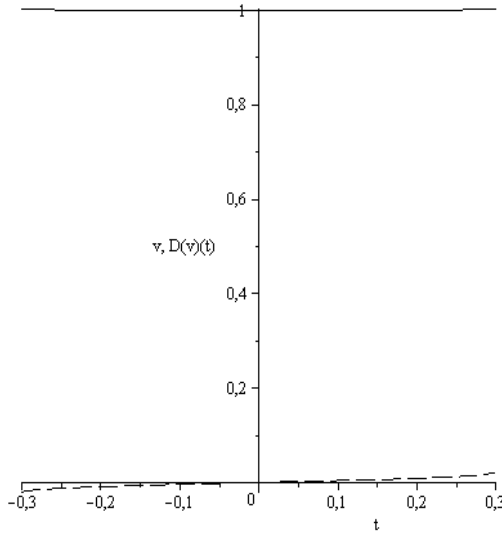


Figure 22. v – potential $\tilde{\varphi}$ (solid line),
 $D(v)(t)$.
 (the second approximation, Variant 2).

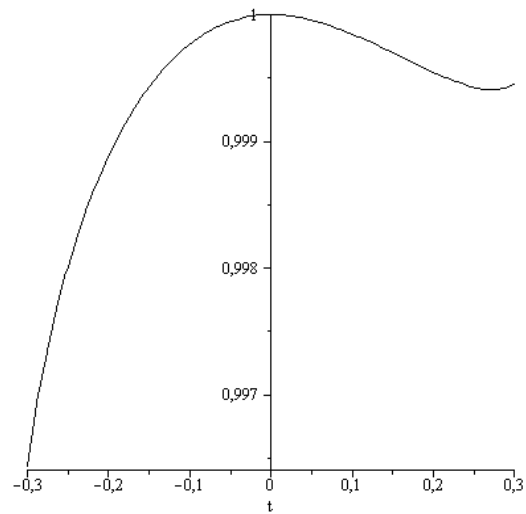


Figure 23. q – electron pressure.
 (the second approximation, Variant 2).

From comparison of figures 2 - 9 and 16 - 23 follow that numerical diminishing of the lattice potential (by the practically the same value of the self-consistent potential) does not influence on soliton size. But at the same time the solitons gain the more symmetrical forms. Therefore namely the self-consistent potential plays the basic role in the soliton formation.

Let us analyze now the influence of H - parameter, practically the influence of the non-locality parameter. Figures 24 – 31 (Variant 5) correspond to increasing of the parameter H in 100 times in comparison with Variant 1.

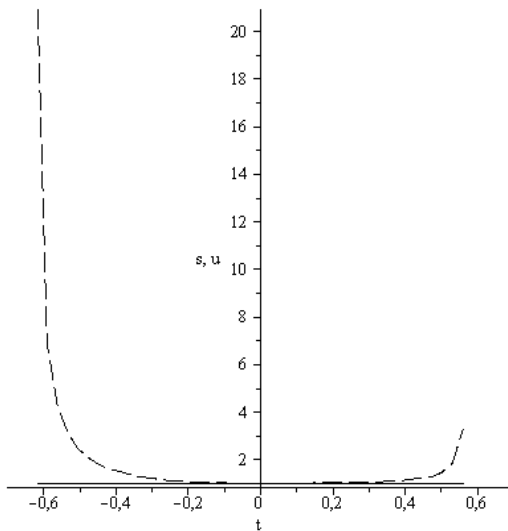


Figure 24. s – electron density $\tilde{\rho}_e$,
 u – velocity \tilde{u} (solid line).
 (the first approximation, Variant 5).

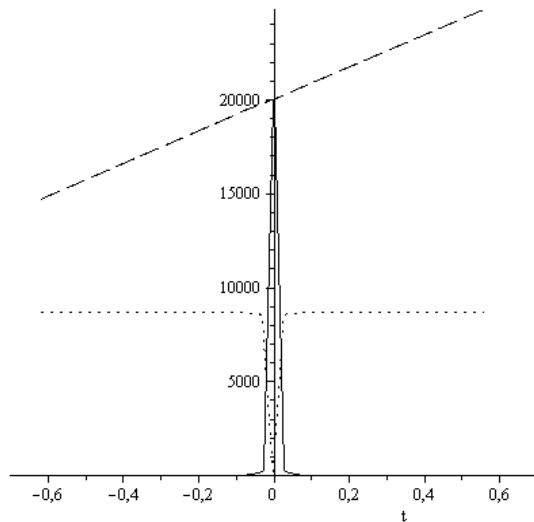
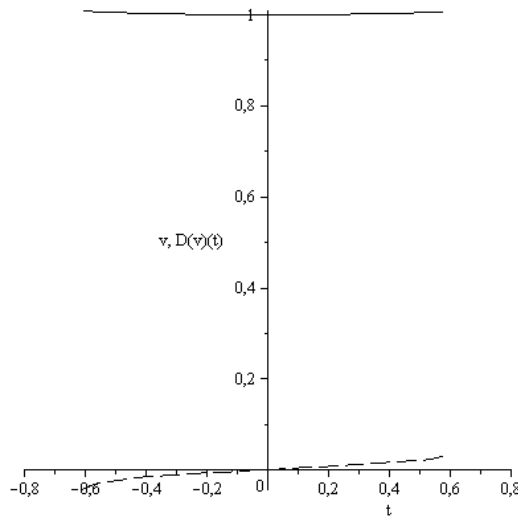


Figure 25. r – the positive particles density,
 (solid line); p – the positive particles pressure
 (dashed line), $D(p)(t)$ - dotted line.
 (the first approximation, Variant 5).

865



866

867

868

869

Figure 26. v – potential $\tilde{\varphi}$ (solid line);
 $D(v)(t)$, (the first approximation, Variant 5).

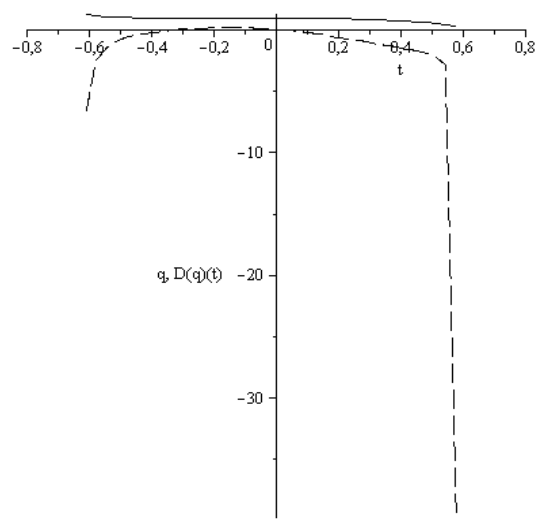
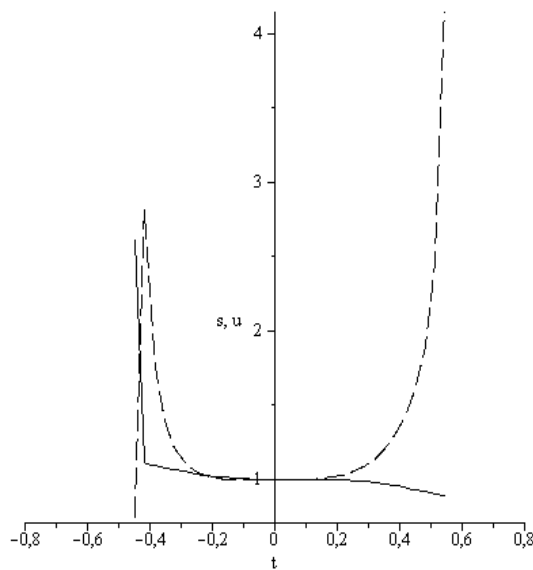


Figure 27. q – electron pressure.
(solid line), $D(q)(t)$,
(the first approximation, Variant 5)



870

871

872

873

874

Figure 28. s – electron density $\tilde{\rho}_e$,
 u – velocity \tilde{u} (solid line).
(the second approximation, Variant 5)

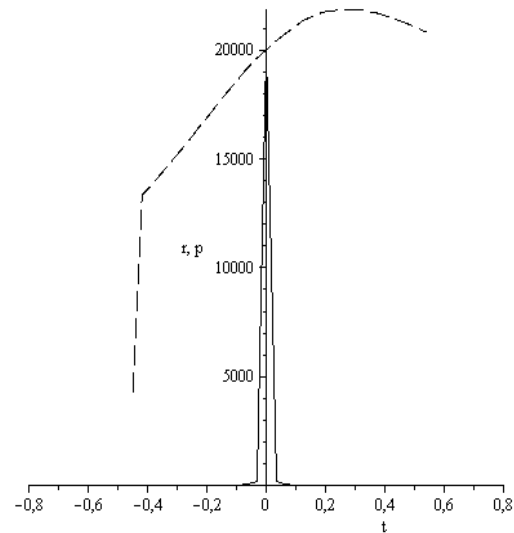
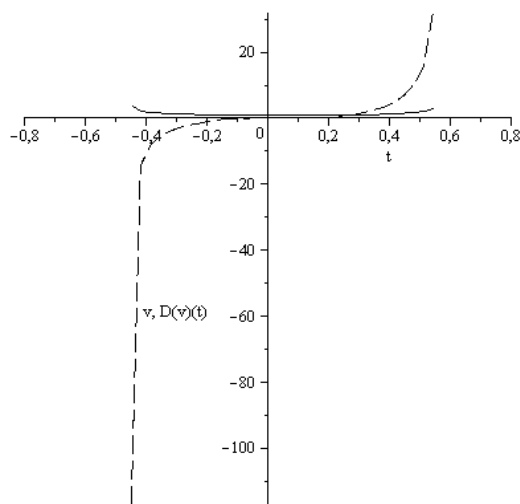


Figure 29. r – the positive particles density,
(solid line); p – the positive particles pressure
(the second approximation, Variant 5).



875
876

877 Figure 30. v – potential $\tilde{\varphi}$ (solid line);
878 $D(v)(t)$, (the second approximation, Variant 5).

879
880
881

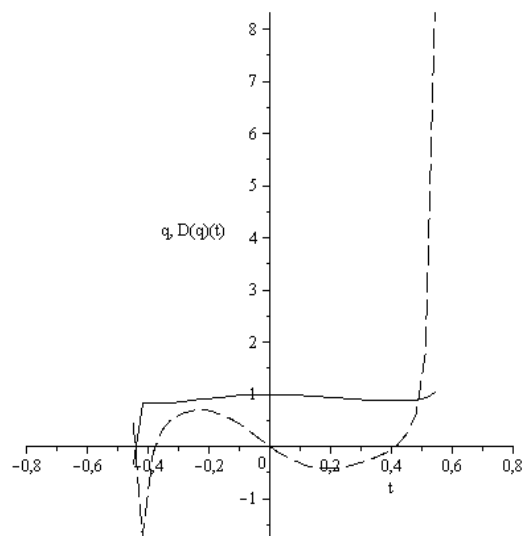
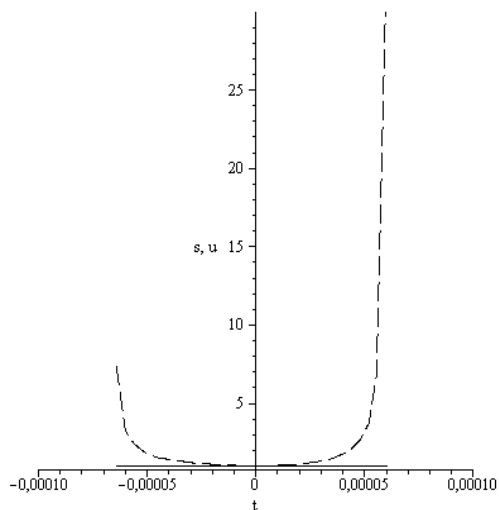


Figure 31. q – electron pressure
(solid line), $D(q)(t)$, (the second
approximation, Variant 5).

882 The comparison of figures 2 - 5 and 24 - 27 indicates that in the first approximation
883 the very significant increasing in of the H value in 100 times leads to increasing of the soliton
884 size only in two times without significant changing of the soliton structure. The comparison of
885 calculations (see figures 6 and 28) in the second approximation leads to conclusion that the
886 region (where the velocity \tilde{u} is constant) has practically the same size.

887 Consider now the calculations responding to Variant 4 (Table 3). Increasing in 10^4
888 times of the scale φ_0 denotes increasing the self consistent potential and the lattice
889 potential introduced in the process of the mathematical modeling. This case leads to the
890 drastic diminishing of the soliton size. Figures 32 - 35 demonstrate that in the calculations of
891 the first approximation the soliton size is $\sim 10^{-4} a = 1.42 \cdot 10^{-12} cm$ and exceeds the nuclei
892 size only in several times. The positive kernel of the soliton decreasing in the less degree
893 and occupies now the half of the soliton size. It is no surprise because the low boundary of
894 this kernel size is the character size of the nuclei. Application of the second approximation
895 for the lattice potential function in the mathematical modeling leads to the significant soliton
896 deformation but the same soliton size (see figures 36-39).



897
898 Figure 32. s – electron density $\tilde{\rho}_e$,
899 u – velocity \tilde{u} (solid line).
900 (the first approximation, Variant 4).
901

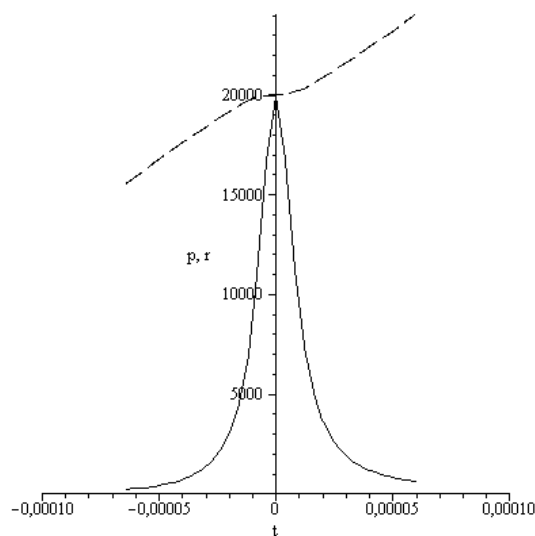
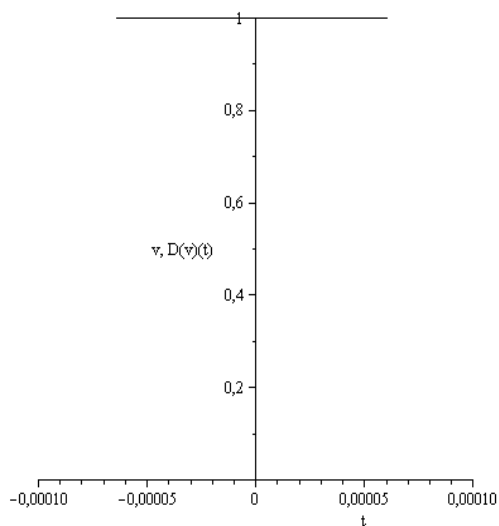


Figure 33. r – the positive particles density,
(solid line); p – the positive particles pressure
(the first approximation, Variant 4).



902
903 Figure 34. v – potential $\tilde{\varphi}$ (solid line).
904 (the first approximation, Variant 4).
905

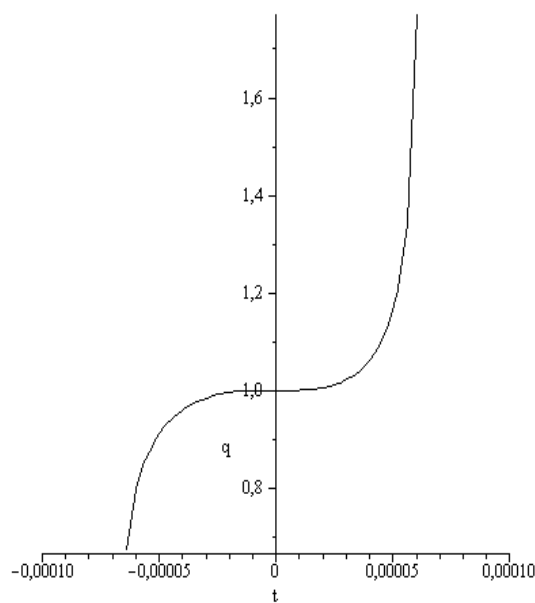
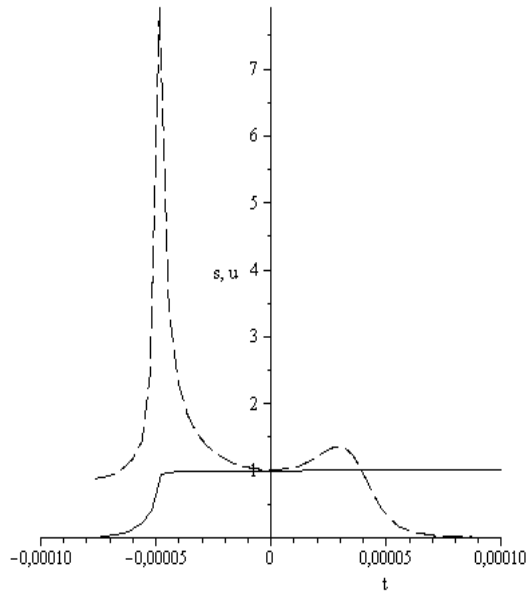


Figure 35. q – electron pressure.
(the first approximation, Variant 4).



906

907 Figure 36. s – electron density $\tilde{\rho}_e$,
 908 u – velocity \tilde{u} (solid line).
 909 (the second approximation, Variant 4).
 910

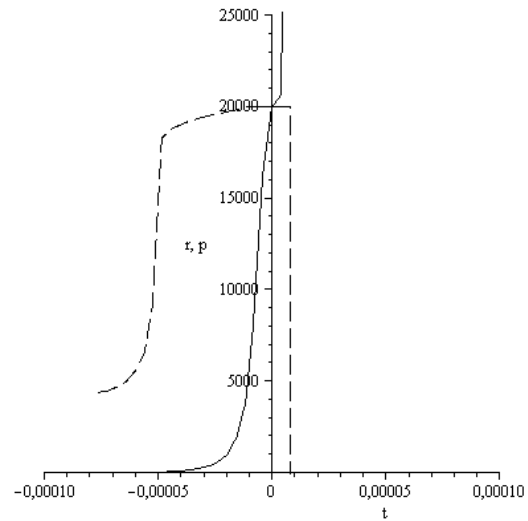
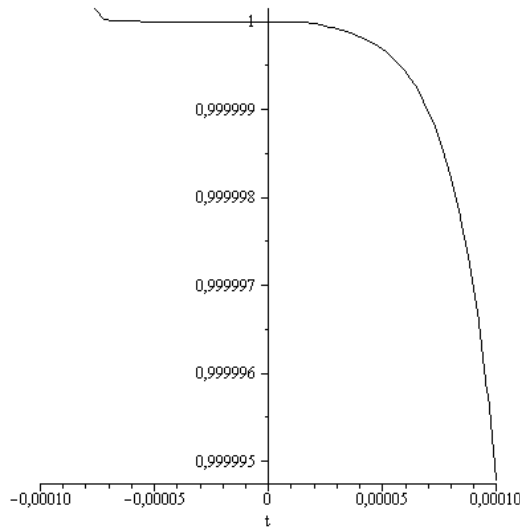


Figure 37. r – the positive particles density,
 (solid line); p – the positive particles pressure
 (the second approximation, Variant 4)



911

912 Figure 38. v – potential $\tilde{\varphi}$ (solid line).
 913 (the second approximation, Variant 4)
 914

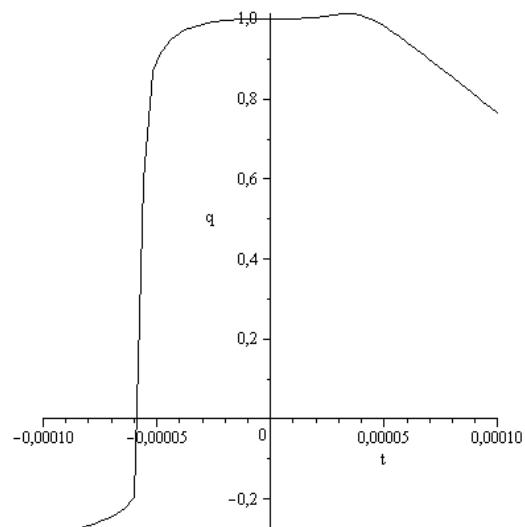
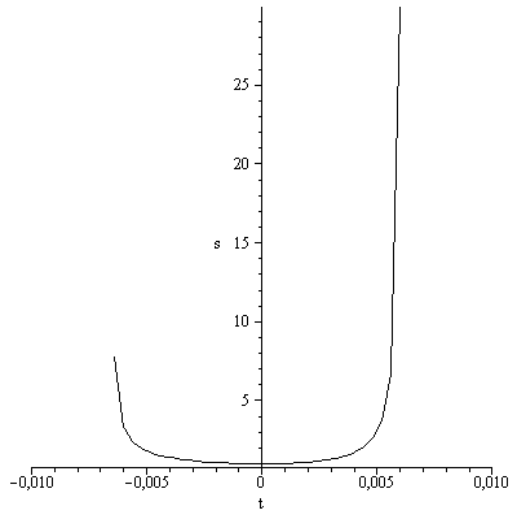


Figure 39. q – electron pressure.
 (the second approximation, Variant 4)

915 The drastic increasing of the periodic potential of the crystal lattice (in hundred
 916 times, see figures 40 – 48) in comparison with the self-consistent potential also leads to
 917 diminishing of the soliton size. For the case Variant 6, Table 3 this size consists only
 918 $\sim 10^{-2}a$. But this increasing does not lead to the relative increasing of the soliton kernel
 919 and to the mentioned above the soliton deformation in the second approximation (see

920 figures 45 – 48). Figure 41 demonstrates the extremely high accuracy of the soliton stability,
 921 the velocity fluctuation inside the soliton is only $\sim 10^{-16} \tilde{u}$.



922
 923 Figure 40. s – electron density $\tilde{\rho}_e$,
 924 (the first approximation, Variant 6).
 925

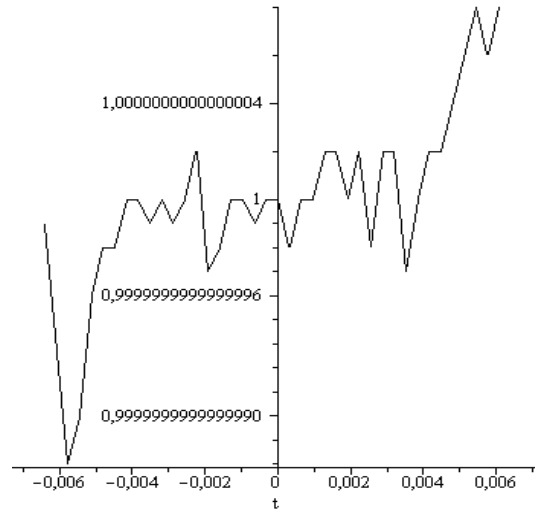
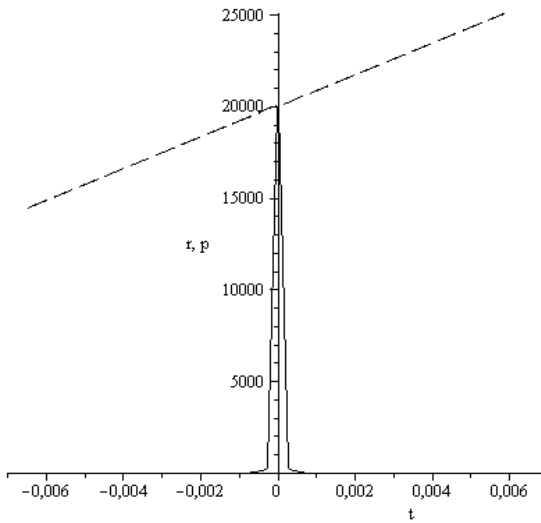


Figure 41. u – velocity \tilde{u} .
 (the first approximation, Variant 6).



926
 927 Figure 42. r – the positive particles density,
 928 (solid line); p – the positive particles pressure
 929 (the first approximation, Variant 6).

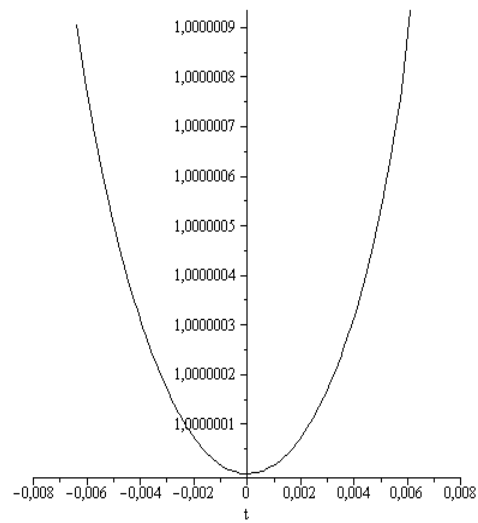
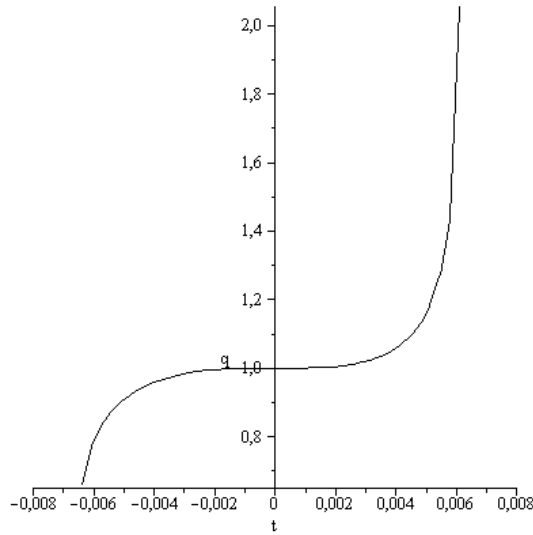


Figure 43. v – potential $\tilde{\phi}$.
 (the first approximation, Variant 6).



930
931 Figure 44. q – electron pressure.
932 (the first approximation, Variant 6).
933
934
935

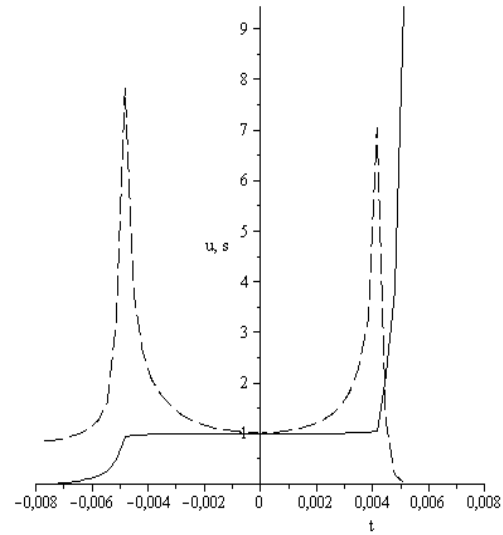
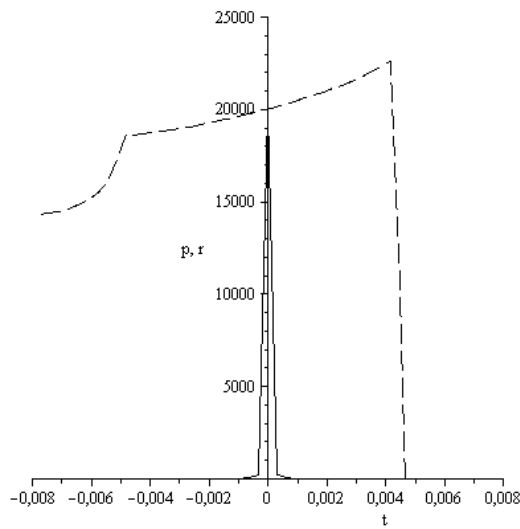


Figure 45. s – electron density $\tilde{\rho}_e$,
 u – velocity \tilde{u} (solid line).
(the second approximation, Variant 6).



936
937 Figure 46. r – the positive particles density.
938 (solid line); p – the positive particles
939 pressure, (the second approximation, Variant 6).
940

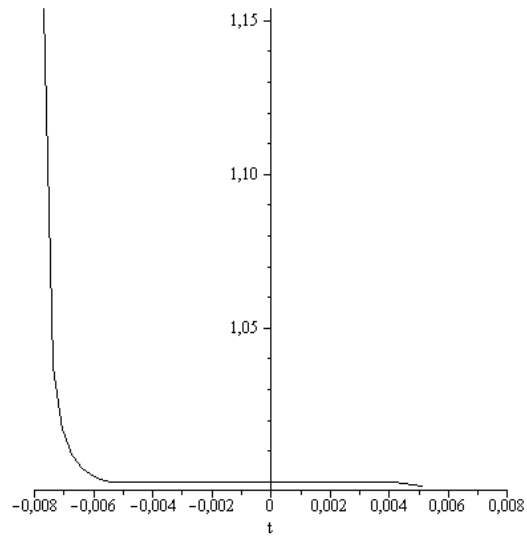


Figure 47. v – potential $\tilde{\phi}$.
(the second approximation, Variant 6).

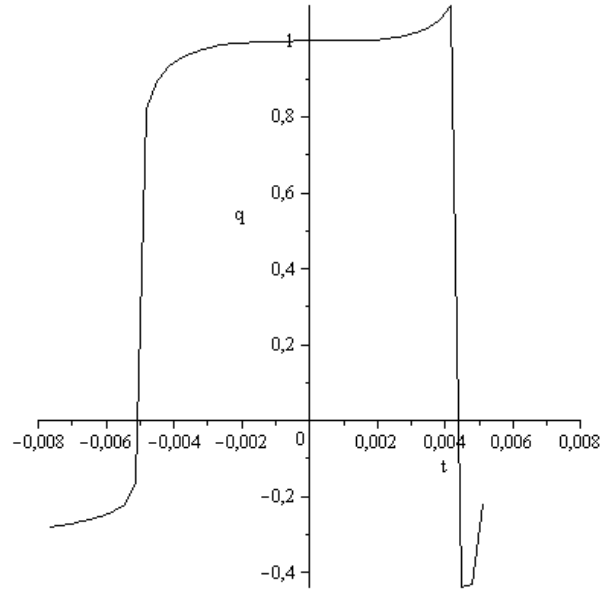


Figure 48. q – electron pressure.
(the second approximation, Variant 6).

6. RESULTS OF THE MATHEMATICAL MODELING WITH THE EXTERNAL ELECTRIC FIELD

Let us consider now the results of the mathematical modeling with taking into account the intensity of the external electric field which does not depend on y . In this case the solution of the hydrodynamic system (3.10) – (3.15) should be found. After averaging and in the moving coordinate system it leads to the following equations written in the first approximation (compare with the system (3.34) – (3.39)):

Poisson equation for the self-consistent electric field:

$$\frac{\partial^2 \tilde{\varphi}}{\partial \tilde{\xi}^2} = -4\pi R \left\{ \frac{m_e}{m_p} \left[\tilde{\rho}_p - \frac{m_e H}{m_p \tilde{u}^2} \frac{\partial}{\partial \tilde{\xi}} (\tilde{\rho}_p (\tilde{u} - 1)) \right] - \left[\tilde{\rho}_e - \frac{H}{\tilde{u}^2} \frac{\partial}{\partial \tilde{\xi}} (\tilde{\rho}_e (\tilde{u} - 1)) \right] \right\}. \quad (6.1)$$

Continuity equation for the positive particles:

$$\begin{aligned} \frac{\partial}{\partial \tilde{\xi}} [\tilde{\rho}_p (1 - \tilde{u})] + \frac{m_e}{m_p} \frac{\partial}{\partial \tilde{\xi}} \left\{ \frac{H}{\tilde{u}^2} \frac{\partial}{\partial \tilde{\xi}} [\tilde{\rho}_p (\tilde{u} - 1)^2] \right\} + \frac{m_e}{m_p} \frac{\partial}{\partial \tilde{\xi}} \left\{ \frac{H}{\tilde{u}^2} \left[\frac{V_{0p}^2}{u_0^2} \frac{\partial}{\partial \tilde{\xi}} \tilde{p}_p - \right. \right. \\ \left. \left. \frac{m_e}{m_p} \tilde{\rho}_p E \left(-\frac{\partial \tilde{\varphi}}{\partial \tilde{\xi}} + \tilde{U}'_{11} \sin \left(\frac{4\pi}{3\tilde{a}} \tilde{\xi} - \frac{\pi}{3} \right) + \tilde{E}_0 \right) \right] \right\} = 0 \end{aligned} \quad (6.2)$$

Continuity equation for electrons:

$$\begin{aligned} \frac{\partial}{\partial \tilde{\xi}} [\tilde{\rho}_e (1 - \tilde{u})] + \frac{\partial}{\partial \tilde{\xi}} \left\{ \frac{H}{\tilde{u}^2} \frac{\partial}{\partial \tilde{\xi}} [\tilde{\rho}_e (\tilde{u} - 1)^2] \right\} + \frac{\partial}{\partial \tilde{\xi}} \left\{ \frac{H}{\tilde{u}^2} \left[\frac{V_{0e}^2}{u_0^2} \frac{\partial}{\partial \tilde{\xi}} \tilde{p}_e - \right. \right. \\ \left. \left. \tilde{\rho}_e E \left(\frac{\partial \tilde{\varphi}}{\partial \tilde{\xi}} - \tilde{U}'_{11} \sin \left(\frac{4\pi}{3\tilde{a}} \tilde{\xi} - \frac{\pi}{3} \right) - \tilde{E}_0 \right) \right] \right\} = 0 \end{aligned} \quad (6.3)$$

960
961

Momentum equation for the x direction:

$$\begin{aligned}
& \frac{\partial}{\partial \tilde{\xi}} \left\{ (\tilde{\rho}_p + \tilde{\rho}_e) \tilde{u} (\tilde{u} - 1) + \frac{V_{0p}^2}{u_0^2} \tilde{p}_p + \frac{V_{0e}^2}{u_0^2} \tilde{p}_e \right\} - \\
962 & \frac{m_e}{m_p} \tilde{\rho}_p E \left(-\frac{\partial \tilde{\phi}}{\partial \tilde{\xi}} + \tilde{U}'_{11} \sin \left(\frac{4\pi}{3\tilde{a}} \tilde{\xi} - \frac{\pi}{3} \right) + \tilde{E}_0 \right) - \\
& \tilde{\rho}_e E \left(\frac{\partial \tilde{\phi}}{\partial \tilde{\xi}} - \tilde{U}'_{11} \sin \left(\frac{4\pi}{3\tilde{a}} \tilde{\xi} - \frac{\pi}{3} \right) - \tilde{E}_0 \right) + \\
& \frac{m_e}{m_p} \frac{\partial}{\partial \tilde{\xi}} \left\{ \frac{H}{\tilde{u}^2} \left[\frac{\partial}{\partial \tilde{\xi}} \left(2 \frac{V_{0p}^2}{u_0^2} \tilde{p}_p (1 - \tilde{u}) - \tilde{\rho}_p \tilde{u} (1 - \tilde{u})^2 \right) - \right. \right. \\
963 & \left. \left. \frac{m_e}{m_p} \tilde{\rho}_p (1 - \tilde{u}) E \left(-\frac{\partial \tilde{\phi}}{\partial \tilde{\xi}} + \tilde{U}'_{11} \sin \left(\frac{4\pi}{3\tilde{a}} \tilde{\xi} - \frac{\pi}{3} \right) + \tilde{E}_0 \right) \right] \right\} + \\
& \frac{\partial}{\partial \tilde{\xi}} \left\{ \frac{H}{\tilde{u}^2} \left[\frac{\partial}{\partial \tilde{\xi}} \left(2 \frac{V_{0e}^2}{u_0^2} \tilde{p}_e (1 - \tilde{u}) - \tilde{\rho}_e \tilde{u} (1 - \tilde{u})^2 \right) - \right. \right. \\
& \left. \left. \tilde{\rho}_e (1 - \tilde{u}) E \left(\frac{\partial \tilde{\phi}}{\partial \tilde{\xi}} - \tilde{U}'_{11} \sin \left(\frac{4\pi}{3\tilde{a}} \tilde{\xi} - \frac{\pi}{3} \right) - \tilde{E}_0 \right) \right] \right\} + \\
& \frac{H}{\tilde{u}^2} E \left(\frac{m_e}{m_p} \right)^2 \left(-\frac{\partial \tilde{\phi}}{\partial \tilde{\xi}} + \tilde{U}'_{11} \sin \left(\frac{4\pi}{3\tilde{a}} \tilde{\xi} - \frac{\pi}{3} \right) + \tilde{E}_0 \right) \left(\frac{\partial}{\partial \tilde{\xi}} (\tilde{\rho}_p (\tilde{u} - 1)) \right) + \\
964 & \frac{H}{\tilde{u}^2} E \left(\frac{\partial \tilde{\phi}}{\partial \tilde{\xi}} - \tilde{U}'_{11} \sin \left(\frac{4\pi}{3\tilde{a}} \tilde{\xi} - \frac{\pi}{3} \right) - \tilde{E}_0 \right) \left(\frac{\partial}{\partial \tilde{\xi}} (\tilde{\rho}_e (\tilde{u} - 1)) \right) - \\
965 & \frac{m_e}{m_p} \frac{\partial}{\partial \tilde{\xi}} \left\{ \frac{H}{\tilde{u}^2} \frac{V_{0p}^2}{u_0^2} \frac{\partial}{\partial \tilde{\xi}} (\tilde{p}_p \tilde{u}) \right\} - \frac{\partial}{\partial \tilde{\xi}} \left\{ \frac{H}{\tilde{u}^2} \frac{V_{0e}^2}{u_0^2} \frac{\partial}{\partial \tilde{\xi}} (\tilde{p}_e \tilde{u}) \right\} + \\
& \left(\frac{m_e}{m_p} \right)^2 E \frac{\partial}{\partial \tilde{\xi}} \left\{ \frac{H}{\tilde{u}^2} \left[\left(-\frac{\partial \tilde{\phi}}{\partial \tilde{\xi}} + \tilde{U}'_{11} \sin \left(\frac{4\pi}{3\tilde{a}} \tilde{\xi} - \frac{\pi}{3} \right) + \tilde{E}_0 \right) \tilde{\rho}_p \tilde{u} \right] \right\} + \\
966 & E \frac{\partial}{\partial \tilde{\xi}} \left\{ \frac{H}{\tilde{u}^2} \left[\left(\frac{\partial \tilde{\phi}}{\partial \tilde{\xi}} - \tilde{U}'_{11} \sin \left(\frac{4\pi}{3\tilde{a}} \tilde{\xi} - \frac{\pi}{3} \right) - \tilde{E}_0 \right) \tilde{\rho}_e \tilde{u} \right] \right\} = 0
\end{aligned} \tag{6.4}$$

967
968
969

Energy equation for the positive particles:

$$\begin{aligned}
970 & \frac{\partial}{\partial \tilde{\xi}} \left[\tilde{\rho}_p \tilde{u}^2 (\tilde{u} - 1) + 5 \frac{V_{0p}^2}{u_0^2} \tilde{p}_p \tilde{u} - 3 \frac{V_{0p}^2}{u_0^2} \tilde{p}_p \right] - 2 \frac{m_e}{m_p} \tilde{\rho}_p E \left(-\frac{\partial \tilde{\phi}}{\partial \tilde{\xi}} + \tilde{U}'_{11} \sin \left(\frac{4\pi}{3\tilde{a}} \tilde{\xi} - \frac{\pi}{3} \right) + \tilde{E}_0 \right) \tilde{u} + \\
971 &
\end{aligned}$$

$$\begin{aligned}
& \frac{\partial}{\partial \tilde{\xi}} \left\{ \frac{H}{\tilde{u}^2} \frac{m_e}{m_p} \left[\frac{\partial}{\partial \tilde{\xi}} \left(-\tilde{\rho}_p \tilde{u}^2 (1-\tilde{u})^2 + 7 \frac{V_{0p}^2}{u_0^2} \tilde{p}_p \tilde{u} (1-\tilde{u}) + 3 \frac{V_{0p}^2}{u_0^2} \tilde{p}_p (\tilde{u}-1) - \frac{V_{0p}^2}{u_0^2} \tilde{p}_p \tilde{u}^2 - \right. \right. \right. \\
972 & \left. \left. \left. 5 \frac{V_{0p}^4}{u_0^4} \frac{\tilde{p}_p^2}{\tilde{\rho}_p} \right) + E \left(-2 \frac{m_e}{m_p} \tilde{\rho}_p \tilde{u} (1-\tilde{u}) + \frac{m_e}{m_p} \tilde{\rho}_p \tilde{u}^2 + 5 \frac{m_e}{m_p} \frac{V_{0p}^2}{u_0^2} \tilde{p}_p \right) \left(-\frac{\partial \tilde{\varphi}}{\partial \tilde{\xi}} + \right. \right. \\
& \left. \left. \tilde{U}'_{11} \sin \left(\frac{4\pi}{3\tilde{a}} \tilde{\xi} - \frac{\pi}{3} \right) + \tilde{E}_0 \right) \right] \right\} + 2 \frac{H}{\tilde{u}^2} E \left(\frac{m_e}{m_p} \right) \left[-\frac{\partial}{\partial \tilde{\xi}} (\tilde{\rho}_p \tilde{u} (1-\tilde{u})) + \right. \\
973 & \left. \frac{V_{0p}^2}{u_0^2} \frac{\partial}{\partial \tilde{\xi}} \tilde{p}_p \right] \left(-\frac{\partial \tilde{\varphi}}{\partial \tilde{\xi}} + \tilde{U}'_{11} \sin \left(\frac{4\pi}{3\tilde{a}} \tilde{\xi} - \frac{\pi}{3} \right) + \tilde{E}_0 \right) - \\
974 & 2 \frac{H}{\tilde{u}^2} E^2 \left(\frac{m_e}{m_p} \right) \tilde{\rho}_p \left[\left(-\frac{\partial \tilde{\varphi}}{\partial \tilde{\xi}} + \tilde{U}'_{11} \sin \left(\frac{4\pi}{3\tilde{a}} \tilde{\xi} - \frac{\pi}{3} \right) + \tilde{E}_0 \right)^2 + \frac{1}{2} \left(\tilde{U}'_{10} \sin \left(\frac{2\pi}{3\tilde{a}} \tilde{\xi} + \frac{\pi}{3} \right) \right)^2 + \right. \\
975 & \left. \frac{3}{2} \left(\tilde{U}'_{10} \cos \left(\frac{2\pi}{3\tilde{a}} \tilde{\xi} + \frac{\pi}{3} \right) \right)^2 + 6(\tilde{U}'_{11})^2 + \frac{16}{\pi} (\tilde{U}'_{10} \tilde{U}'_{11}) \cos \left(\frac{2\pi}{3\tilde{a}} \tilde{\xi} + \frac{\pi}{3} \right) \right] = \\
976 & -\frac{\tilde{u}^2}{Hu_0^2} (V_{0p}^2 \tilde{p}_p - \tilde{p}_e V_{0e}^2) \left(1 + \frac{m_p}{m_e} \right) \quad (6.5)
\end{aligned}$$

977
978
979

Energy equation for electrons:

$$\begin{aligned}
980 & \frac{\partial}{\partial \tilde{\xi}} \left[\tilde{\rho}_e \tilde{u}^2 (\tilde{u}-1) + 5 \frac{V_{0e}^2}{u_0^2} \tilde{p}_e \tilde{u} - 3 \frac{V_{0e}^2}{u_0^2} \tilde{p}_e \right] - 2 \tilde{\rho}_e \tilde{u} E \left(\frac{\partial \tilde{\varphi}}{\partial \tilde{\xi}} - \tilde{U}'_{11} \sin \left(\frac{4\pi}{3\tilde{a}} \tilde{\xi} - \frac{\pi}{3} \right) - \tilde{E}_0 \right) + \\
& \frac{\partial}{\partial \tilde{\xi}} \left\{ \frac{H}{\tilde{u}^2} \left[\frac{\partial}{\partial \tilde{\xi}} \left(-\tilde{\rho}_e \tilde{u}^2 (1-\tilde{u})^2 + 7 \frac{V_{0e}^2}{u_0^2} \tilde{p}_e \tilde{u} (1-\tilde{u}) + 3 \frac{V_{0e}^2}{u_0^2} \tilde{p}_e (\tilde{u}-1) - \frac{V_{0e}^2}{u_0^2} \tilde{p}_e \tilde{u}^2 - \right. \right. \right. \\
981 & \left. \left. \left. 5 \frac{V_{0e}^4}{u_0^4} \frac{\tilde{p}_e^2}{\tilde{\rho}_e} \right) + E \left(-2 \tilde{\rho}_e \tilde{u} (1-\tilde{u}) + \tilde{\rho}_e \tilde{u}^2 + 5 \frac{V_{0e}^2}{u_0^2} \tilde{p}_e \right) \left(\frac{\partial \tilde{\varphi}}{\partial \tilde{\xi}} - \tilde{U}'_{11} \sin \left(\frac{4\pi}{3\tilde{a}} \tilde{\xi} - \frac{\pi}{3} \right) - \tilde{E}_0 \right) \right] \right\} + \\
982 & E \left(-2 \frac{H}{\tilde{u}^2} \frac{\partial}{\partial \tilde{\xi}} (\tilde{\rho}_e \tilde{u} (1-\tilde{u})) + 2 \frac{H}{\tilde{u}^2} \frac{V_{0e}^2}{u_0^2} \frac{\partial}{\partial \tilde{\xi}} \tilde{p}_e \right) \left(\frac{\partial \tilde{\varphi}}{\partial \tilde{\xi}} - \tilde{U}'_{11} \sin \left(\frac{4\pi}{3\tilde{a}} \tilde{\xi} - \frac{\pi}{3} \right) - \tilde{E}_0 \right) -
\end{aligned}$$

$$\begin{aligned}
& 2E^2 \frac{H}{\tilde{u}^2} \tilde{\rho}_e \left[\left(-\frac{\partial \tilde{\varphi}}{\partial \tilde{\xi}} + \tilde{U}'_{11} \sin \left(\frac{4\pi}{3\tilde{a}} \tilde{\xi} - \frac{\pi}{3} \right) + \tilde{E}_0 \right)^2 + \right. \\
& \frac{1}{2} \left(\tilde{U}'_{10} \sin \left(\frac{2\pi}{3\tilde{a}} \tilde{\xi} + \frac{\pi}{3} \right) \right)^2 + \frac{3}{2} \left(\tilde{U}'_{10} \cos \left(\frac{2\pi}{3\tilde{a}} \tilde{\xi} + \frac{\pi}{3} \right) \right)^2 + \\
& \left. 6(\tilde{U}'_{11})^2 + \frac{16}{\pi} (\tilde{U}'_{10} \tilde{U}'_{11}) \cos \left(\frac{2\pi}{3\tilde{a}} \tilde{\xi} + \frac{\pi}{3} \right) \right] = -\frac{\tilde{u}^2}{Hu_0^2} (V_{0e}^2 \tilde{p}_e - V_{0p}^2 \tilde{p}_p) \left(1 + \frac{m_p}{m_e} \right)
\end{aligned} \tag{6.6}$$

Two classes of parameters were used by the mathematical modeling – parameters and scales which were not changed during calculations and varied parameters indicated in Table 4.

Parameters, scales and Cauchy conditions which are common for modeling with the external field:

$\frac{m_e}{m_p} = 5 \cdot 10^{-5}$, the scales $\rho_0 = 10^{-10} \text{ g/cm}^3$, $u_0 = 5 \cdot 10^6 \text{ cm/s}$, $V_{0e} = 5 \cdot 10^6 \text{ cm/s}$,

$V_{0p} = 5 \cdot 10^4 \text{ cm/s}$, $x_0 = a = 0.142 \text{ nm}$, $\varphi_0 = 10^{-4} \frac{e}{a} = 3.4 \cdot 10^{-6} \text{ CGSE}_\varphi$.

Dimensionless parameters $R = 3 \cdot 10^{-3}$, $E = 0.1$, $H = 15$ (by $N_R = 1$). Admit that for the lattice

$U \sim V_{1,(10)} \sim V_{1,(11)} \sim \varphi_0$ and choose $\tilde{U}'_{10} = 10$, $\tilde{U}'_{11} = 10$.

Cauchy conditions $\tilde{\rho}_e(0) = 1$, $\tilde{\rho}_p(0) = 2 \cdot 10^4$, $\tilde{p}_e(0) = 1$, $\tilde{p}_p(0) = 2 \cdot 10^4$, $\tilde{\varphi}(0) = 1$,

$\frac{\partial \tilde{\rho}_e}{\partial \tilde{\xi}}(0) = 0$, $\frac{\partial \tilde{\rho}_p}{\partial \tilde{\xi}}(0) = 0$.

Table 4. Varied parameters in calculations with the external electric field.

| Variant № | \tilde{E}_0 | $\frac{\partial \tilde{\varphi}}{\partial \tilde{\xi}}(0)$ | $\frac{\partial \tilde{p}_p}{\partial \tilde{\xi}}(0)$ | $\frac{\partial \tilde{p}_e}{\partial \tilde{\xi}}(0)$ |
|-----------|---------------|--|--|--|
| 1 | 0 | 0 | 0 | 0 |
| 7.0 | 10 | 10 | 0 | 0 |
| 7.1 | 10 | 10 | 10 | -1 |
| 8.0 | 100 | 100 | 0 | 0 |
| 8.1 | 100 | 100 | 10 | 0 |
| 9.0 | 10000 | 10000 | 0 | 0 |
| 9.1 | 10000 | 10000 | 10 | -1 |

The external intensity of the electric field is written as

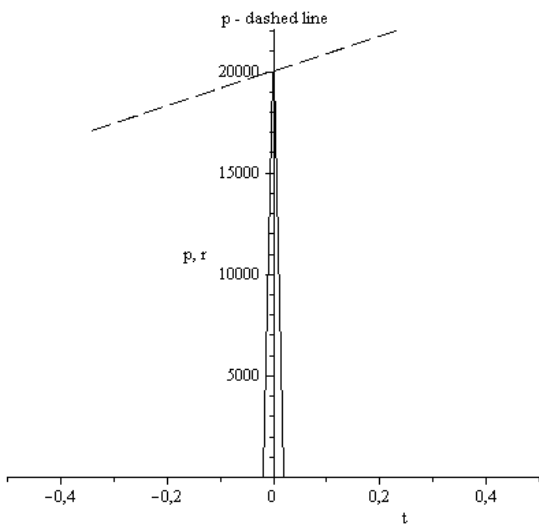
$E_0 = \frac{\varphi_0}{x_0} \tilde{E}_0 = 10^{-4} \frac{e}{a^2} \tilde{E}_0 = 238 \text{ CGSE}_E \tilde{E}_0 = 7.14 \cdot 10^6 \frac{V}{m} \tilde{E}_0$. It means that even by

$\tilde{E}_0 = 1$ we are dealing with the rather strong fields. But namely strong external fields can exert the influence on the soliton structures compared with the Coulomb forces in the lattice. For example in [39] the influence of the external electric field in graphene up to

1004 $10^7 - 10^8 V/m$. The values \tilde{E}_0 are indicated in Table 4, variants 9.0 and 9.1 respond to
 1005 the extremely strong external field.

1006 Table 4 contains in the first line the reminder about the first variant of calculations
 1007 reflected on figures 2 – 5. These data (in the absence of the external field, $\tilde{E}_0 = 0$) are
 1008 convenient for the following result comparison. The variants of calculations in Table 4 are
 1009 grouped on principle of the \tilde{E}_0 increasing. In more details: figures 49 – 58 correspond to
 1010 $\tilde{E}_0 = 10$, figures 59 – 68 correspond to $\tilde{E}_0 = 100$, figures 69 – 80 correspond to
 1011 $\tilde{E}_0 = 10000$.

1012
 1013



1014
 1015
 1016
 1017
 1018
 1019
 1020

Figure 49. r – the positive particles density, (solid line); p – the positive particles pressure. (Variant 7.0).

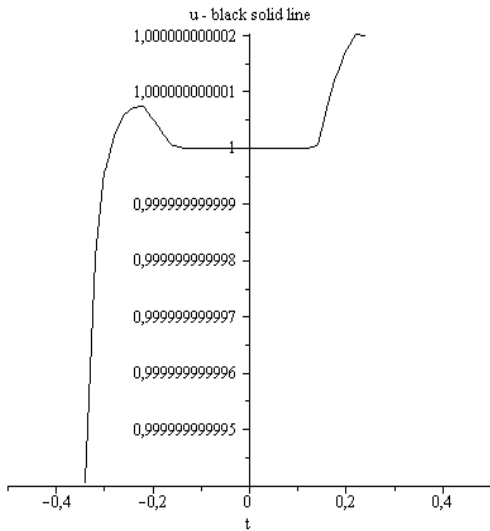


Figure 50. u – velocity \tilde{u} . (Variant 7.0).

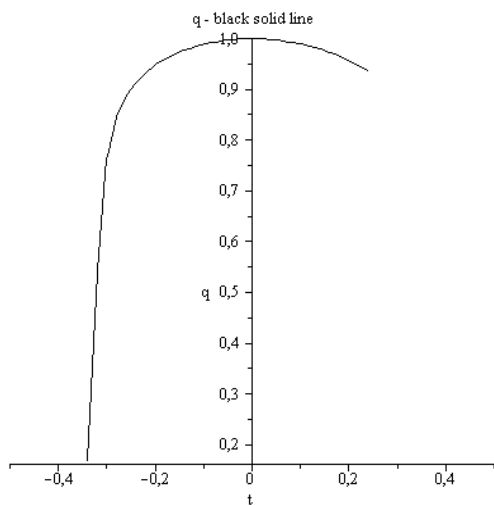


Figure 51. q – electron pressure .
(Variant 7.0).

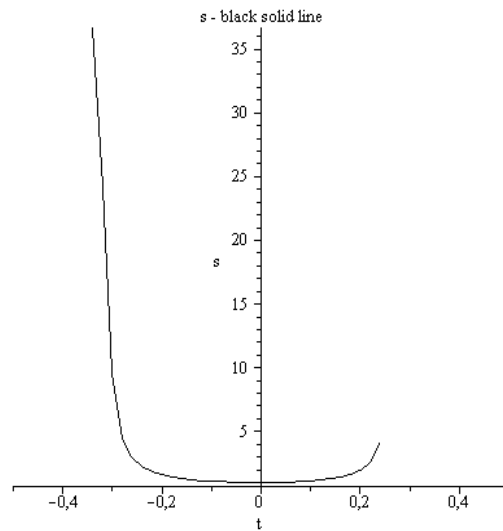


Figure 52. s – electron density $\tilde{\rho}_e$,
(Variant 7.0).

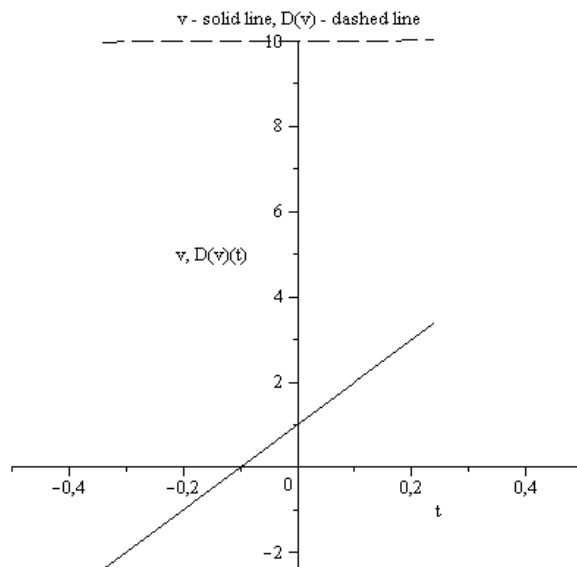


Figure 53. v – potential $\tilde{\varphi}$ (solid line);
 $D(v)(t)$, (Variant 7.0).

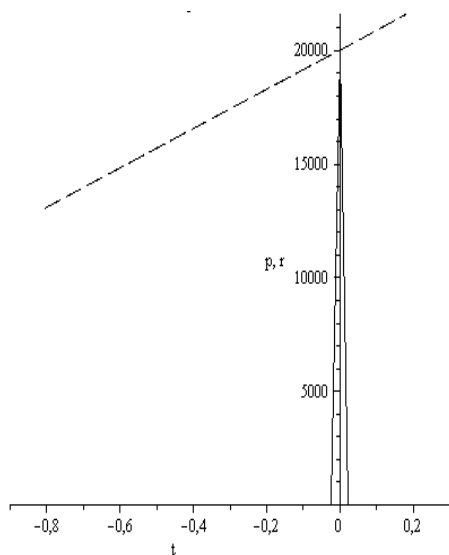


Figure 54. r – the positive particles density, (solid line); p – the positive particles pressure. (Variant 7.1).

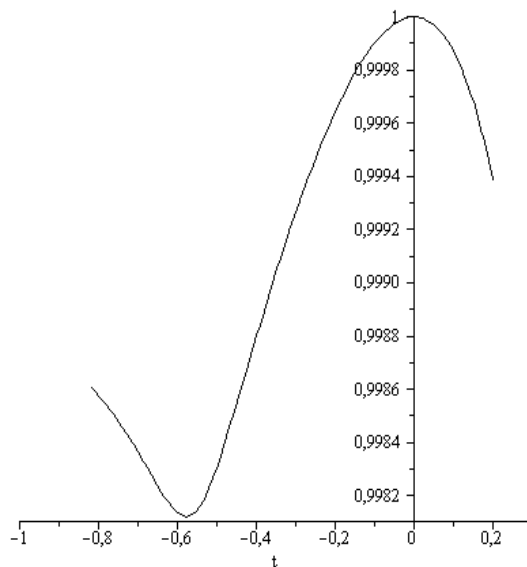


Figure 55. u – velocity \tilde{u} . (Variant 7.1).

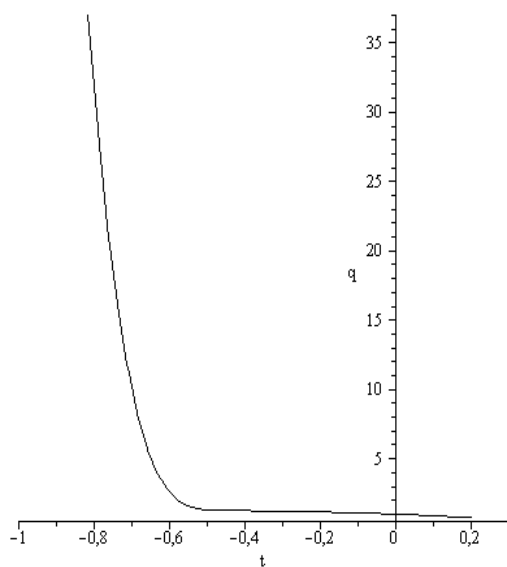


Figure 56. q – electron pressure. (Variant 7.1).

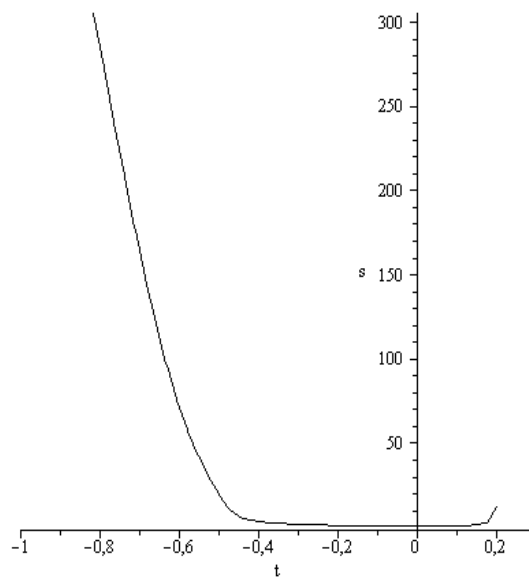


Figure 57. s – electron density $\tilde{\rho}_e$, (Variant 7.1).

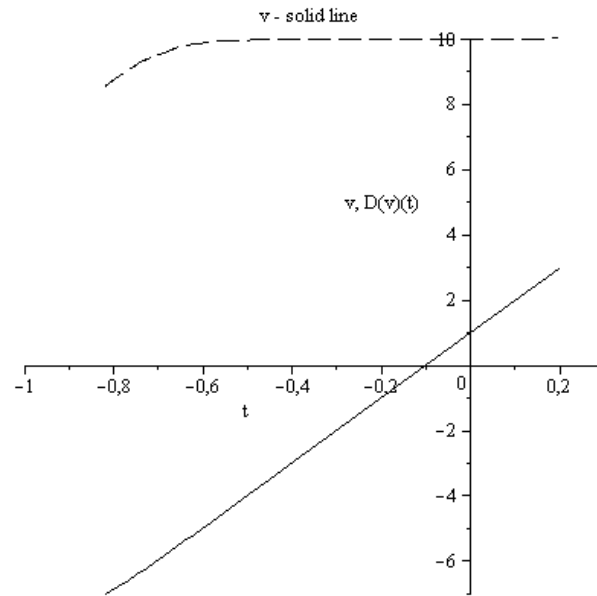


Figure 58. v – potential $\tilde{\varphi}$ (solid line);
 $D(v)(t)$, (Variant 7.1).

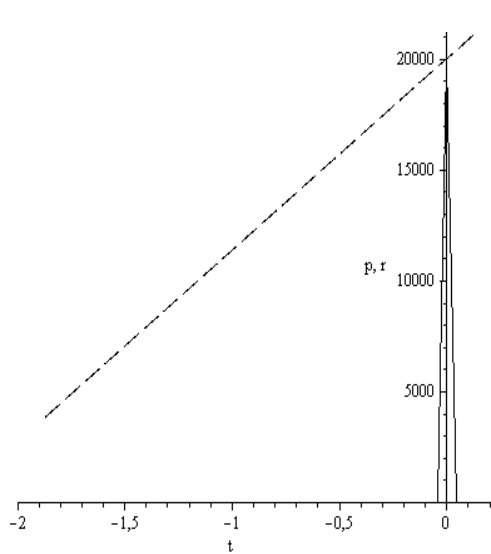


Figure 59. r – the positive particles density,
(solid line); p – the positive particles pressure.
(Variant 8.0).

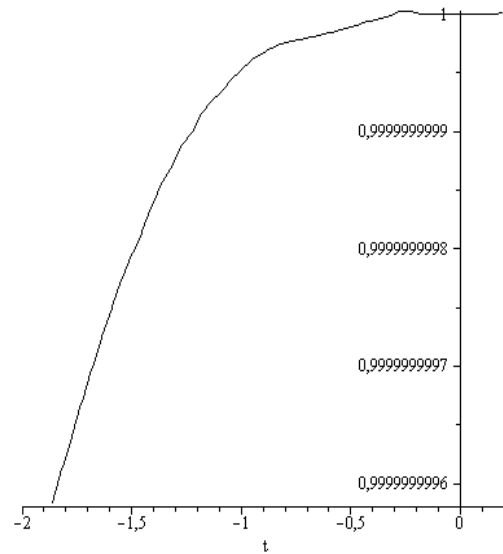


Figure 60. u – velocity \tilde{u} . (Variant 8.0).

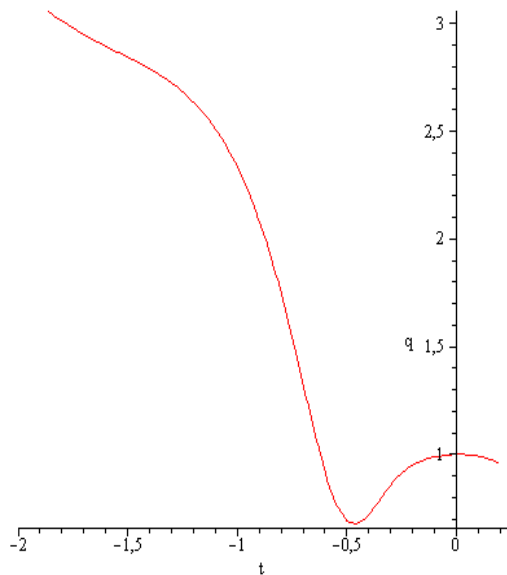


Figure 61. q – electron pressure.
(Variant 8.0).

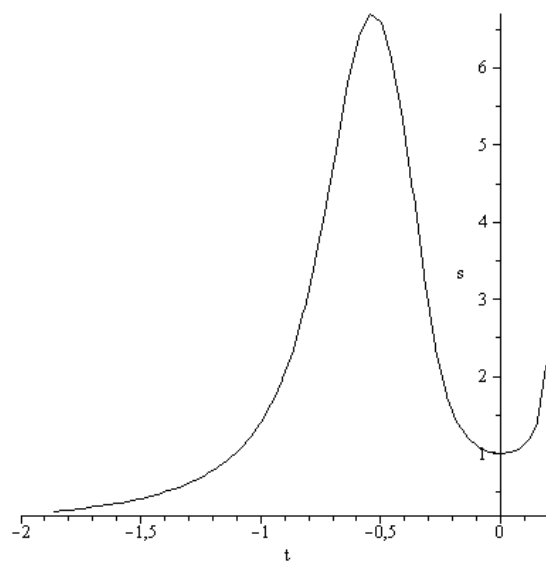


Figure 62. s – electron density $\tilde{\rho}_e$,
(Variant 8.0).

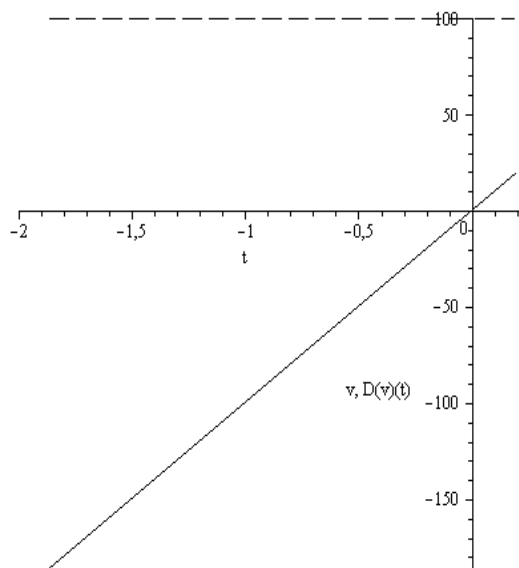


Figure 63. v – potential $\tilde{\phi}$ (solid line);
 $D(v)(t)$, (Variant 8.0).

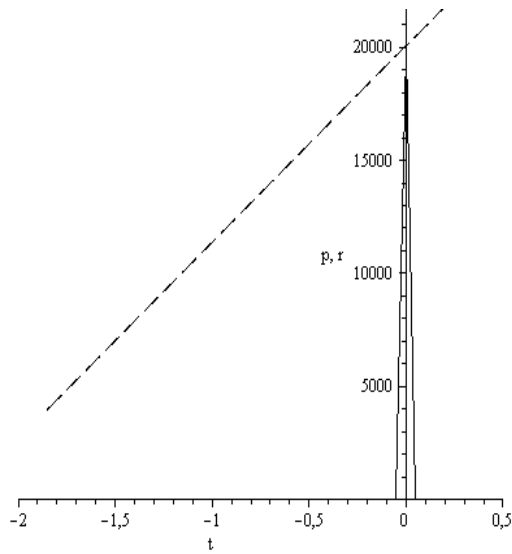


Figure 64. r – the positive particles density, (solid line); p – the positive particles pressure. (Variant 8.1).

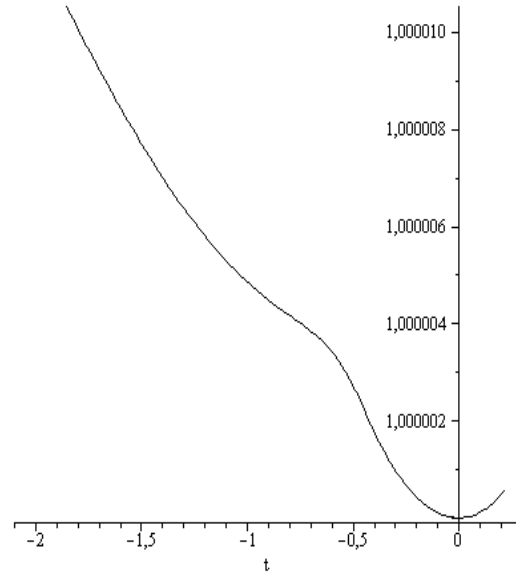


Figure 65. u – velocity \tilde{u} . (Variant 8.1).

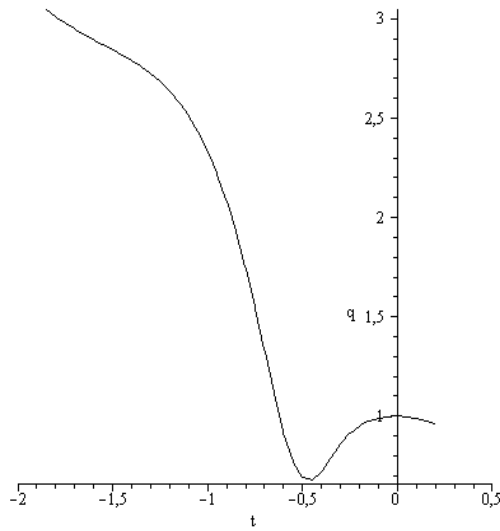


Figure 66. q – electron pressure. (Variant 8.1).

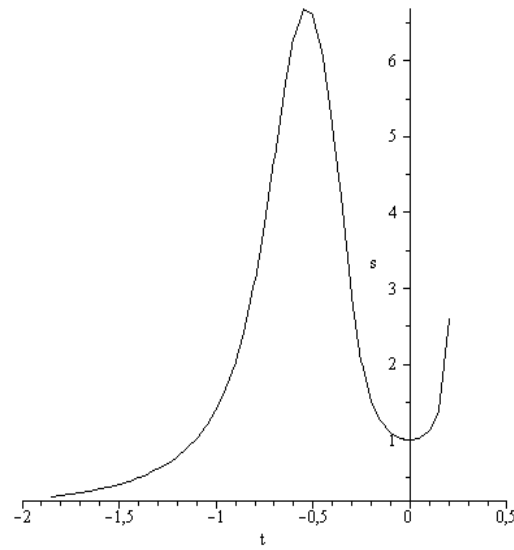


Figure 67. s – electron density $\tilde{\rho}_e$, (Variant 8.1).

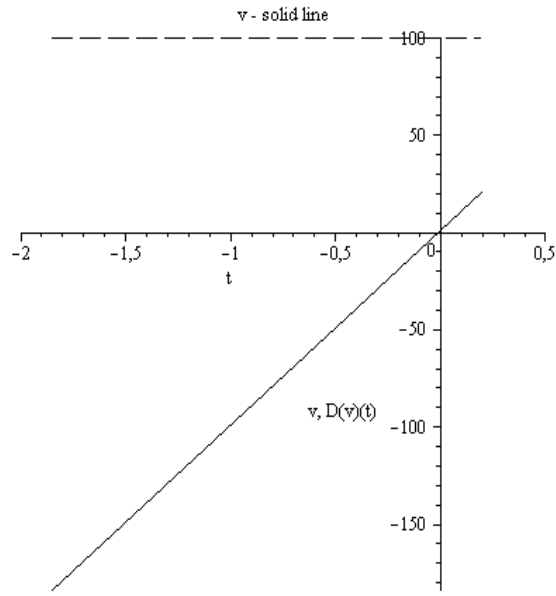


Figure 68. v – potential $\tilde{\phi}$ (solid line);
 $D(v)(t)$, (Variant 8.1).

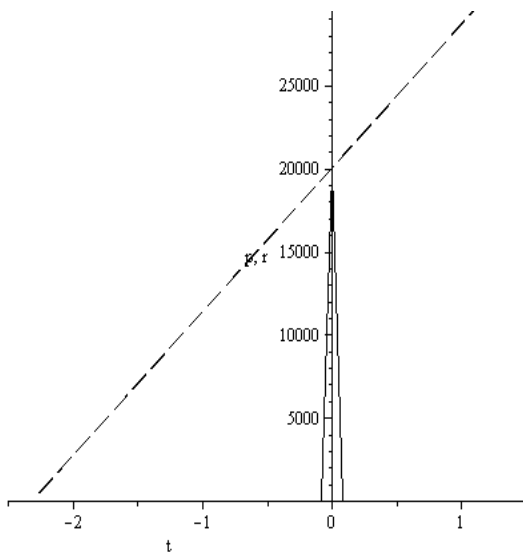


Figure 69. r – the positive particles density,
(solid line); p – the positive particles pressure.
(Variant 9.0).

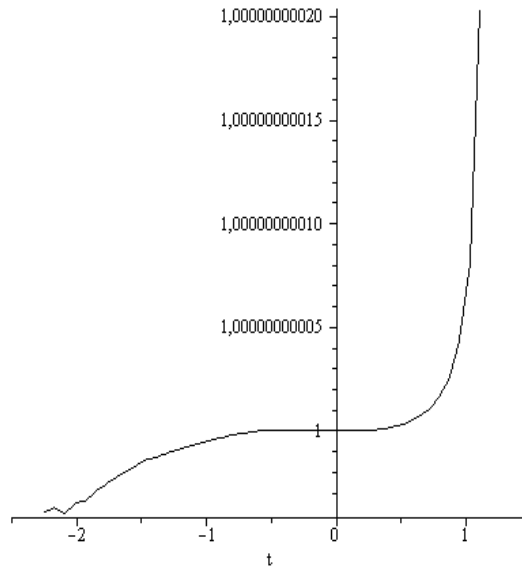


Figure 70. u – velocity \tilde{u} . (Variant 9.0).

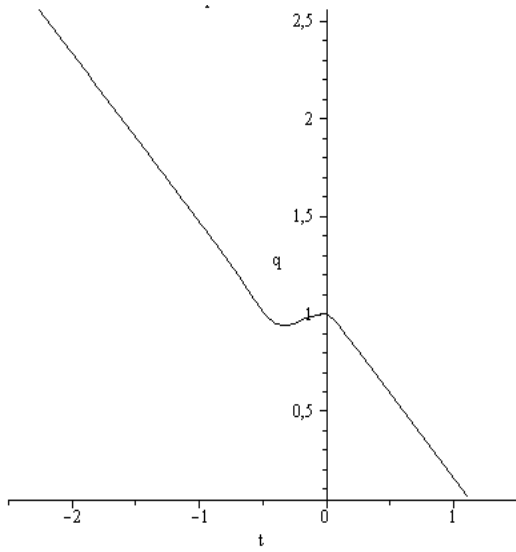


Figure 71. q – electron pressure.
(Variant 9.0).

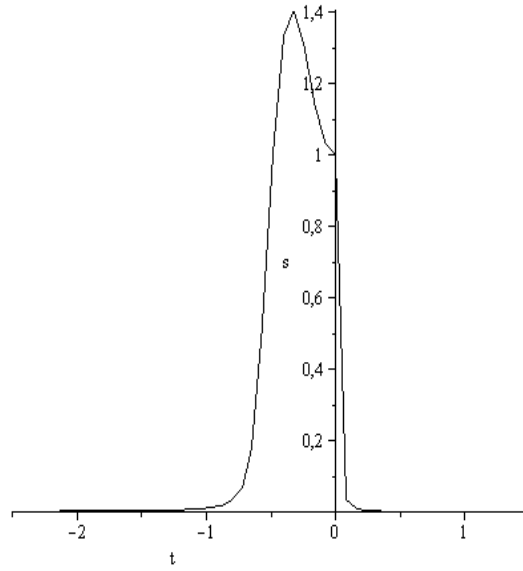


Figure 72. s – electron density $\tilde{\rho}_e$,
(Variant 9.0).

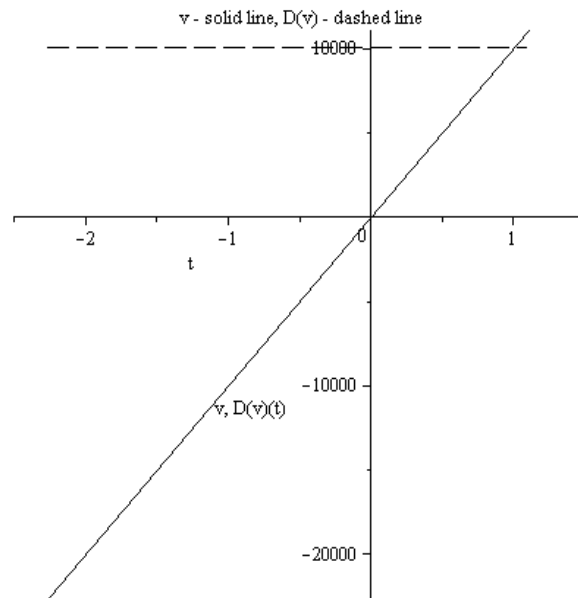


Figure 73. v – potential $\tilde{\varphi}$ (solid line);
 $D(v)(t)$, (Variant 9.0).

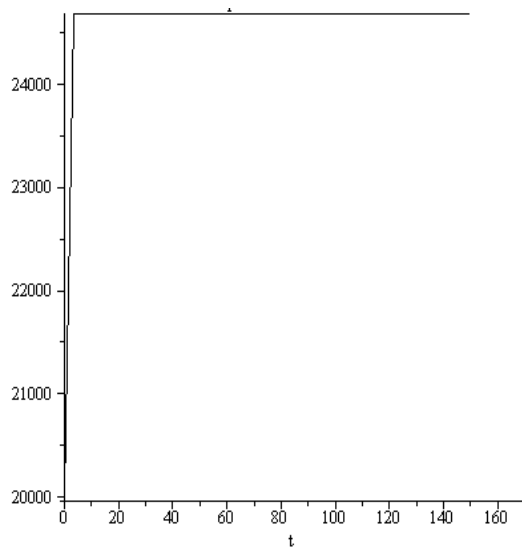


Figure 74. p – the positive particles pressure.
(Variant 9.1).

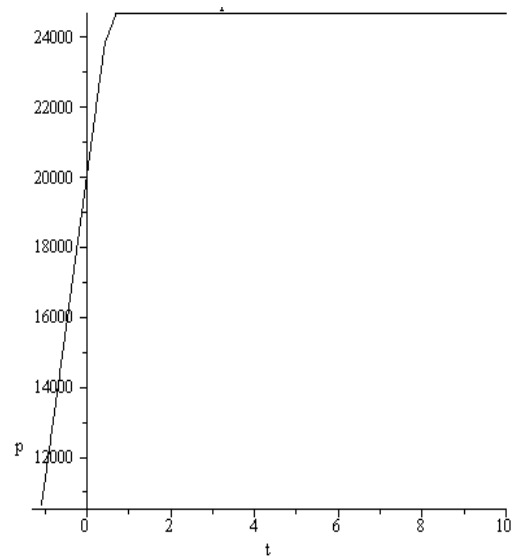


Figure 75. p – the positive particles pressure.
(Variant 9.1).

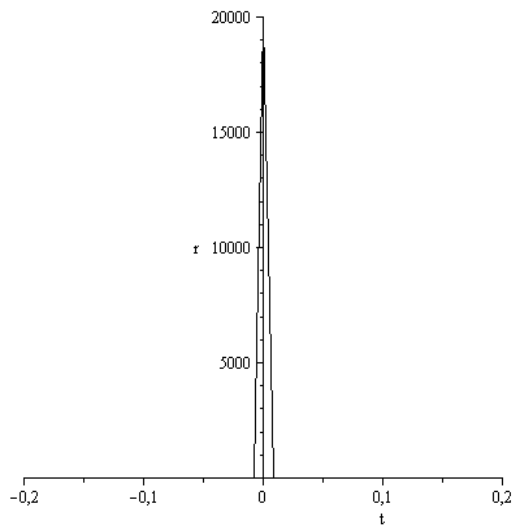


Figure 76. r – the positive particles density,
(Variant 9.1).

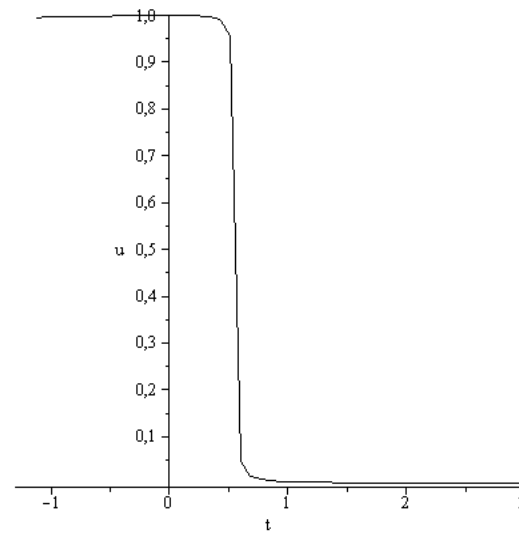


Figure 77. u – velocity \tilde{u} . (Variant 9.1).

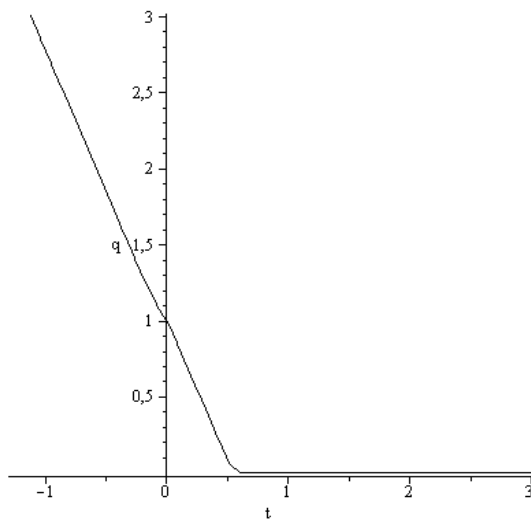


Figure 78. q – electron pressure.
(Variant 9.1).

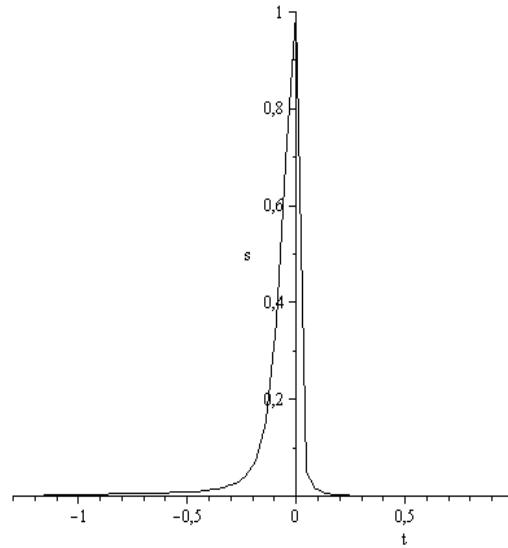


Figure 79. s – electron density $\tilde{\rho}_e$,
(Variant 9.1).

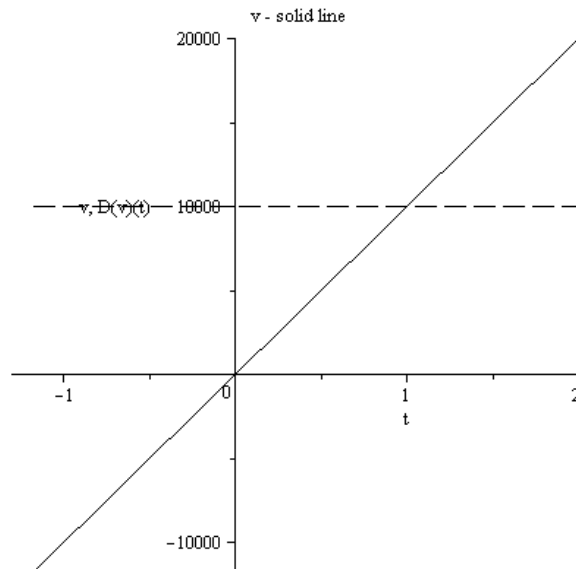


Figure 80. v – potential $\tilde{\varphi}$ (solid line);
 $D(v)(t)$, (Variant 9.1).

Consider now the character features of the soliton evolution and the change of the charge distribution in solitons with growing of the external field intensity:

1. The character soliton size is defined by the area where $\tilde{u} = 1$. It means that all part of the soliton wave are moving without destruction. The size of this area is practically independent on choosing of the numerical method of calculations.

2. Figures 75 – 77 demonstrate the typical situation when the area of possible numerical calculations for a physical variable does not coincide with area $\tilde{u} = 1$ where the soliton regime exists.
3. In the area of the soliton existence the condition $\tilde{u} = 1$ is fulfilled with the high accuracy defined practically by accuracy of the choosed numerical method (see figures 50, 55, 60, 65, 70, 77).
4. As a rule for the choosed topology of the electric field the size of the soliton existence is growing with increasing of the electric field intensity.
5. Under the influence of the external electric field the captured electron cloud is displacing in the opposite direction (of the negative variable $\tilde{\xi}$). The soliton kernel is loosing its symmetry.
6. The redistribution of the self-consistent effective charge creates the self-consistence field with the opposite (to the external field) direction, (see figures 53, 58, 63, 68, 73, 80).
7. The quantum pressure of the positive particle is growing with the $\tilde{\xi}$ increase. On the whole the specific features of the \tilde{p} , \tilde{q} pressures are defined by the process of the soliton formation.

7. CONCLUSION

The origin of the charge density waves (CDW) is a long-standing problem relevant to a number of important issues in condensed matter physics. Mathematical modeling of the CDW expansion as well as the problem of the high temperature superconduction can be solved only on the basement of the nonlocal quantum hydrodynamics in particular on the basement of the Alexeev non-local quantum hydrodynamics. It is known that the Schrödinger – Madelung quantum physics leads to the destruction of the wave packets and can not be used for the solution of this kind of problems. **The appearance of the soliton solutions in mathematics is the rare and remarkable effect.** As we see the soliton's appearance in the generalized hydrodynamics created by Alexeev is an “ordinary” oft-recurring fact. The realized here mathematical modeling CDW expansion support established in [22, 24] mechanism of the relay (“estafette”) motion of the soliton' system (“lattice ion – electron”) **which is realizing without creation of additional chemical bonds.** Important to underline that the soliton mechanism of CDW expansion in graphene (and other substances like NbSe₂) takes place in the extremely large diapason of physical parameters. But CDW existence belongs to effects conveying the high temperature superconductivity. It means that the high temperature superconductivity can be explained in the frame of the non-local soliton quantum hydrodynamics.

Important to underline that the problem of existing and propagation of solitons in graphene and in the perspective high superconducting materials belong to the class of significantly non-local non-linear problems which can be sold only in the frame of vast numerical modeling.

REFERENCES

- [1] Alekseev, B.V. (1982). Matematicheskaya Kinetika Reagiruyushchikh Gazov. (Mathematical Theory of Reacting Gases) Moscow, Nauka.
- [2] Alexeev, B.V. (1994) The Generalized Boltzmann Equation, Generalized Hydrodynamic Equations and their Applications, Phil. Trans. Roy. Soc. Lond. Vol. 349, 417-443.

- doi:10.1098/rsta.1994.0140
- [3] Alexeev, B.V. The Generalized Boltzmann Equation (1995), *Physica A*, Vol. 216, 459 - 468. doi:10.1016/0378-4371(95)00044-8
- [4] Alekseev, B.V. Physical Basements of the Generalized Boltzmann Kinetic Theory of Gases. (2000), *Physics-Uspekhi*, Vol. 43, No 6, 601 – 629. doi:10.1070/PU2000v043n06ABEH000694
- [5] Alekseev, B.V. (2003). Physical Fundamentals of the Generalized Boltzmann Kinetic Theory of Ionized Gases, *Physics-Uspekhi*, Vol 46, No 2, 139 – 167. doi:10.1070/PU2003v046n02ABEH001221
- [6] Alexeev, B.V. (2004) *Generalized Boltzmann Physical Kinetics*. Elsevier, Amsterdam, The Netherlands.
- [7] Alexeev, B.V. (2008). Generalized Quantum Hydrodynamics and Principles of Non-Local Physics”, *J. Nanoelectron. Optoelectron.* No. 3, 143 - 158. doi:10.1166/jno.2008.207
- [8] Alexeev, B.V. (2008). Application of Generalized Quantum Hydrodynamics in the Theory of Quantum Soliton Evolution”, *J. Nanoelectron. Optoelectron.* No. 3, 316 - 328. doi:10.1166/jno.2008.311
- [9] Alexeev, B.V. (2012) Application of Generalized Non-Local Quantum Hydrodynamics to the Calculation of the Charge Inner Structures for Proton and Electron” *Journal of Modern Physics*, 3, 1895-1906 doi:10.4236/jmp.2012.312239 Published Online December 2012 (<http://www.SciRP.org/journal/jmp>)
- [10] Alexeev, B.V. (2012) To the Theory of Galaxies Rotation and the Hubble Expansion in the Frame of Non-Local Physics” *Journal of Modern Physics*, 3, 1103-1122 doi:10.4236/jmp.2012.329145 Published Online September 2012 (<http://www.SciRP.org/journal/jmp>)
- [11] Boltzmann, L. (1872) Weitere Studien über das Wärmegleichgewicht unter Gasmolekülen, *Sitz. Ber. Kaiserl. Akad. Wiss.* 66 (2), 275.
- [12] Boltzmann L. (1912) *Vorlesungen über Gastheorie*, Leipzig: Verlag von Johann Barth.
- [13] Chapman, S. and Cowling T.G. (1952). *The Mathematical Theory of Non-uniform Gases*, Cambridge: At the University Press.
- [14] Hirschfelder I.O., Ch. F. Curtiss Ch. F. and, Bird R.B., (1954). *Molecular Theory of Gases and Liquids*, John Wiley and sons, inc. New York. Chapman and Hall, lim., London.
- [15] Bell, J.S. (1964) On the Einstein Podolsky Rosen Paradox, *Physics*, v. 1, 195 - 200.
- [16] Madelung, E. (1927). Quantum Theory in Hydrodynamical Form”, *Zeit. f. Phys.* 40, 322 - 325. doi:10.1007/BF01400372
- [17] Landau, L.D. (1932). Zur Theorie der Energieübertragung. II 2, *Physics of the Soviet Union*, 46 - 51.
- [18] Zener C. (1932). Non-adiabatic Crossing of Energy Levels. *Proceedings of the Royal Society of London A* **137** (6), 696–702. Bibcode 1932RSPSA.137..696Z. doi:10.1098/rspa.1932.0165. JSTOR 19320901
- [19] Gell-Mann, M. and F. Low F. (1951). Bound States in Quantum Field Theory, *Phys. Rev.*, 84, 350. doi:10.1103/PhysRev.84.350
- [20] Berry, M.V. (1984). Quantal Phase Factors Accompanying Adiabatic Changes, *Proc. Royal Soc. London A*, 392, 45. doi:10.1098/rspa.1984.0023
- [21] Simon, B. (1983) Holonomy, the Quantum Adiabatic Theorem and Berry's Phase, *Phys. Rev. Letters*, 51, 2167 - 2170. doi:10.1103/PhysRevLett.51.2167
- [22] Alexeev, B.V. (2012). To the Non-Local Theory of the High Temperature Superconductivity. ArXiv: 0804.3489 [physics.gen-ph] Submitted on 30 Jan 2012.
- [23] Алексеев, Б.В. (2008). Обобщенная квантовая гидродинамика //Вестник МИТХТ. Т.3. №3. С.3-19 (Alexeev B.V. Generalized Quantum Hydrodynamics. Vestnik MITHT, in Russian).
- [24] Алексеев, Б.В. (2012). К нелокальной теории высокотемпературной

- 1225 сверхпроводимости. Вестник МИТХТ, Т. 7, №3, 3 – 21. (Alexeev B.V. To the
1226 Non-Local Theory of the High Temperature Superconductivity. Vestnik MITHT, in
1227 Russian).
- 1228 [25]. Dürkop T., Getty S.A., Cobas Enrique, and Fuhrer M.S., Nano Letters 4, 35 (2004)).
- 1229 [26] Kohsaka Y., Hanaguri T., Azuma M., Takano M., Davis J.C., Takagi H. (2012).
1230 Visualization of the emergence of the pseudogap state and the evolution to
1231 superconductivity in a lightly hole-doped Mott insulator. Nature Physics. 8. 534 – 538.
1232 doi:10.1038/nphys2321
- 1233 [27] Chang, J, Blackburn, E., Holmes, A.T., Christensen, N.B., Larsen, J., Mesot, J, Ruixing,
1234 Liang, Bonn, D.A., Hardy, W.N., Watenphul, A., v. Zimmermann, M., Forgan, E.M.,
1235 Hayden, S.M. (2012). Direct observation of competition between superconductivity
1236 and charge density wave order in $\text{YBa}_2\text{Cu}_3\text{O}_y$. ArXiv:1206.4333[v2], 3 Jul 2012.
1237 Condensed Matter. Superconductivity.
- 1238 [28] Alexeev, B.V., Abakumov, A.I., Vinogradov, V.S., (1986). Mathematical Modeling of
1239 Elastic Interactions of Fast Electrons with Atoms and Molecules. Communications on
1240 the Applied Mathematics. Computer Centre of the USSR Academy of Sciences.
1241 Moscow.
- 1242 [29] Alexeev, B.V. (2011). Non-local Physics. Non-relativistic Theory, Lambert Academic
1243 Press (in Russian).
- 1244 [30] Лозовик, Ю.Е., Меркулова, С.П., Соколик, А.А. (2008). Коллективные электронные
1245 явления в графене//Успехи физических наук. Т.178. №7. 757-776.
- 1246 [31] Barlas Y., Pereg-Barnea T., Polini M., Asgari R., MacDonald A.H. (2007) Chirality and
1247 Correlations in Graphene. Phys. Rev. Letters, 98, 236601.
- 1248 [32]. Castro Neto, A.H., Guinea, F., Peres, N.M.R., Novoselov, K.S., Geim, A.K. (2009). The
1249 Electronic Properties of Graphene. Reviews of Modern Physics, 81,109-162.
- 1250 [33]. Vasko, F.T., Ryzhii, V. (2008) Photoconductivity of an intrinsic graphene.
1251 ArXiv,0801/3476v2 [cond-mat.mtrl-sci].
- 1252 [34] Alexeev, B.V. and Ovchinnikova, I.V. (2011). Non-local Physics. Relativistic Theory,
1253 Lambert Academic Press (in Russian).
- 1254 [35] Pisana, S., Lazzeri, M., Casiraghi, C., Novoselov, K.S., Geim, A.K., Ferrari, A.C., Mauri
1255 F. (2007). Breakdown of the adiabatic Born – Oppenheimer approximation in
1256 graphene. Nature Materials. Vol.6, 198-201.
- 1257 [36] Завьялов, Д.В., Крючков, С.В., Тюлькина, Т.А. (2010). Численное моделирование
1258 эффекта выпрямления тока, индуцированного электромагнитной волной в
1259 графене. Физика и техника полупроводников 44, вып.7, 910-914 (Zavjalov, D.V.,
1260 Krychkov, S.V., Tyul'kina, T.A. Numerical simulation of the current rectification effect
1261 induced by an electromagnetic wave in graphene. Fisika and Tehnika
1262 Poluprovodnikov. in Russian)
- 1263 [37] Завьялов, Д.В., Крючков, С.В., Мещерякова, Н.Е. (2010). Влияние нелинейной
1264 электромагнитной волны на плотность тока в поверхностной сверхрешетке в
1265 сильном электрическом поле. Физика и техника полупроводников 39, вып.2, 214-
1266 217.(Zavjalov, D.V., Kruchkov, S.V., Mestcheryakova, N.E. Influence of a nonlinear
1267 electromagnetic wave on the electric current density in a superficial superlattice in a
1268 strong electric field. Fisika i Tehnika Poluprovodnikov. in Russian)
- 1269 [38] Hwang, E.H., Adam, S., Sarma, S.D. (2007). Carrier transport in 2D graphene layers.
1270 ArXiv,0610157v2 [cond-mat.mes-hall].
- 1271 [39] Белоненко, М.Б., Лебедев, Н.Г., Пак, А.В., Янюшкина, Н.Н. (2011). Спонтанное
1272 поперечное поле в примесном графене. Журнал технической физики Т. 81. Вып.
1273 8. 64-69. (Belonenko, M.B., Lebedev, N.G., Pak, A.V., Yanushkina, N.N. Spontaneous
1274 transverse field in doped graphene. Journal of Technical Physics, in Russian).